NUCLEAR ENGINEERING

MASSACHUSETTS INSTITUTE
OF TECHNOLOGY

ANALYSIS OF DESIGN STRATEGIES FOR MITIGATING THE CONSEQUENCES OF LITHIUM FIRE WITHIN CONTAINMENT OF CONTROLLED THERMONUCLEAR REACTORS

by

D. A. Dube and M. S. Kazimi

DEPARTMENT OF NUCLEAR ENGINEERING
MASSACHUSETTS INSTITUTE OF TECHNOLOGY
Cambridge, Massachusetts 02139

July 1978

ANALYSIS OF DESIGN STRATEGIES FOR MITIGATING THE CONSEQUENCES OF LITHIUM FIRE WITHIN CONTAINMENT OF CONTROLLED THERMONUCLEAR REACTORS

by

D. A. Dube and M. S. Kazimi

Report Issued Under Contract EY-76-02-2431
U.S. Department of Energy

ABSTRACT

A lithium combustion model (LITFIRE) was developed to describe the physical and chemical processes which occur during a hypothetical lithium spill and fire. The model was used to study the effectiveness of various design strategies for mitigating the consequences of lithium fire, using the UWMAK-III features as a reference design. Calculations show that without any special fire protection measures, the containment may reach pressures of up to 32 psig when one coolant loop is spilled inside the reactor building. Temperatures as high as 2000 °F would also be experienced by some of the containment structures. These consequences were found to diminish greatly by the incorporation of a number of design strategies including initially subatmospheric containment pressures, enhanced structural surface heat removal capability, initially low oxygen concentrations, and active post-accident cooling of the containment gas. The EBTR modular design was found to limit the consequences of a lithium spill, and hence offers a potential safety advantage. Calculations of the maximum flame temperature resulting from lithium fire indicate that none of the radioactive first wall materials under consideration would vaporize, and only a few could possibly melt.

PUBLICATIONS UNDER CONTRACT EY-76-02-2431

1. R. Sawdye, J. A. Sefcik and M. S. Kazimi, "Reliability Requirements for Admissible Radiological Hazards from Fusion Reactors," Trans. Am. Nucl. Soc. 27, 65-66, November 1977.

2. M. S. Kazimi et al., "Aspects of Environmental and Safety Analysis of Fusion Reactors," MITNE-212, Dept. Nucl. Eng., M.I.T., October 1977.

3. D. Dube, M. S. Kazimi and L. M. Lidsky, "Thermal Response of Fusion Reactor Containment to Lithium Fire," Paper presented at Third Top. Meeting on Fusion Reactor Technology, Santa Fe, N.M., May 1978.

4. R. W. Sawdye and M. S. Kazimi, "Application of Probabilistic Consequence Analysis to the Assessment of Potential Radiological Hazards of Fusion Reactors," MITNE-220, Dept. Nucl. Eng., M.I.T., July 1978.

5. D. A. Dube and M. S. Kazimi, "Analysis of Design Strategies for Mitigating the Consequences of Lithium Fire within Containment of Controlled Thermonuclear Reactors," MITNE-219, Dept. Nucl. Eng., M.I.T., July 1978.

ACKNOWLEDGEMENTS

This report is based on a thesis submitted by the first author to M.I.T. in fullfillment of the requirements for the degree of Master of Science in Nuclear Engineering.

The authors would like to thank Lenny Andexler for his help with graphing, Robert Green for his help in getting the computer code SPOOL-FIRE working and Gail Jacobson for her patience and effort in getting this report typed.

TABLE OF CONTENTS

LIST OF FIGURES

LIST OF TABLES

I. INTRODUCTION

Development of controlled thermonuclear reactors (CTR) designs must include evaluation, elimination and/or minimization of the mechanisms for the release of large amounts of energy, and subsequent release of radioactivity to the environment. One such mechanism is the chemical reaction of liquid lithium with air or other gases resulting from a rupture of the lithium coolant piping or equipment. A possible consequence of liquid lithium fires is the overpressurization and rupture of the reactor containment. In addition, the high temperatures and pressures accompanying lithium fires can potentially provide the means for mobilizing a significant portion of the radioactive inventory, which includes the activated first wall and structures, and tritium.

Many fusion reactor designs use liquid lithium as coolant and breeding material because of its low melting point, high boiling point, low vapor pressure, low density, high heat capacity, high thermal conductivity, and low viscosity. Lithium requires less pumping power when flowing across magnetic field lines than most other liquid metals, and lithium is not activated to long-lived gamma emitting isotopes by neutron capture.[1]

However, liquid lithium reacts strongly in air, liberating about 3.7 times more energy on a weight basis than liquid sodium (which is itself being considered for use in the secondary loop). Lithium temperatures as high as 982°C will

be reached in some designs where a refractory metal or alloy is employed as structural material.[2]

Should a large amount of liquid lithium become exposed to air within the reactor containment building, there is a potential for release of substantial amounts of energy. (Examples of the energy sources and sinks in Tokamak reactors are given in Table 1.1). Furthermore, lithium may interact with the concrete floors or structures, releasing still more energy. The designer of the reactor containment must take such hypothetical accidents from lithium spills into consideration.

Examples of the CTR containment designs so far proposed are those of UWMAK-I, UWMAK-III, and EBTR reactors.

The UWMAK-I CTR design includes a double containment.[3] The inner primary containment is evacuated to a pressure of 1 Torr. It is designed to withstand an overpressure of 10 psig caused by liquid helium coolant leakage and vaporization. It would have a 0.5 in. steel liner to prevent lithium-concrete reactions should a spill occur. The UWMAK-III design utilizes a single containment of roughly one and one-half the free volume of UWMAK-I (8.85×10^6 ft.^{3} compared to 5.65×10^6 ft.^{3}). The containment atmosphere is an inert gas and the structure is lined with 0.25 in. steel plate. The design overpressure is 15 psig. The ELMO Bumby Torus Reactor reference design (EBTR)[4] has a much larger aspect ratio than the Tokamak-type fusion reactor designs and hence employs a primary containment similar to those used for large underground particle

TABLE 1.1

Energy and Heat Sources and Sinks in UWMAK-I and III

SOURCES	UWMAK-I	UWMAK-III
Superconducting magnets	350×10^9 J	Approximately same
Kinetic energy of plasma	3×10^9 J	Approximately same
Thermal energy of liquid lithium	32.5×10^9 J/% Li	15.8×10^9 J/% Li
Li-air reactions	$280\text{-}731 \times 10^9$ J/% Li	$65\text{-}170 \times 10^9$ J/% Li
Li-concrete reactions	1200×10^9 J/% Li	278×10^9 J/% Li
Thermal energy of gaseous helium*	$.34 \times 10^9$ J (from shield)	27×10^9 J (inner blanket)
SINKS		
Liquid helium*	84×10^9 J	same
Heat capacity of air*	61.1×10^6 J/°C	95.7×10^6 J/°C
Heat conduction through the concrete containment	$.8\text{-}1.0 \times 10^4 \frac{W}{°C} (T-T_{amb})$	$1.2 \times 10^4 \frac{W}{°C} (T-T_{amb})$
Heat capacity of containment structures	7.3×10^9 J/°C	9.8×10^9 J/°C

* Ambient is taken as zero-base in calculation of thermal energy

accelerators. EBTR is modularized into as many as 48 units, with each section containing 3.5×10^4 ft.^{3} of free volume. No provision has yet been made for partial evacuation of the containment.

Air could be introduced into an otherwise evacuated environment by a breach of the primary containment by a missle or seismic activity. In these cases it would be impossible to prevent leakage of air into the containment and the main concern would lie in minimizing lithium leakage and peak flame temperatures. Also, under some circumstances, it may be preferable to operate with an atmospheric environment. If an inert containment atmosphere were properly maintained, and the steel liner were effective in separating the lithium from concrete, a lithium spill by itself would pose little danger to the containment integrity.

Because the lithium would be contained in a multiplicity of parallel systems (12 for UWMAK-I, 18 for UWMAK-III, and up to 48 for EBTR), rupture of a single lithium system could not release more than a small fraction of the total lithium inventory. However, in absolute terms, this could amount to a large spill nonetheless (312,000 lbs. in UWMAK-I, 48,400 lbs. in UWMAK-III, and approximately 62,500 lbs. in EBTR). A spill of this size might cause large thermal stresses in the steel liner possibly causing it to buckle and allowing lithium to contact the concrete structure beneath. Lithium reacts readily with concrete giving off hydrogen, oxygen, carbon dioxide, and

water vapor. Release of these gases might further displace the liner, allowing still more leakage.

If a lithium spill occurs, the lithium's tritium inventory would be released into the containment atmosphere creating a radiation hazard. The lithium also contains activated blanket wall erosion and corrosion products. If a fire occurs it is possible that some products be volatilized and released into the containment atmosphere. The fire might also supply the energy needed to disrupt the first wall and other activated reactor structures. This radiological hazard combined with the very large potential energy release necessitates that we develop a detailed understanding of lithium fires and means of mitigating their consequences.

In this work, a lithium pool combustion model is developed to account for the reaction of liquid lithium with both oxygen and nitrogen. The model includes the effects from moisture in the atmosphere and subsequent hydrogen gas generation resulting from lithium-water reaction. Radiative and convective heat transfer from the combustion zone to the containment walls and to the cell gases are considered. Convective mass transport of oxygen and nitrogen, and diffusive lithium vapor transport to the zone are also included. The model also considers heat loss from the containment to the ambient, and heat absorption by internal structures.

The design strategies analyzed for mitigating the consequences of lithium fires include:

1) emergency space cooling of the containment atmosphere;

2) inert gas flooding of the containment;

3) containment ventilation;

4) surface cooling of the lihtium pool;

5) modularization of the reactor as employed in the EBTR design;

6) reduction of the initial concentration of oxygen within the containment;

7) reduction of the initial containment gas pressure;

8) employing structural materials with high heat capacities and thermal conductivities;

9) employing a multiplicity of parallel cooling systems;

10) the use of "catch pans," dump tanks, and chemical fire fighting methods.

II. COMBUSTION OF LIQUID LITHIUM

2.1 Thermochemical Considerations

The major safety concern when using liquid lithium as a fusion reactor coolant is its exothermic reaction with air as well as with the concrete containment should a lithium spill occur. Unlike sodium, liquid lithium also reacts exothermically with nitrogen gas at elevated temperatures. The reactions in air of greatest interest are:[1]

	ΔH°_{298} kcal/mole	ΔG°_{298} kcal/mole
$2\,Li(c) + \frac{1}{2}O_2 \rightarrow Li_2O(c)$	-142.75	-133.95
$2\,Li(c) + O_2 \rightarrow Li_2O_2(c)$	-151.9	-133.1
$Li(c) + \frac{1}{2}H_2 + \frac{1}{2}O_2 \rightarrow LiOH(c)$	-166.58	-105.68
$3\,Li(c) + \frac{1}{2}N_2(g) \rightarrow Li_3N(c)$	- 47.5	-37.3

where ΔH° is the change in enthalpy between the products and reactants (also known as the heat of formation), and ΔG° is the change in Gibbs free energy. Negative values of ΔH° indicate exothermic reactions. The zero superscript refers to enthalpy changes with respect to the standard state (1 atmosphere of pressure).

The heat of formation ΔH° is a function of reaction temperature as well. Most thermodynamic data give values of ΔH° at room temperature (298.15°K to be precise). However, one would expect the heat of formation at a given temperature ΔH°_T to more

accurately reflect the energy release for reactions which occur at temperatures other than 209.15°K. Table 2.1 gives the heats of formation and the change in Gibbs free energy of $Li_2O(c)$ and $Li_3N(c)$ for various temperatures.[5]

In any chemical situation the forward reaction may be expressed as

$$A + B \rightarrow C \tag{2.1}$$

while the reverse reaction may be expressed as

$$C \rightarrow A + B \tag{2.2}$$

At chemical equilibrium, one obtains the standard form

$$A + B \rightleftharpoons C \tag{2.3}$$

Large negative values of ΔG_T° indicate, in general, that the forward reaction goes nearly to completion, while large positive values of ΔG_T° indicate that the reverse reaction is preferred thermodynamically.

One can represent a chemical transformation for ideal gases, for example, by the equation

$$aA + bB \rightleftharpoons cC + dD, \tag{2.4}$$

where the lower-case letters represent the number of moles and the upper-case letters represent the reactants and products. One can then represent ΔG_T° mathematically by

$$\Delta G_T^\circ = -RT \ln K \tag{2.5}$$

TABLE 2.1

Heats of Formation and Changes in Gibbs Free Energy for $Li_3N(c)$ and $Li_2O(c)$*

TEMP (°K)	ΔH_T° (kcal/mole)		ΔG_T° (kcal/mole)	
	$Li_3N(c)$	$Li_2O(c)$	$Li_3N(c)$	$Li_2O(c)$
298	-47.2	-143.1	-36.8	-134.3
400	-47.4	-143.3	-33.3	-131.3
500	-49.8	-144.9	-29.5	-128.2
600	-49.9	-145.0	-25.4	-124.8
700	-49.7	-145.0	-21.3	-121.5
800	-49.2	-144.9	-17.3	-118.1
900	-48.7	-144.7	-13.3	-114.8
1000	-48.0	-144.5	- 9.5	-111.5
1100	-47.2	-144.1	- 5.7	-108.2
1500	-43.8	-142.5	+ 8.9	- 95.4

*Janaf Thermochemical Tables
(Dow Chemical Co., Midland, Mich., 1970)

where

$$K = \frac{[C]^c \ [D]^d}{[A]^a \ [B]^b} \tag{2.6}$$

and is called the thermodynamic equilibrium constant. R is the universal gas constant (1.987 cal/gm-mole °K) and T is the absolute temperature. The values in the brackets refer to the corresponding mole concentrations of the products, while the lower-case letters are exponents in the above expression for K. Hence, large negative values of ΔG°_T indicate relatively high concentrations of the products C and D, and the forward reaction more nearly goes to completion at chemical equilibrium.

Gibbs free energy can be represented more accurately by

$$G^\circ = H^\circ - TS^\circ \tag{2.7}$$

while the change in Gibbs free energy is represented by

$$\Delta G^\circ_T = \Delta H^\circ - T\Delta S^\circ \tag{2.8}$$

for infinitesimal changes under isothermal conditions. ΔS° represents the change in entropy for the reaction in the standard state. A more complete discussion of chemical thermodynamics for reactions involving liquids, solids, and changes in state is treated by Klotz[6] for example.

2.2 Lithium-Air Adiabatic Flame Temperature

Of primary concern in lithium fires is the peak flame temperature which can be achieved. To a large extent, this will

determine whether many radioactive species become airborne by vaporization or aerosol formation in fusion reactor accidents. The standard procedure is to assume a number of constraints on the lithium-air reaction to establish peak flame temperatures - in essence, 1) reactant stoichiometry, 2) chemical equilibrium between the product species, and 3) overall adiabatic conditions. In reality, one can expect significantly lower temperatures to be achieved because of radiative transfer and constraints on the reaction rates. These further constraints will be considered later. However, the present analysis does provide an absolute upper bound for the flame temperature, albeit a very conservative one.

The procedure used in determining chemical equilibrium is an established one and is treated especially well by Zeggeren and Storrey.[7] Briefly, the procedure involves the minimization of Gibbs free energy for all the reactants, products, and their concentrations under consideration. It is assumed that all of the energy released from the chemical reactions is used in heating the product species to the equilibrium temperature.

Gordon and McBride[8] have developed a special computer program, CEC 71, for calculating thermochemical values in rocket engines. This code, developed for NASA, and available at MIT under the name TRAN72, includes other options used in studying jet propulsion, but are not considered here. Thermochemical and physical data for some 62 reactants and 421 reaction species in liquid, solid, and gaseous states are included. The

input requires specifying the reactant concentrations (by weight or moles) and the initial enthalpies (or temperatures) of these reactants. The resulting output provides information on the product concentrations, equilibrium temperature, density, effective molecular weight, and so forth. Of greatest interest is of course the equilibrium temperature, but the product concentrations further provide information on which reactions are dominant.

Using this computer code, a number of cases were run under similar conditions except for reactant concentrations to note the contribution of the various reactants to the total energy release.

In case 1, it is assumed that a leakage of 16% of the total lithium inventory of UWMAK-III (about three coolant loops) has resulted and reacted with the volume of air within the containment. The reaction is assumed to occur with air at room temperature, 1 atmosphere of pressure, and 50% relative humidity. Case 2 was similar to case 1 but dry air was used instead. Case 3 considered only lithium, oxygen, and nitrogen as reactants. In case 4, only nitrogen and lithium were used as reactants. Table 2.2 summarizes the assumptions and the results of all four cases.

It is significant to note that the equilibrium temperature reached is quite insensitive to those reactants considered other than nitrogen and oxygen. Further analysis shows that in the presence of small concentrations of oxygen, the percen-

TABLE 2.2

Thermodynamic Results from Sample Calculations for Determining Adiabatic Flame Temperature.

		Case 1	Case 2	Case 3	Case 4
INPUT					
Reactants Considered and Mole Fractions	Li(l)	.45800	Similar	.468	.27
	N_2	.41000	but	.419	.73
	O_2	.11000	no H_2O	.113	-
	H_2O	.01862		-	-
	Ar	.00495		-	-
	CO_2	.00026		-	-
	H_2	.00005		-	-
OUTPUT					
Equilibrium °K Temperature		2498	2498	2500	1094
Energy Released (kcal/gm Li reacting)		10.4	10.4	10.4	2.3
Products resulting and mole fractions (greater than 1×10^{-5})	Ar	.00722	.00722	-	-
	Co	.00010	.00010	-	-
	Co_2	.00028	.00028	-	-
	Li	.08670	.08670	.08767	.00151
	LiO	.00767	.00767	.00778	-
	LiOH	.00014	.00014	-	-
	$Li_2(g)$	.00006	.00006	.00006	.00002
	$Li_2O(l)$	.11990	.11990	.12012	-
	Li_2O	.16524	.16524	.16703	-
	Li_2O_2	.00156	.00156	.00158	-
	NO	.00446	.00446	.00452	-
	N_2	.59579	.59579	.60024	.88433
	O	.00131	.00131	.00133	-
	O_2	.00957	.00957	.00968	-
	$Li_3N(s)$	-	-	-	.11414

tage of nitrogen which underwent reaction is very small. Several reasons can be given to account for this observation.

For one, the lithium-oxygen reaction is significantly more exothermic than the lithium-nitrogen reaction. Hence, one would assume that in establishing equilibrium, reaction with oxygen would be preferred over nitrogen. In addition, the change in Gibbs free energy for the reaction is greater for oxygen than nitrogen, indicating that the forward reaction with oxygen is carried to greater completion than with nitrogen. Although the heat of formation of Li_3N is fairly constant over a wide range of temperatures, the value of ΔG°_T increases significantly with temperature. At 298 °K, the value of ΔG°_T is -36.8 kcal/mole, while it increases to -17.3 kcal/mole at 800 °K and still higher to +8.9 kcal/mole at 1500 °K. This would indicate that the forward reaction of lithium-nitrogen at elevated temperatures is very slow. Note also that the melting point of Li_3N is 1123 °K so that Table 2.1 should not be used above this temperature.

Close examination of lithium-oxygen reaction, on the other hand, shows that for $Li_2O(c)$, ΔG° = -134.3 kcal/mole at 298 °K, -118.1 kcal/mole at 800 °K, and -95.4 kcal/mole at 1500 °K. Hence, the forward lithium-oxygen reaction is still very important at elevated temperatures. Indeed, these observations imply that liquid lithium-nitrogen reaction would be important at relatively low combustion temperatures of 400-500 °K, and unimportant in the regime of temperatures above 1000 °K.

However, the fact that lithium-nitrogen reactions are exothermic at all temperatures still means that nitrogen would be insufficient for the extinguishment of lithium fires.

Several other cases were investigated to determine the effects of the relative mole fraction of Li-to-air and Li-to-nitrogen on the final equilibrium temperature. Figures 2.1 and 2.2 illustrate this as well as the effect of the lithium release temperature on the final temperature. Calculations were made for lithium release temperatures of 1173 °K, 1000 °K, 800 °K, and 600 °K, but only the curves for 1173 °K and 600 °K are plotted. The peak flame temperature obtained for lithium fires in air is 2502 °K, while the peak flame temperature for Li in N_2 is 1315 °K. The value of 2502 °K compares quite closely with the value of 2400 °K obtained by Okrent et al.[9] It was also found that for environments of low oxygen concentration (4 and 8%), the peak flame temperatures were reduced significantly to 1580 °K and 1800 °K respectively at Li release temperatures of 1173 °K. Moreover, it was found that except for environments with low oxygen concentrations (<5% volume), lithium-nitrogen reactions were unimportant at chemical equilibrium.

This leads to the following conclusions:

1) The lithium-oxygen reactions predominate in atmospheric environments, while the lithium-nitrogen reactions are relatively unimportant except at very low concentrations of oxygen.

FIGURE 2.1

EQUILIBRIUM TEMPERATURE VS. LITHIUM TO AIR MOLE RATIO FOR TWO LI RELEASE TEMPERATURES

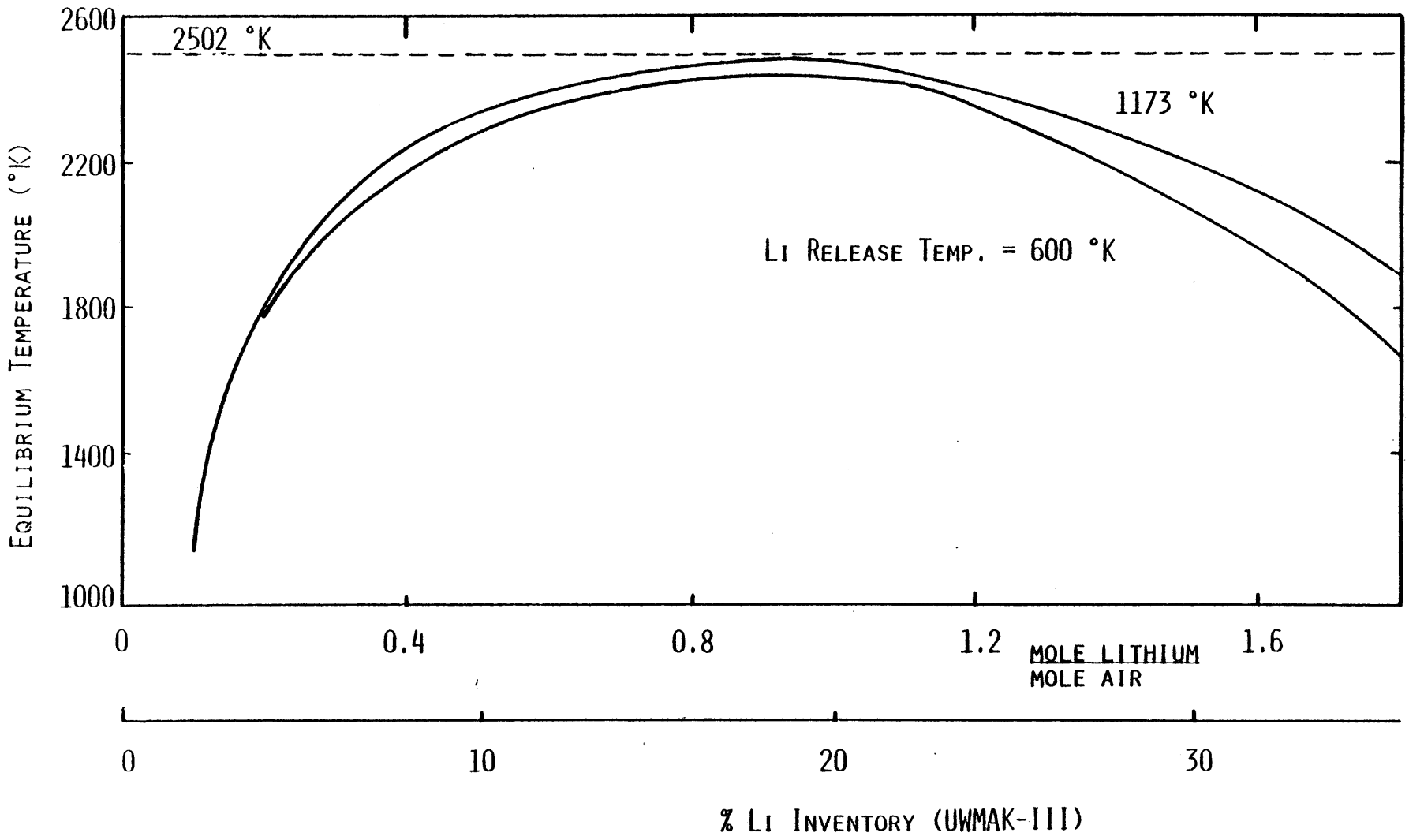

FIGURE 2.2
EQUILIBRIUM TEMPERATURE VS. LITHIUM TO NITROGEN MOLE RATIO FOR TWO LI RELEASE TEMPERATURES

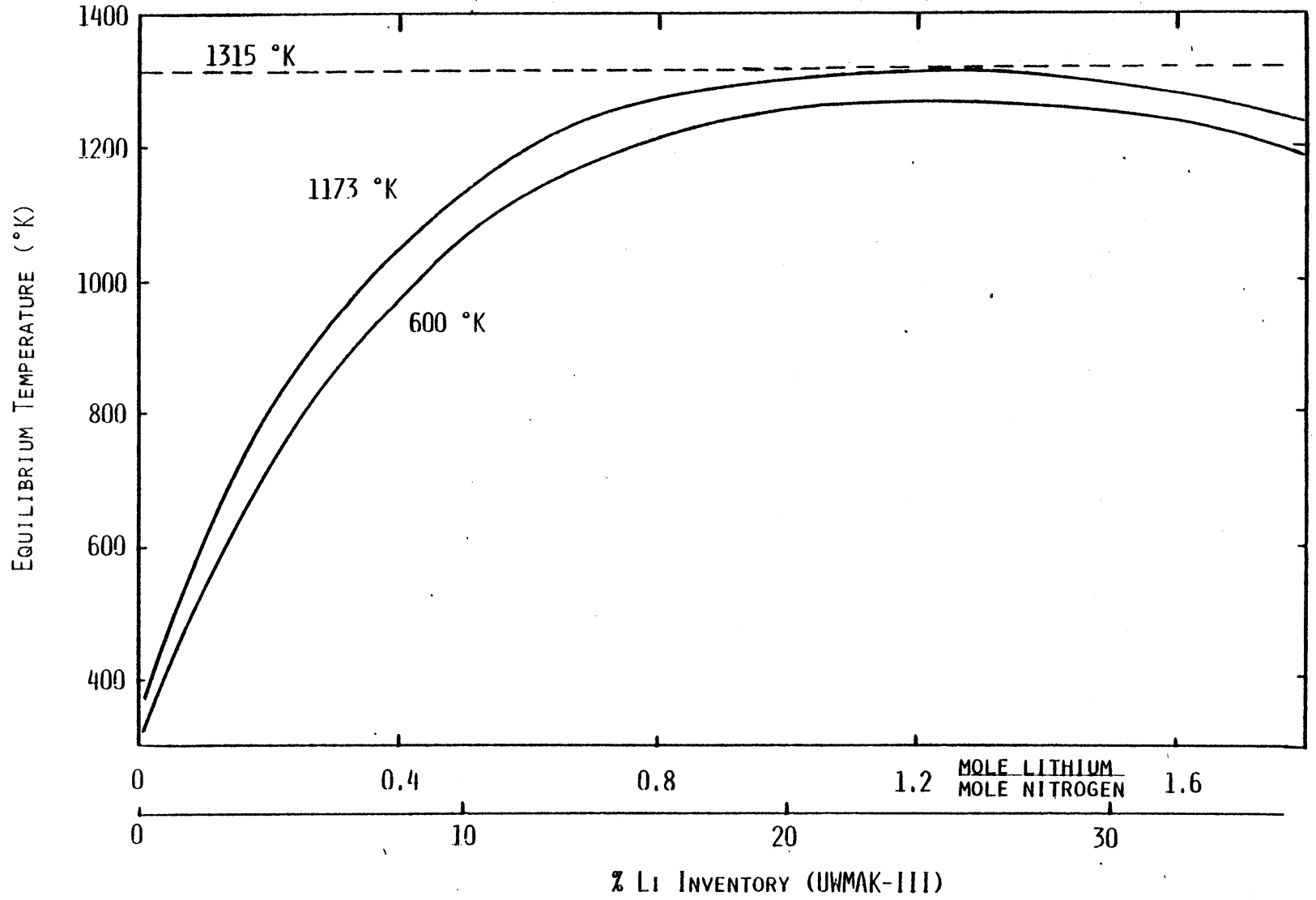

2) In an N_2 environment, lithium reacts exothermically with the nitrogen gas, although the forward reaction is constrained by thermodynamic considerations, resulting in peak flame temperatures which are significantly lower than those found in an air environment.

The first conclusion suggests that it is possible to model lithium-oxygen reactions in an atmospheric environment in much the same way as was done in several studies to sodium fires in LMFBRs.[10-13] This would make it possible to predict the temperature-pressure history of containment resulting from lithium fires. At lower oxygen concentrations, the model can be modified to account for lithium reactions with nitrogen.

Of considerable interest is the possible vaporization of reactor materials in the event of a lithium fire. Table 2.3 gives the melting points and some vaporization points for those metals considered likely to be used as first wall or as structural material. It can be seen that even at temperatures of 2502 °K (which is the highest peak flame temperature calculated from this investigation), none of the materials would vaporize, although several would melt. Further study would have to be made to determine if aerosol formation is significant at these temperatures when assessing the overall mobilization of radioactive species.

TABLE 2.3

Melting and Boiling Points of Some Metals
Being Considered as First Wall or Structural Materials

	M.P. (°K)	B.P. (°K)
Titanium	2000	3550
Molybdenum	2883	-
Zirconium	2125	3900
Aluminun	932	2600
Stainless Steel	>1700	>3000
Niobium	2760	5000
Vanadium	1890	3800

2.3 Experimental Observations

Most of the experimental research conducted on lithium reactions thus far have dealt with small scale quantities at low temperatures, and with lithium in the solid phase. Hence, there is a lack of information pertaining to large scale tests which would more accurately simulate accident conditions. A number of studies, however, describe at least qualitatively the reactions between liquid lithium and various gases.

Good reviews of lithium's properties and interactions are provided by Cowles and Pasternak[1] and Ballif *et al*.[14] At high temperatures, it is found that molten lithium reacts with all known molecular gases but can be handled up to 200 °C in paraffin vapors. Liquid lithium is considered inert in helium under most conditions. Trace amounts of moisture catalyze lithium-gas reactions. Liquid lithium will not react with oxygen or carbon dioxide in air at its melting point in the absence of water; but 10 to 15 parts-per-million moisture will cause lithium to react with air, nitrogen, oxygen, and carbon dioxide at room temperature.[1]

Actual reaction rates, products, and temperatures for lithium-air reactions are uncertain and contradictory. Values between 180 °C and 640 °C have been reported for the ignition temperature of lithium metal in air. The discrepancy is mainly due to purity and moisture conditions. However, information regarding liquid lithium-air reactions is lacking.[14]

In a stream of dry nitrogen, the reaction between lithium and nitrogen is 10 to 15 times more rapid than in air. Oxygen and hydrogen inhibit the interaction of lithium and nitrogen. The presence of oxygen in nitrogen greater than 14 volume % may completely prevent reaction at lower temperatures. With lesser amounts, the reaction proceeds much slower.[15] These findings are in general agreement with the conclusions drawn in section 2.2 involving liquid lithium-nitrogen reactions under conditions of moderate-to-high concentrations of oxygen and at chemical equilibrium.

The combustion of lithium is characterized by the emission of a dazzling actinic flame and the evolution of copius clouds of white irritating 'smoke'. Fires involving lithium are more intense than those in which an equivalent volume of sodium is burning. 'Wicking' action is very pronounced in lithium oxide sponge and the build-up of oxide deposits on containment walls permits the metal to migrate readily.[16] However, information on the aerosol properties of lithium reaction products is lacking.

When exposed to normal atmospheric conditions and heated to 600 °F, liquid lithium is found to ignite and give a maximum flame temperature, as measured 1 inch above the combustion vessel, of 1420 °F (1044 °K). Under conditions of varied relative humidity (40 to 55%) and wind velocity (0 to 30 ft/sec), the maximum temperatures are found to be in excess of 2000 °F (1367 °K).[16] As expected, these values are well below the

maximum adiabatic flame temperature of 2502 °K calculated in Section 2.2.

III. THE LITFIRE MODEL FOR LITHIUM COMBUSTION IN CTR CONTAINMENTS

3.1 Introduction

In the past few years several models have been developed to describe sodium fires in LMFBR containment buildings. Because of the similarity between most alkali metal fires, computer codes developed for analyzing liquid sodium fires in LMFBRs can potentially be modified to study liquid lithium fires. In particular, the SPRAY,[43-45] SOFIRE II,[12] CACECO,[13,46] and SPOOL-FIRE[10,47] codes have been considered for this study. With the exception of SPOOL-FIRE, the analytical modeling and recommended improvements in these codes have been reviewed by Sarma et al.[32,48] and Tsai et al.[49]

SPRAY utilizes a dynamic combustion zone model about a moving spray droplet to provide the time-temperature-pressure history of a spray fire. CACECO models a combined spray-pool fire within a four-cell containment. Heat and mass may be transferred between all cells and between each cell and the ambient exterior. Options include sodium-concrete reactions, water release from heated concrete, ventilation in and out of the containment, emergency space cooling and the effects of equipment heat sinks within the containment. SOFIRE II is a two cell pool fire code which models the containment heat transfer using the finite difference technique. SPOOL-FIRE is an adaptation of the SOFIRE II computer model combined

with a simple spray fire model first proposed by Humphreys.[51] Because of the simplicity of the computer code SPOOL-FIRE, this program is used as a stepping ground for the formulation of LITFIRE (an acronym for lithium fire) which describes the thermal response of fusion reactor containments to hypothetical lithium spills.

A number of major modifications have been made to SPOOL-FIRE to more accurately account for the physical and chemical processes occurring in lithium pool fires. These modifications include:

1) the inclusion of a model for lithium-nitrogen reaction;

2) consideration of lithium-water vapor reactions and subsequent release of hydrogen;

3) the inclusion of a "combustion zone" model in pool fires;

4) the inclusion of a model for describing the effect of aerosols in the containment on radiation heat transfer.

In addition, a number of options have been included for mitigating the consequences of lithium pool fires. These design strategies are examined in greater detail in Chapter IV. A flow diagram of the LITFIRE program for finding the thermal response of CTR containments to lithium fires is shown in Figure 3.1. A complete listing of LITFIRE is given in Appendix A, and samples of the input and output are shown in Appendices B and C.

FIGURE 3.1

FLOW DIAGRAM OF THE LITFIRE PROGRAM

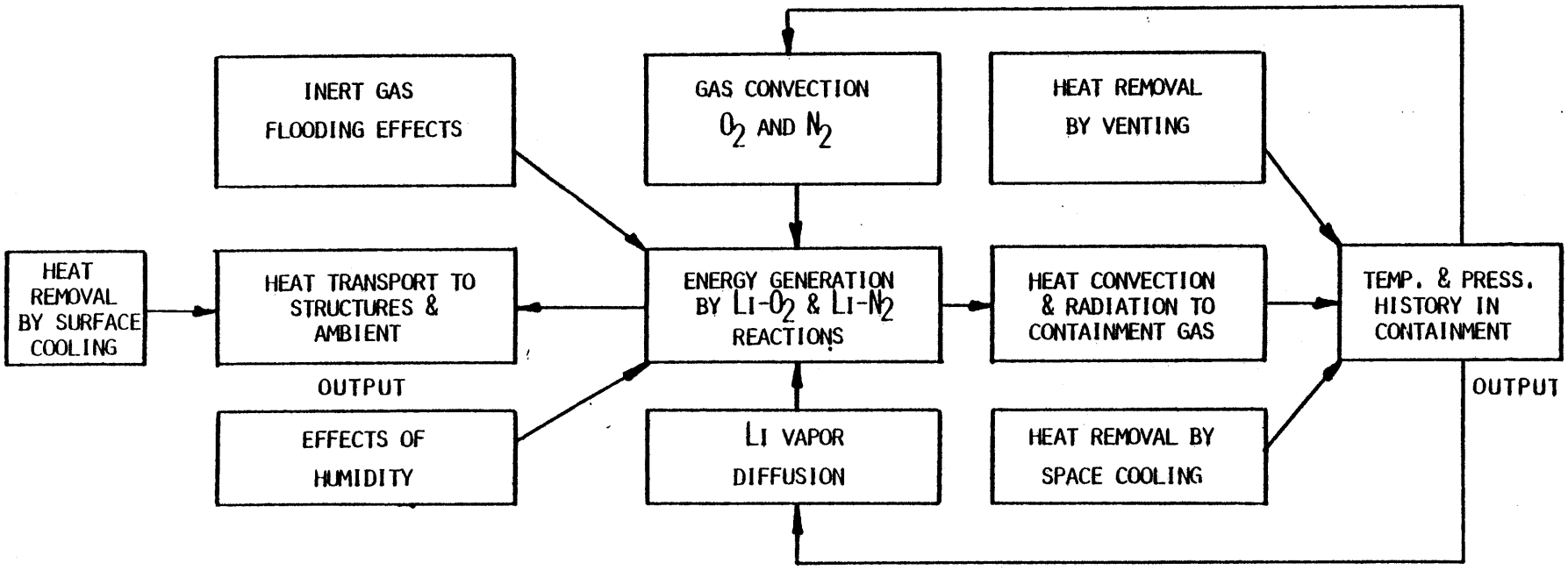

In LITFIRE, combustion occurs in a "combustion zone" separated from and slightly above the pool surface. Lithium is carried to the zone by vaporization. Oxygen and nitrogen are carried by convection and diffusion through a thin boundary layer. Under quasi-steady state conditions of pool combustion, convection of oxygen and other reactive gases to the pool surface is the limiting effect on the combustion rate. The heat of combustion is transferred to the pool surface by radiation and conduction, and to the containment gas and structures by convection and radiation. Figures 3.2 and 3.3 illustrate the heat and mass flow diagrams for the combustion zone, lithium pool, containment gas, and containment structures.

Although very little research has been done in the area of liquid lithium pool fires, a number of analytical and experimental studies for pool and tank fires of hydrocarbons support the above picture.[18-25] Huber et al.[29] further suggest the existence of such a combustion zone for liquid sodium fires.

The lithium pool combustion model developed herein is thus an extension of the models used in describing hydrocarbon fires and represents a first attempt at describing liquid metal fires at the pool surface - containment atmosphere interface.

3.2 Major Assumptions of the Combustion Model

The major assumptions made in the combustion model

FIGURE 3.2

HEAT FLOW DIAGRAM FOR LITHIUM POOL COMBUSTION IN CTR CONTAINMENT

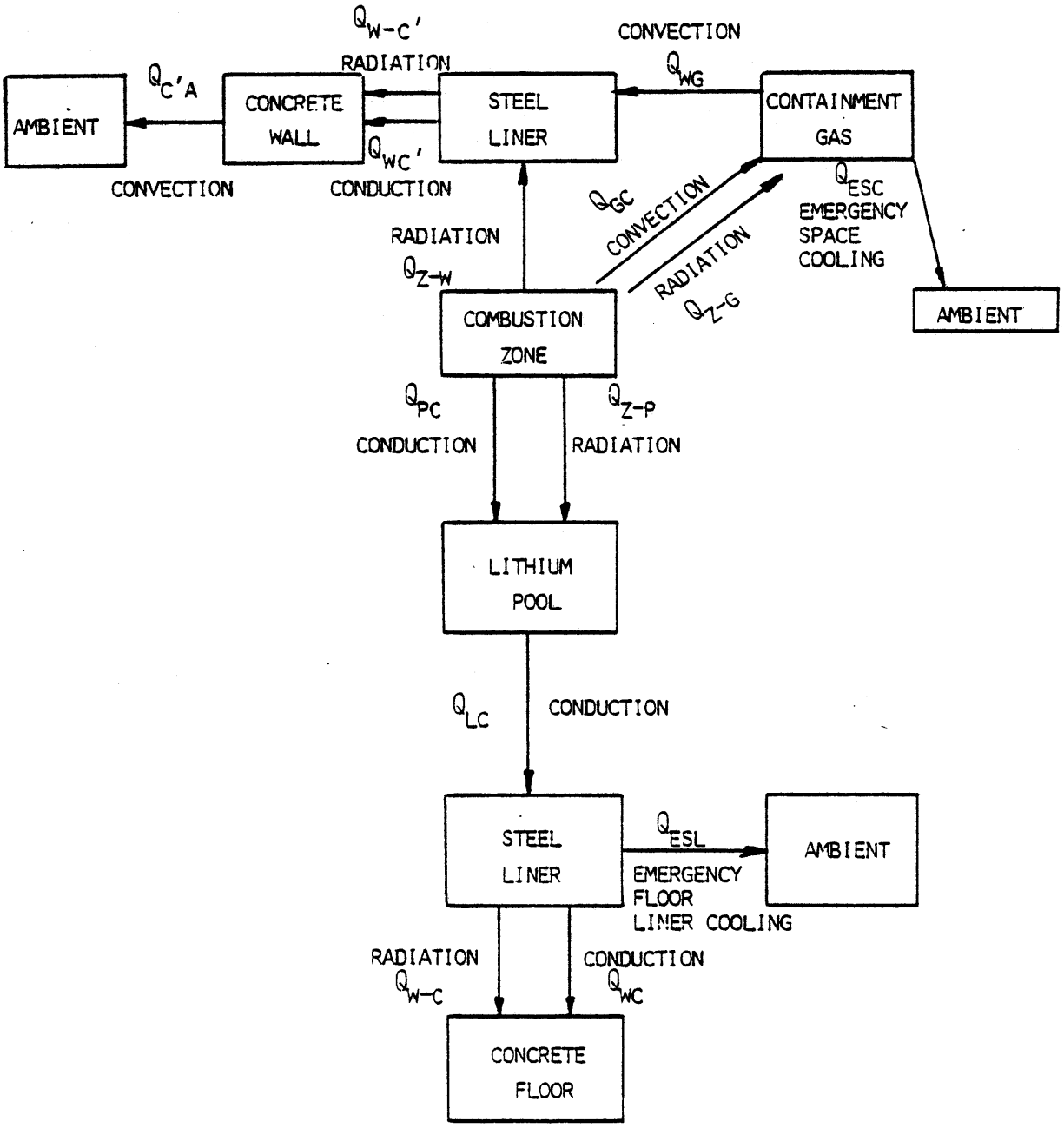

FIGURE 3.3

MASS FLOW DIAGRAM FOR LITHIUM POOL COMBUSTION IN CTR CONTAINMENT

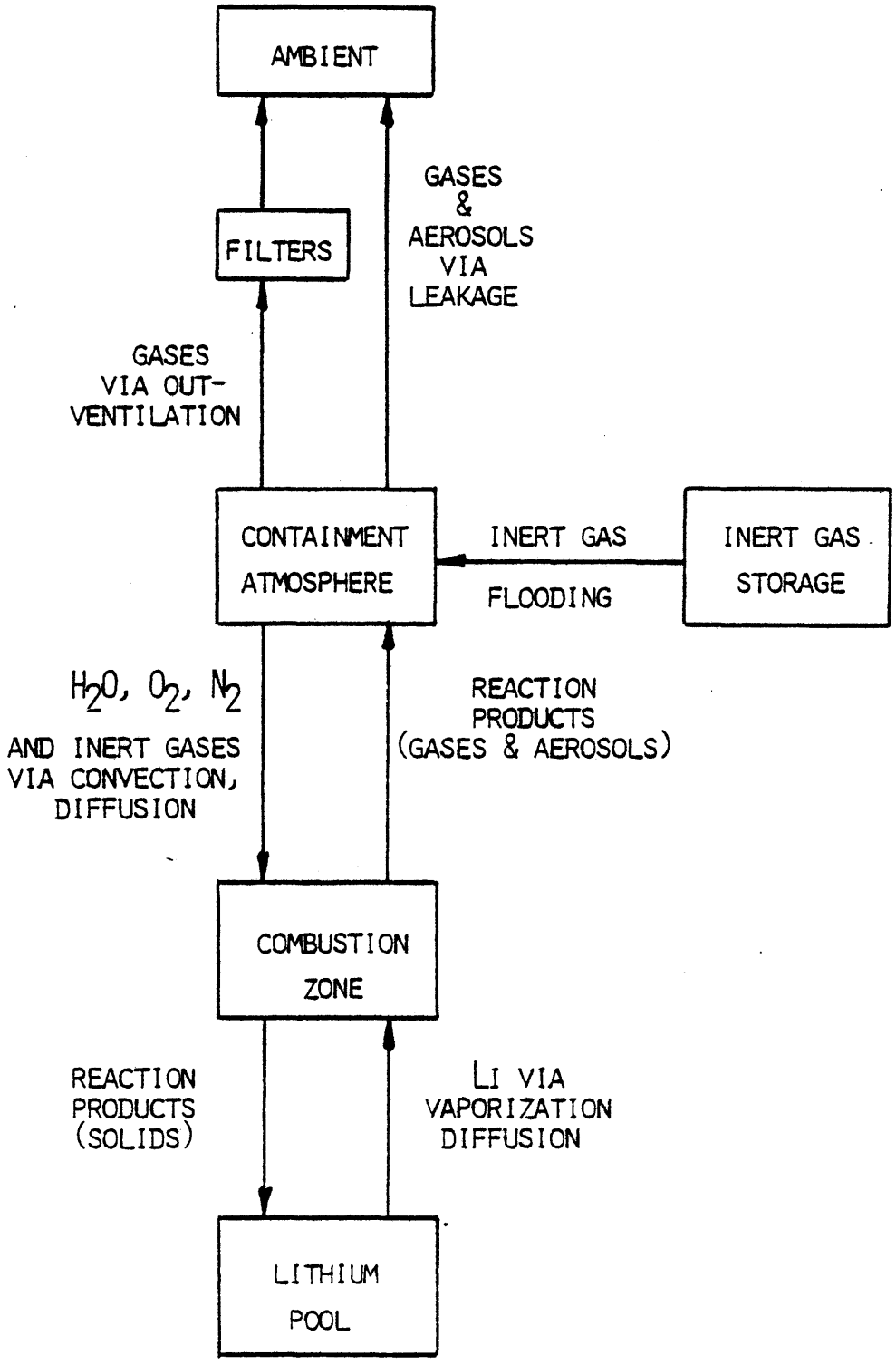

for lithium pool fires within CTR containments include the following:

1) The lithium pool is assumed to be of uniform thickness and temperature throughout the designated spill area on the containment floor.

2) The combustion zone is separated from the pool surface and is uniform in temperature.

3) Lithium combustion occurs in the vapor phase in the combustion zone, and practically all of the chemical energy released is transported to the containment walls, gas, and floor as thermal energy. The sensible heat addition to the combustion zone is negligible in comparison to other heat transfer mechanisms.

4) The containment atmosphere is assumed to be uniform in temperature and well-mixed.

5) Mass transport of oxygen and other reactive gases to the combustion zone limits the combustion rate of liquid lithium. The reaction of liquid lithium with oxygen and water vapor is assumed complete, whereas the reaction rate of nitrogen is dependent on reaction temperatures and oxygen concentrations.

6) A fraction of the reaction products is released into the containment gas as aerosols of uniform size and density. The concentration of aerosols in the gas

is also uniform and increases as the fire progresses.

7) The integrity of the containment wall and floor steel liners is maintained throughout the accident. The temperature history of the steel liners resulting from hypothetical accidents considered in this study can be used for assuring an adequate safety margin in the design of the containment structures.

8) The combustion zone is terminated when liquid lithium is cooled to below its ignition temperature, or when oxygen and nitrogen have been exhausted from the containment atmosphere.

3.3 Heat Transfer Mechanisms

3.3.1 Heat Conduction from the Combustion Zone to the Pool Surface

As suggested by Hottel,[18] the heat flux to the liquid surface that provides evaporation to feed the flame in a combustion zone is the sum of conductive, convective, and radiative terms. Convection is an edge effect in the pools of small tanks, and it is important only at the smallest diameters (on the order of 10 cm). In small hydrocarbon pool fires, it was observed that many flames sweep back and forth across the liquid surface at this diameter, thus accounting for the convection effect. In large pool fires on the order of several tens of meters in diameter, the convection effect becomes negligible.[23] The primary heat transfer mechanisms between the combustion zone and pool are thus

radiation and conduction.

Heat conduction from the combustion zone to the pool surface arises from the presence of air, lithium vapor, and other gases in this space. In general, one would expect heat conduction to be a small fraction of total heat transfer from flame to pool because of the high temperature of the flame. The heat conduction term can be expressed as:

$$Q_{pc} = k_f A_p (T_z - T_L)/d \qquad (3.1)$$

where k_f = thermal conductivity of the gaseous film

A_p = liquid lithium pool surface area

T_z = combustion zone temperature

T_L = liquid lithium temperature

d = separation distance between combustion zone and pool surface

The thermal conductivity of the gases is a function of pressure and temperature. Because of the rather low vapor pressure of lithium over the temperature range of interest (less than 0.07 atm. for lithium temperatures below 1300 °K), and because of the low concentrations of oxygen, the thermal conductivity can be given as a function of temperature and pressure of nitrogen gas in the film between the pool surface and combustion zone temperatures, while the film pressure is equal to the containment gas pressure.

The separation distance between the zone and pool is determined by conditions of the fire itself. Under quasi-steady state conditions, the diffusion of lithium to the

combustion zone is controlled by its reaction with other reactants. Fick's Law gives:

$$\dot{M}_L = -D_L \frac{\Delta\rho}{d} \tag{3.2}$$

where $\dot{M}_L$ = mass flow rate of lithium to the combustion zone

D_L = diffusion coefficient of lithium in air

$\Delta\rho$ = difference in concentration of lithium at the pool surface (determined by lithium's vapor pressure) and concentration in combustion zone (assumed zero).

Rearrangement of 3.2 gives the solution for d. Hence, the separation distance is a function of several important parameters. The required mass transfer expressions will be considered in greater detail in section 3.4.

3.3.2 Heat Convection from the Combustion Zone to the Containment Atmosphere

The convection of heat from the combustion zone to the gas occurs according to:

$$Q_{gc} = h_c A_p (T_z - T_g) \tag{3.3}$$

where h_c is the heat transfer coefficient between the combustion zone and the containment gas, and T_g is the containment gas temperature. The gas is assumed to be well mixed and isothermal throughout the containment for the application of the above expression.

Little research has been done for turbulent natural convection from diffusion flames. The most widely accepted correlation for the heat transfer coefficient, h_c, was derived

by Fishender and Saunders[30] for free convection from isothermal horizontal plates. The expression is written as

$$\overline{Nu} = 0.14\ (Gr \cdot Pr)^{1/3} \tag{3.4}$$

where $\overline{Nu}$ is the average Nusselt number and is related to the average heat transfer coefficient $\bar{h}_c$ by:

$$\overline{Nu} = \frac{\bar{h}_c\ L}{k} \tag{3.5}$$

Gr and Pr are the Grashof and Prandtl numbers, while L is the characteristic length of the square plate. Equation 3.4 necessarily applies to horizontal plates with the heated surface facing upwards and for flows in the turbulent regime, i.e.

$$2 \times 10^7 \leq Gr \cdot Pr \leq 3 \times 10^{10} \tag{3.6}$$

For natural convection inside spherical containments, Kreith[31] recommends using the expression

$$\overline{Nu} = 0.13\ (Gr \cdot Pr)^{1/3} \tag{3.7}$$

$$\text{for} \qquad 10^9 \leq Gr \cdot Pr \leq 10^{12} \tag{3.8}$$

where heat transfer is assumed to occur between the internal gas and the isothermal walls of the containment. However, Sarma et al. has found that in an attempt to model and analyze several sodium pool fires conducted by Atomics

International, the coefficient 0.14 in equation 3.4 was in some instances too high by almost a factor of two. In low O_2 environments (<2% O_2 by volume), Sarma found that the coefficient 0.14 was adequate. However, in high oxygen environments it was necessary to reduce the value of the leading coefficient in the empirical correlation used to determine the heat transfer (and analogous mass transfer) of oxygen from 0.14 to 0.075. Both SOFIRE II[36] and CACECO[13] use the coefficient of 0.14 in the Fishender and Saunders expression.

Several experimental investigations have been made for natural convection heat transfer for fluids confined by two horizontal plates and heated from below.[33-35] Specifically, Jakob in his analysis of the data of Mull and Reiher on air gives the relationship

$$\overline{Nu} = 0.068\ (Gr)^{1/3} \tag{3.9}$$

which, for Prandtl numbers of 0.71 for air, differs from equation 3.4 by a factor of two. Similarly, Globe and Dropkin obtained the expression

$$\overline{Nu} = 0.060\ (Gr)^{1/3} \tag{3.10}$$

for air. Malkus, basing his relationship on the data of water and acetone at room temperature, proposed the expression

$$\overline{Nu} = 0.085\ (Ra)^{0.325} \tag{3.11}$$

where

$$Ra = Pr \cdot Gr \tag{3.12}$$

These investigations suggest that the heat and mass transfer coefficients used by SOFIRE II and CACECO may be high by a

factor of two.

Torrance et al.[58-59] have performed experimental and analytical studies of natural convection in enclosures with localized heating from below. For Grashof numbers in the laminar region

$$4 \times 10^7 \leq Gr \leq 4 \times 10^8 \tag{3.13}$$

where

$$Gr = \frac{g\beta\Delta T L^3}{\nu^2} \tag{3.14}$$

and

L = characteristic length of heated region

β = coefficient of gas expansion

ν = kinematic viscosity

g = gravitational acceleration constant

ΔT = temperature difference getween heated region and gas

they theoretically predicted

$$\overline{Nu} = 0.02\ (Gr)^{1/2} \tag{3.15}$$

with an assumed Pr = 0.71. However, a better empirical curve fit for the available data in this region, derived by this author, gives

$$\overline{Nu} = 0.21\ (Gr)^{1/3} \pm 25\% \tag{3.16}$$

The onset of turbulence occurred for $Gr \geq 1.2 \times 10^9$. In liquid metal fires of the kind predicted in this study, Grashof

numbers on the order of 10^{12} to 10^{15} are predicted and so the applicability of the above correlation is doubtful.

Kanury[25] has used the experimental results of steady turbulent, free-convective diffusional burning of various polymers to model heat and mass transfer to and from horizontal circular pools. A simple one-dimensional diffusion flame theory is used to correlate mass transfer rates, history of burning, and radiant-emission rates. The combustion of fuel is assumed to occur in an extremely thin flame sheet or combustion zone. The flame sheet is assumed to radiate as an optically thick body at a temperature T_z. Kanury uses the Fishender-Saunders correlation for heat (and mass transfer) from the combustion zone to the ambient, i.e.

$$\overline{Nu} = 0.14\ (Gr \cdot Pr)^{1/3} \tag{3.4}$$

Whereas SOFIRE II and CACECO use ΔT as the temperature difference between the gas and pool surface, Kanury suggests

$$\Delta T = T_z - T_g \tag{3.17}$$

where T_z = combustion zone temperature

T_g = well-mixed, isothermal containment gas temperature

Hence, equation 3.4 is used in the correlation of convective heat transfer for this study, with the acknowledgement that the leading coefficient may be too high by a factor of two,

or too low by 50% with regards to values determined in the literature. The heat convection is thus expressed as:

$$Q_{gc} = A_p \, k \left(\frac{g\beta}{\nu^2}\right)^{1/3} Pr^{1/3} \, (T_z - T_g)^{4/3} \qquad (3.18)$$

3.3.3 Thermal Radiation from the Combustion Zone

As reported by Bulmer,[16] the combustion of lithium is characterized by the emission of a dazzling actinic flame and the evolution of copious clouds of white irritating "smoke". For such luminous flames, it is possible to approximate the flames as gray bodies with high thermal emissivities.[24] Hence, the lithium pool surface becomes "invisible" to the containment gas and walls during combustion, and vice versa.

An equivalent "circuit" for radiation heat exchange between the lithium pool surface, cell gas, containment walls, and combustion zone is shown in Figure 3.4. The net radiation exchange between any two gray surfaces 1 and 2 is described by

$$Q_{1-2} = f \, A_1 \, \sigma \, (T_1^4 - T_2^4) \qquad \text{BTU/sec} \qquad (3.19)$$

where σ = Stephen - Boltzman constant

A_1 = area of surface 1

f = radiation interchange factor between surfaces 1 and 2 based on surface area A_1

FIGURE 3.4

EQUIVALENT CIRCUIT FOR RADIATION HEAT EXCHANGE BETWEEN LITHIUM POOL SURFACE, CELL GAS, COMBUSTION ZONE, AND CONTAINMENT WALLS

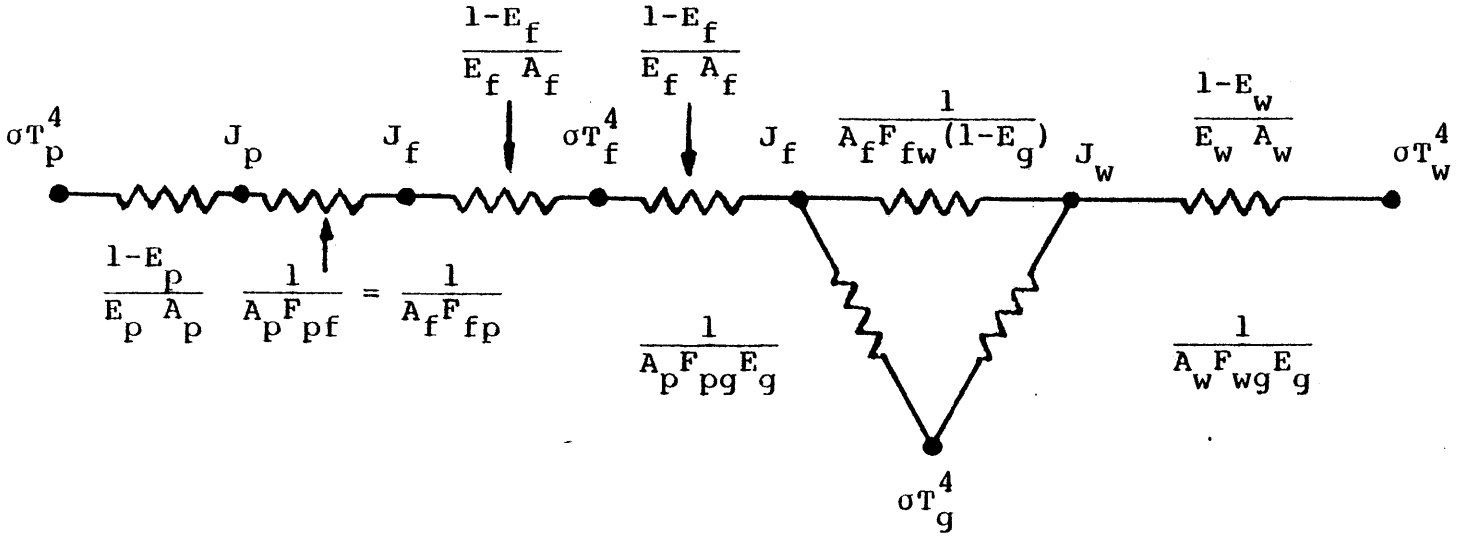

The value of f is determined by the thermal emissivities of the two surfaces and the view factor between the two. Note that the view factors and areas between the two surfaces can be expressed as

$$A_1 F_{12} = A_2 F_{21} \tag{3.20}$$

By circuit reduction,[31] the heat transfer from the combustion zone to the pool is given by

$$Q_{z-p} = \frac{A_p \sigma (T_z^4 - T_p^4)}{\frac{1}{E_p} + \frac{1}{E_z} - 1} \tag{3.21}$$

where $A_p = A_z$, and the pool and combustion zone are considered to be two infinitely large parallel plates because of their relatively small separation distances. Hence,

$$F_{12} = F_{21} = 1 \tag{3.22}$$

E_p and E_z are the thermal emissivities of the lithium pool and combustion zone respectively.

Likewise, the heat transfer form the combustion zone to the walls can be given by

$$Q_{z-w} = \frac{A_p \sigma (T_z^4 - T_w^4)}{\frac{1-E_z}{E_z} + \frac{1-E_w}{E_w}\frac{A_p}{A_w} + \left[F_{zw}(1-E_g) + \left(\frac{1}{F_{zg}E_g} + \frac{A_p}{A_w F_{fg} E_g} \right)^{-1} \right]^{-1}} \tag{3.23}$$

where E_z, E_w and E_g are the thermal emissivities of the combustion zone, containment wall, and containment gas respectively; A_p and A_w are the pool and wall areas; and F_{zw}, F_{zg}, and F_{wg} are corresponding view factors between the combustion zone, containment wall, and containment gas. For radiation from the containment zone in such enclosures, the following relation holds:

$$F_{zw} = F_{wg} = F_{zg} = 1 \tag{3.24}$$

Similarly, the radiation from the combustion to the gas can be expressed as:

$$Q_{z-g} = \frac{A_p \sigma (T_z^4 - T_g^4)}{\frac{1-E_z}{E_z} + \frac{1}{E_g}} \tag{3.25}$$

Between the steel wall liner and the concrete wall lies a gap of approximately 0.025 inches. Because of the low thermal conductivity of air within this gap, thermal radiation between the steel liner and concrete floor is an important heat transfer mechanism. This thermal radiation can be expressed as:

$$Q_{w-c} = \frac{A_w \sigma (T_w^4 - T_c^4)}{\frac{1}{E_w} + \frac{1}{E_c} - 1} \tag{3.26}$$

where A_w is the containment wall area. A similar expression describes thermal radiation from the steel floor liner to the

concrete below. The thermal emissivities of concrete and carbon-steel lie in the range 0.85 to 0.94, while that of liquid lithium lies in the range of 0.1 to 0.3. The emissivity of the combustion zone is in the range of 0.5 to 0.9.[40]

The thermal emissivity of the containment gas is a function of the aerosol concentration resulting from lithium combustion. In most sodium fire codes such as SOFIRE II, there is no modelling of this change in emissivity with time. Rather, the value of the thermal emissivity, or "view factor," is changed at some point in time to more nearly fit experimental observation. In this study, the suggestion of Blackshear[24] is used for changing the gas emissivity with aerosol concentration and time, i.e.

$$E_g = 1 - \exp(-C\ A_a\ L/4) \qquad (3.27)$$

where C = aerosol concentration (particles/ft^3)

A_a = aerosol particle surface area

L = optical path length

The path length is taken to be the distance from the floor of the containment to the containment walls. The aerosol concentration and surface area are dependent on the mean aerosol particle radium for lithium products.

3.3.4 Heats of Combustion for Lithium Reactions

Liquid lithium reacts exothermically with both oxygen and nitrogen. The presence of moisture further encourages the ignition of lithium.[14] The heats of combustion for lithium

reaction with oxygen, nitrogen, and water are approximately constant over a wide range of temperatures. Although the formation of Li_2O_2 releases 152 kcal. per mole of product, this reaction of lithium with oxygen is not important because of the instability of the peroxide above 250 °C. The heats of combustion can be summarized as follows:

$$Q_o = \text{lithium-oxygen heat of combustion} = 18{,}510 \text{ BTU/lb. Li} \tag{3.28}$$

$$Q_n = \text{lithium-nitrogen heat of combustion} = 4080 \text{ BTU/lb. Li} \tag{3.29}$$

$$Q_w = \text{lithium-water heat of combustion} = 13{,}784 \text{ BTU/lb. Li} \tag{3.30}$$

If R_o, R_n, and R_w represent the combustion rates of lithium with oxygen, nitrogen, and water respectively in terms of lb. Li/sec/ft^2, then the total heat generation rate inside the combustion zone can be given by:

$$Q = A_p[Q_oR_o + Q_nR_n + Q_wR_w] \text{ BTU/sec} \tag{3.31}$$

3.3.5 Sensible Heat Addition to the Reaction Products and Reactants in the Combustion Zone

A portion of the heat of combustion is used to heat the reaction products and reactants to the combustion zone temperature T_z. This can be written as:

$$Q_s = \sum_i \dot{m}_i c_i (T_L - T_i) + \sum_j \dot{m}_j c_j (T_z - T_L) \frac{\text{BTU}}{\text{sec}} \tag{3.32}$$

where $\dot{m}_i$ = mass flow rate of reactant i

c_i = specific heat of reactant i

T_L = lithium pool temperature

T_i = original temperature of reactant i

$\dot{m}_j$ = mass flow rate of product j

c_j = specific heat of product j

T_z = combustion zone temperature

In this expression, it is assumed that the reactants N_2, O_2, and H_2O are raised from their original temperature T_g to the temperature of the lithium surface T_L. Because of the high thermal conductivity of liquid lithium and the expected small thickness of the pool in practical considerations, it is assumed that the lithium pool has a uniform temperature with depth. The lithium vapor is also at the pool temperature.

The subsequent reaction between lithium vapor and the other reactants then occurs at temperature T_L. The reaction products and unreacted gases are then raised to the temperature of the combustion zone T_z. In this model, it is assumed that complete combustion occurs between lithium and the other reactants, i.e. all of the lithium is consumed. In reality, a small fraction of lithium will not react according to thermodynamic considerations. However, because of the large value of $|\Delta G^\circ_T|$ for the Li - O_2 reaction, the assumption that combustion is complete is reasonable. Likewise, reaction of lithium with water is assumed to go to completion. For Li - N_2 reaction, this formulation does not necessarily hold and corrections

must be made as will be shown later in section 3.4.3.

3.3.6 Combustion Zone Heat Balance

The production of heat from lithium combustion in the burning zone is balanced by the removal of heat by various heat transfer mechanisms. The basic heat balance equation can be expressed as

$$Q + Q_v = Q_{pc} + Q_{gc} + Q_{z-p} + Q_{z-w} + Q_s \quad \text{BTU/sec} \qquad (3.33)$$

The Q_v term represents the heat of vaporization of liquid lithium. This term is necessary because the heats of combustion in expressions 3.28 - 3.30 are based on liquid lithium combustion, whereas the combustion model in this study assumes vapor-phase reaction of lithium with other gases. In the overall heat balance equation for the lithium pool, the Q_v term represents a loss of energy from the pool. Under the assumed conditions of lithium pool fires observed in Rodgers and Everson,[17] the radiation terms Q_{z-p}, Q_{z-w}, and Q_{z-g} dominate the right side of equation 3.33 because of the high combustion zone temperatures and fourth power dependence of radiation.

3.4 Mass Transport Mechanisms

3.4.1 Mass Transfer of Oxygen, Nitrogen, and Water Vapor

In the combustion model developed, the fire resulting from Li-air reactions is assumed to induce gas free convective flow, and hence the fluid mechanical characteristics are governed by the Grashof number Gr. It is assumed that the

viscosity ν and the coefficient of gas expansion β in equation 3.14 are independent of containment pressure, but depend greatly on the cell gas temperature.

It is further assumed that chemical reactions between lithium and oxygen occur infinitely fast in the combustion zone where the fuel vapor and oxygen combine stoichiometrically. The partial pressure of lithium vapor and oxygen are assumed to be zero in this combustion zone. The air side of this combustion zone is comprised of gases i.e. nitrogen, oxygen, water vapor, and inert gases, while the fuel-side is comprised of fuel vapor, inert gases, and unreacted nitrogen.

Oxygen and nitrogen are carried to the combustion zone by natural convection, and mass transport at the combustion zone occurs by molecular diffusion through a boundary layer. In the case of sodium fires, Huber et al.[29] assume that the reaction rate is mainly determined by diffusion of oxygen through a boundary layer of nitrogen. Using calculated diffusion coefficients and experimentally determined reaction rates, they were able to estimate the diffusion layer thickness above the combustion zone. Under various conditions of combustion, the diffusion layer thickness is found to be less than 5 mm.

Bulk mass transfer can be expressed using the mass transfer - heat transfer analogy (Reynold's analogy). Such an analogy is valid when the Schmidt number Sc ($\equiv \nu/D$) and the Prandtl number Pr ($\equiv C_p \rho \nu/k$) are both approximately equal to one. In such instances, the Lewis relation[37] necessarily holds

with

$$D \simeq a \tag{3.34}$$

where D = mass diffusivity (ft^2/hr)

a = thermal diffusivity $\equiv k/C_p\rho$

For oxygen in air, Eckert and Drake[37] give:

$$D(ft^2/sec) = 1.46 \times 10^{-4} P^{-1} (T/460)^{1.81} \tag{3.35}$$

where P is the gas pressure in atmospheres and T the absolute temperature in degrees Rankine. Using the formulation developed by Chen and Othmer[38] for determining mass diffusivities of binary gas mixtures, one obtains

$$D(N_2 \text{ in air}) \simeq 0.98\, D(O_2 \text{ in air}) \tag{3.36}$$

The values of a are obtained from Kreith.[31] Table 3.1 gives values of D and a for oxygen and nitrogen in air. The close agreement of the values for D and a indicate that the assumption is valid. Hence, under such conditions one obtains:

$$h_m = \frac{h_c}{C_p} \quad \frac{\text{lb.}}{\text{hr.} - \text{ft}^2 - {}^\circ\text{F}} \tag{3.37}$$

where h_c = heat transfer coefficient for natural convection

C_p = specific heat of gas

h_m = mass transfer coefficient

TABLE 3.1

Values of D (Mass Diffusivity) and of a (Thermal Diffusivity) for Oxygen and Nitrogen in Air as Functions of Temperature*

	O_2 in air.		N_2 in air	
T	D	a	D	a
(°F)	(ft^2/sec)	(ft^2/sec)	(ft^2/sec)	(ft^2/sec)
0	1.46×10^{-4}	1.74×10^{-4}	1.43×10^{-4}	1.76×10^{-4}
100	2.08×10^{-4}	2.44×10^{-4}	2.04×10^{-4}	2.49×10^{-4}
500	5.48×10^{-4}	6.57×10^{-4}	5.38×10^{-4}	6.36×10^{-4}
1000	11.67×10^{-4}	13.13×10^{-4}	11.46×10^{-4}	12.92×10^{-4}
1500	19.84×10^{-4}	21.88×10^{-4}	19.49×10^{-4}	21.05×10^{-4}
2000	29.80×10^{-4}	31.05×10^{-4}	29.27×10^{-4}	28.33×10^{-4}

*Values of a obtained from Kreith, Reference 31.

Oxygen, nitrogen, and water vapor are transported to the combustion zone by diffusion through the boundary layer arising from concentration gradients. Fick's law, given by equation 3.2, can be used for describing this mass transfer mechanism. Under quasi-steady state conditions of combustion considered here, the assumption that bulk transport of the gas to the combustion zone limits the burning rate is a conservative one. Future research should concentrate on removing some of this conservatism through a better understanding of the physical processes by which oxygen and nitrogen are transported to the combustion zone in large pool fires.

3.4.2 Lithium Mass Transport to the Combustion Zone

Lithium vapor is transported to the combustion zone by diffusion through the gas layer (composed mainly of inert gases) between the pool surface and the combustion zone. The heat of vaporization is supplied by heat transfer from the combustion zone to the pool surface. Because of the high thermal conductivity of lithium, the energy transferred is assumed to be deposited uniformly with depth in the lithium pool, unlike hydrocarbon fires. With increasing temperature and pressure, the combustion zone moves away from the lithium surface as evidenced by

$$d = -D_L \frac{\Delta\rho}{\dot{M}_L} \tag{3.38}$$

where $\Delta\rho = \rho_z - \rho_L$

and ρ_z = density (concentration) of lithium in the combustion zone

ρ_L = density (concentration) of lithium at the pool surface

The density of lithium is assumed zero in the combustion zone, while the pool surface density is given as a function of temperature. Cowles and Pasternak[1] give

$$\log_{10} P_L = 4.8831 - \frac{7877.9}{T_L} \tag{3.39}$$

where T_L is the lithium pool temperature in degrees Kelvin, and P is the vapor pressure in atmospheres. The above expression is accurate to within 10 percent for the range of temperatures of interest. The vapor pressure of lithium decreases strongly with temperature and is less then 0.07 atmospheres for temperatures below 1300 °K. The density of lithium vapor at the pool surface is then found by

$$\rho_L = \frac{P_L}{R\ T_L} \tag{3.40}$$

The diffusion coefficient for lithium vapor through air, calculated using the expression suggested by Chen and Othmer, results in

$$D_{12} = 2.42 \times 10^{-4}\ P^{-1}\ (T/460)^{1.81}\ ft^3/sec \tag{3.41}$$

where P is the containment pressure in atmospheres and T the absolute temperature of lithium vapor in degrees Rankine.

The mass transfer rate $\dot{M}_L$ is determined by stoichiometric conditions in the combustion zone and is given by

$$\dot{M}_L = R_o + R_n + R_w \quad \frac{\text{lb. Li}}{\text{sec-ft}^2} \tag{3.42}$$

where the combustion rates R_o, R_n, and R_w have been defined earlier and are dependent on the mass transfer coefficient h_m and the weight fractions of oxygen, nitrogen, and water vapor within the containment.

3.4.3 Lithium-Nitrogen Reaction

In the presence of moisture and at ambient temperatures, lithium reacts exothermically with nitrogen. At temperatures above the melting point of the metal the reaction rate is high.[39] However, from thermochemical considerations, the reaction of lithium with nitrogen proceeds much more slowly than with oxygen for oxygen concentrations greater than a few percent. As discussed in section 2.3, there is no evidence for lithium-nitrogen reaction for oxygen concentrations above 14 percent. Moreover, for reaction temperatures much above 1300 °K, Li_3N strongly dissociates and hence lithium-nitrogen reaction is unimportant.

The contribution of lithium-nitrogen reaction to the overall combustion rate of lithium is thus limited to low concentrations of oxygen, increasing linearly from a value of 2 percent at 13.6 w/o oxygen to 100 percent at 0 w/o oxygen.

3.5 Containment Thermal Model

3.5.1 Containment Pressure

The pressure within the containment is calculated using the ideal gas law,

$$P = \frac{n \cdot RT_g}{V} \tag{3.43}$$

The containment free volume V is assumed constant for a particular CTR containment design. The absolute temperature T is determined from heat transfer considerations as seen in section 3.3. The number of moles of gas n is a function of the initial containment pressure and temperature, the amount of oxygen, with vapor, and nitrogen consumed in the fire, the release of hydrogen, inert gas flooding, and containment leakage.

3.5.2 Containment Leakage

The leakage rate through an intact containment vessel structure is given by Charak and Person[10]

$$LEAK = K\ (OVERP)^a \tag{3.44}$$

where LEAK is the fraction of the containment gas mass which leaks per second, and OVERP is the difference between the containment gas and atmospheric pressures. While each containment will have its own unique leakage characteristics, the above model conservatively assumes that leakage flow is turbulent through a steel-lined concrete vessel. Typical

values of a = 0.5 and K = 2.588 X 10^{-9} / sec-$psi^{0.5}$ give an integrated mass leakage of 0.1% per day at 25 psig overpressure.

3.5.3 Heat Conduction through the Containment Structures to the Ambient

The basic containment structural model is shown in Figure 3.5. The model consists of four major parts: the containment atmosphere, wall structure, floor structure, and the lithium pool and associated combustion zone. These are divided into a number of separate elements. Each element can be lumped into a single node for computational purposes. The nodes are interconnected by thermal admittances equal to the reciprocal of the thermal resistance between the elements.

The containment atmosphere is assumed to be a single, well-mixed mass. It therefore contains only a single node. A single node is also used for describing the lithium pool because of lithium's large thermal conductivity and the small thickness of the pool resulting from hypothetical lithium spills. The containment walls and floor have similar structures, using concrete sheathed with a plate steel liner. Heat transfer through the structures is assumed to be one dimensional. The liner is assumed to be separated from the concrete surface by a small gas gap. Heat is transferred between the two by conduction and radiation. The wall transfers heat out to the ambient surroundings through a convective surface film. The external surface

FIGURE 3.5

BASIC CONTAINMENT STRUCTURAL MODEL

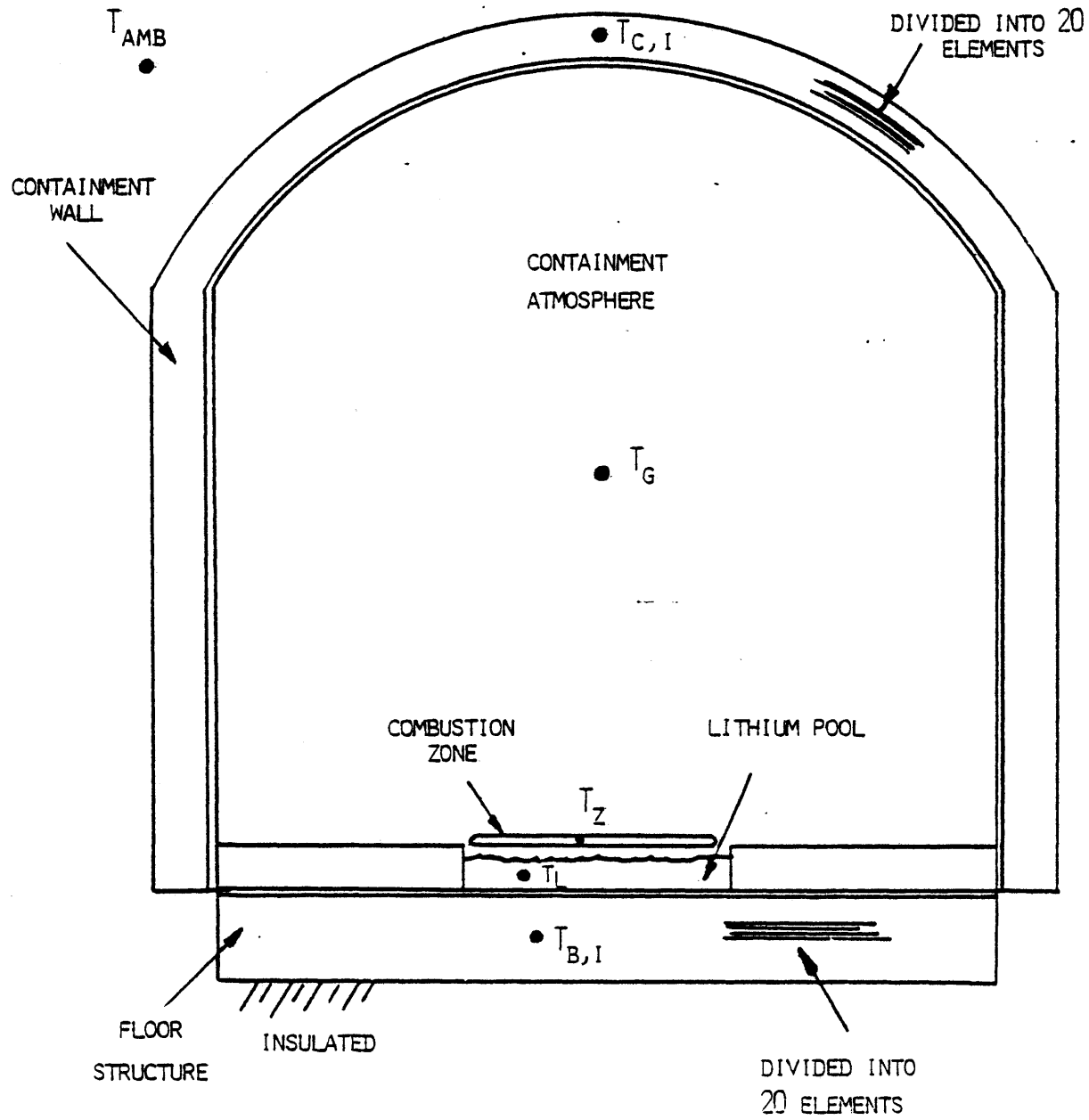

coefficient is taken to be 0.3 BTU/hr - ft^2 - °F, a conservative figure for natural convection. The model assumes that the bottom of the floor is insulated. This is in keeping with the very small heat transfer that will take place into the earth below the containment. For both the floor and the wall, the steel liner is treated as a single element and the concrete is divided into 20 elements. Rebar and tensioning tendon[3] embedded in the concrete are not included. The thermal property values used in the model are shown in Table 3.2.

3.5.4 Containment Spray Fire Model

A liquid metal fire caused by a piping rupture would probably consist of two parts, a spray as the coolant is rapidly expelled out of the broken piping, and a pool fire after the coolant has collected on the containment floor. The spray fire is modeled by assuming that a fixed amount of lithium reacts instantaneously, adiabatically, and stoichiometrically with the oxgyen in the containment atmosphere.[10] The equilibrium temperature of the components, 1, 2 ..., i,...n of the resultant mixture is then given by:

$$\int_{T_o}^{T_p} M_L\, C_L\, dT_L + M_L\, Q_c = \sum_{i=1}^{n} \int_{T_{0,i}}^{T_f} M_i\, C_i\, dT_i \qquad (3.45)$$

where M = mass

C = specific heat = f(T)

TABLE 3.2

Thermophysical Data used in Containment Structures Heat Transport Calculations

Materials	Density (lbm/ft^3)	Specific Heat (Btu/lbm-°F)	Thermal Conductivity (Btu/hr-ft-°F)
Carbon Steel (liner)	490	0.2	30
Concrete	144	0.156	1
Lithium	27.4	1.0	36.3
Air (liner-concrete gap)	--	--	0.015

T = temperature

T_o = initial atmosphere temperature

T_p = lithium spill temperature

T_f = final mixture temperature

Q_c = heat of combustion

Substitution of the formulae for C as a function of temperature of O_2, N_2, and Li_2O, and carrying out the integrations leads to a fourth order polynomial of which the positive real root constitutes the desired solution. A simple iterative technique is used for finding the solution.

The amount of lithium which reacts as spray is dependent on many conditions of the accident itself. To calculate this reaction analytically would be very difficult because it would be a function of droplet size, speed, initial temperature, and the time between ejection and impact on containment walls or lithium pool. These parameters are dependent on the specific accident, and are determined by the size orientation, and location of the break and the driving pressure differential. Krolikowski[41] has studied explosive spray fires with very small droplets ($\sim$572 μ diameter) under very large driving pressure. Shire[42] has studied spray fires resulting from sodium being expelled from a nozzle and impinging on a flat plate. This configuration results in much larger droplets (0.21 in. diameter) but much lower droplet velocities. Both experiments show only a small fraction (5%) of a sodium spray will react before the spray impacts a solid boundary. It may

be possible, however, to postulate conditions under which a larger fraction of the spray is consumed. Although the combustion rate and exposed surface area of sodium droplets are very large, each droplet's time in flight is very short. In such cases, the assumption of instantaneous combustion seems reasonable.

3.5.5 Modeling of Emergency Cooling of the Containment Atmosphere

An option included in the LITFIRE model is the emergency cooling of the containment gas. Under normal operation, the reactor containment atmosphere is assumed to be cooled to prevent an excessively high temperature, and possibly to maintain a slightly negative pressure within the containment with respect to the ambient pressure. During hypothetical accident conditions, the containment atmosphere could possibly be cooled by the same units used for normal operation. The cooling rate provided by the unit will be dependent on the inlet temperature of the cooling fluid, the fluid flow rate, containment air temperature, and overall heat transfer coefficient between the containment air and the coolant. For the purposes of this study, a constant cooling rate Q_{ESC} is assumed to be provided for a given accident situation. However, Q_{ESC} could be represented as a function of containment air temperature with slight modification to LITFIRE.

The overall temperature rate of change of the containment atmosphere is then given by

$$\frac{\Delta T_g}{\Delta t} = (Q_{z-g} + Q_{gc} - Q_{wg} - Q_{ESC})/HTCAPG \quad °F/sec \qquad (3.46)$$

where Q_{wg} is the heat convected from the gas to the containment walls, and HTCAPG is the heat capacity of the containment gas and aerosols. Q_{z-g} and Q_{gc} represent radiative and convective heat transfer from the pool surface to the cell gas as discussed earlier. The sign and magnitude of $\Delta T/\Delta t$ at any given time will then be determined by the relative magnitudes of the above terms at that time.

3.5.6 Modeling of Emergency Cooling of the Steel Floor Liner

Another option included in LITFIRE is the emergency cooling of the steel floor liner. In the event of a hypothetical spill of hot liquid lithium on the containment floor, it may be advantageous to provide cooling to the liner to prevent gross structural deformation from large thermal stresses. Failure of the steel liner would result in contact between liquid lithium and the concrete structures, releasing still more energy and gases as discussed earlier in Chapter 1.

Again, the cooling rate of the steel liner Q_{ESL} will depend on the inlet temperature of the cooling fluid, the fluid flow rate, the steel liner temperature, and overall heat transfer coefficient between the coolant and steel liner. Because of the very exothermic lithium-water reaction and the possibility of liner failure, the use of water as coolant is undesirable. Helium gas would be suitable. Heat from the helium cooling

system could then be rejected to a heat exchanger and secondary cooling system.

The overall temperature rate of change of the steel liner is then given by

$$\frac{\Delta T_s}{\Delta t} = (Q_{Lc} - Q_{w-c} - Q_{ESL})/\text{HTCAPS} \ ^\circ\text{F/sec} \qquad (3.47)$$

where Q_{wc} represents heat conduction between the gap of the steel liner and the concrete, HTCAPS is the heat capacity of the steel liner beneath the lithium pool, Q_{Lc} is the heat conducted from the Li pool to the liner, and Q_{w-c} represents radiative heat transfer from the liner to the concrete. For the purpose of this study the emergency steel liner cooling rate Q_{ESL} is assumed to be constant with steel liner temperature although slight modifications could be made to LITFIRE if desired.

3.5.7 Modeling of Containment Atmosphere Ventilation and Inert Gas Flooding

Two other options included in LITFIRE are the ventilation of the containment air through filters to the ambient, and inert gas flooding of the containment. The former option is applicable mainly to large containments such as the UWMAK-III design, whereas the latter option is practical in small cells such as the EBTR design.

Ventilation of the containment would be desirable when large internal pressures caused by hypothetical lithium fires threaten the integrity of the containment structure. Filters would remove most airborne radioactivity and aerosols. However,

further research is needed to determine the nature and amounts of tritium released into the containment from lithium fire. Tritium gas is more difficult to filter out than the oxide form, and the size of the adsorption beds for tritium oxide removal may also limit the acceptable ventilation rate to unreasonably low values.

Inert gas flooding of the containment or cell is desirable when the amount of oxygen and nitrogen in the cell is the limiting factor on total heat generation from lithium fires. In small cells such as the EBTR design, the combustion of lithium causes the depletion of oxygen and nitrogen in the cell and eventually the gas pressure may become less than ambient atmospheric pressure. Inert gas flooding prevents the cell pressure from becoming too low and hence retards the leakage of more oxygen and nitrogen into the cell. Hilliard et al.[52] have demonstrated the feasibility of this concept for sodium fire protection.

The rate at which the mass of species i in the containment air changes can be expressed as

$$\frac{\Delta m_i}{\Delta t} = \dot{m}_{IN,i} - \dot{m}_{EX,i} - \dot{m}_{LK,i} \quad \text{lb/sec} \qquad (3.48)$$

where $\dot{m}_{IN,i}$, $\dot{m}_{EX,i}$, and $\dot{m}_{LK,i}$ represent the mass flow rates of species i by inert gas flooding, ventilation, and out-leakage respectively. In the case of gas flooding, it is assumed that only one species such as helium or argon is considered although

trace amounts of nitrogen and other gases may be present. The mass flow rate in lb/sec may be converted to the more standard form of SCFM (standard cubic feet per minute) by dividing by the density of the gas considered at standard temperature and pressure.

3.6 The Numerical Scheme

The IBM-CSMP (continuous system modeling program)[50] numerical methodology used in SPOOL-FIRE has been retained since it allows for the change of the lithium combustion model quite readily. With this methodology, a physical problem can be modeled by a set of ordinary differential equations with corresponding initial conditions. For instance, the temperature of a thermal element may be found from the solution to

$$mc \frac{dT}{dt} = q_1 + q_2 + q_3 + \ldots, \; T = T_o \text{ at } t = t_o \tag{3.49}$$

where mc is the element's heat capacity and q_1, q_2, q_3 ... are heat flows into the element. This could also be expressed as

$$T = \int_{t_o}^{t} \frac{1}{mc} (q_1 + q_2 + q_3 \ldots) \, dt + T_o \tag{3.50}$$

In CSMP this is expressed as

$$T = \text{INTGRL}(T_o, \, dT/dt) \tag{3.51}$$

Once the governing equations for the model have been written, it is a relatively simple matter to write a CSMP

program for them. A set of subroutines is used for doing the integrations. Two methods of integration are provided, Simpson's Rule and Fourth Order Runge-Kutta methods.

IV. DESIGN STRATEGIES FOR MITIGATING THE CONSEQUENCES OF LITHIUM FIRES

4.1 Introduction

The immediate consequences of a lithium fire resulting from a hypothetical spill within a CTR containment is the heating of the containment structures as well as the heating and pressurization of the cell gas. The rates at which these temperatures and pressure rise and fall is determined by the containment design, spill conditions, physical properties of structural materials and gases, and engineered safety features. The ultimate heat sinks are the ambient air and ground surrounding the containment building. During the course of the fire, the relatively large heat capacities of the steel and concrete structures provide the primary mechanism for heat removal from the hot lithium and cell gas. It is therefore important to have a good understanding of the physical properties of steel, concrete, lithium, and gases in order to predict and mitigate the consequences of lithium fires.

In this section, a detailed sensitivity study is made using LITFIRE to determine the importance of various input parameters to the code. The inherent safety features of several possible CTR containment and cooling system designs are also investigated. Finally, possible engineered safety features for mitigating the consequences of lithium fires are examined using LITFIRE. The study is performed using the design of UWMAK-III as a reference containment.

4.2 Application of LITFIRE to Lithium Fires in UWMAK-III

4.2.1 Description of UWMAK-III Containment

The UWMAK-III containment building is shown in Figure 4.1. The structure is reinforced concrete lined with a 0.25 in. thick steel plate. To prevent lithium fires, the containment would probably have an inert atmosphere. The structure is designed to withstand a 15 psig over-pressure (caused by a liquid helium pipe rupture). The structure would house the reactor, its piping and immediate peripheries, e.g. neutral beam injectors. Heat exchangers, energy storage devices, refrigeration equipment, hot cells, waste storage, and other auxiliaries would be housed in separate structures located around the circumference of the containment building. This is significantly different from the UWMAK-I containment which utilizes a double containment. The reactor is located in the primary containment vessel and the auxiliaries are located in the surrounding secondary containment building.

4.2.2 Discussion of Important Base Case Parameters

A sensitivity study of the consequences of lithium spills within the UWMAK-III containment was performed using the code LITFIRE. The results are reported in the next section. An attempt was made to realistically estimate the necessary input parameters. This was designated the base case. The parameters were then varied individually to study the effects of the resultant fire. The selection of values for the important parameters were then varied individually to study the effects

FIGURE 4.1

CROSS SECTION OF UWMAK-III PRIMARY CONTAINMENT BUILDING

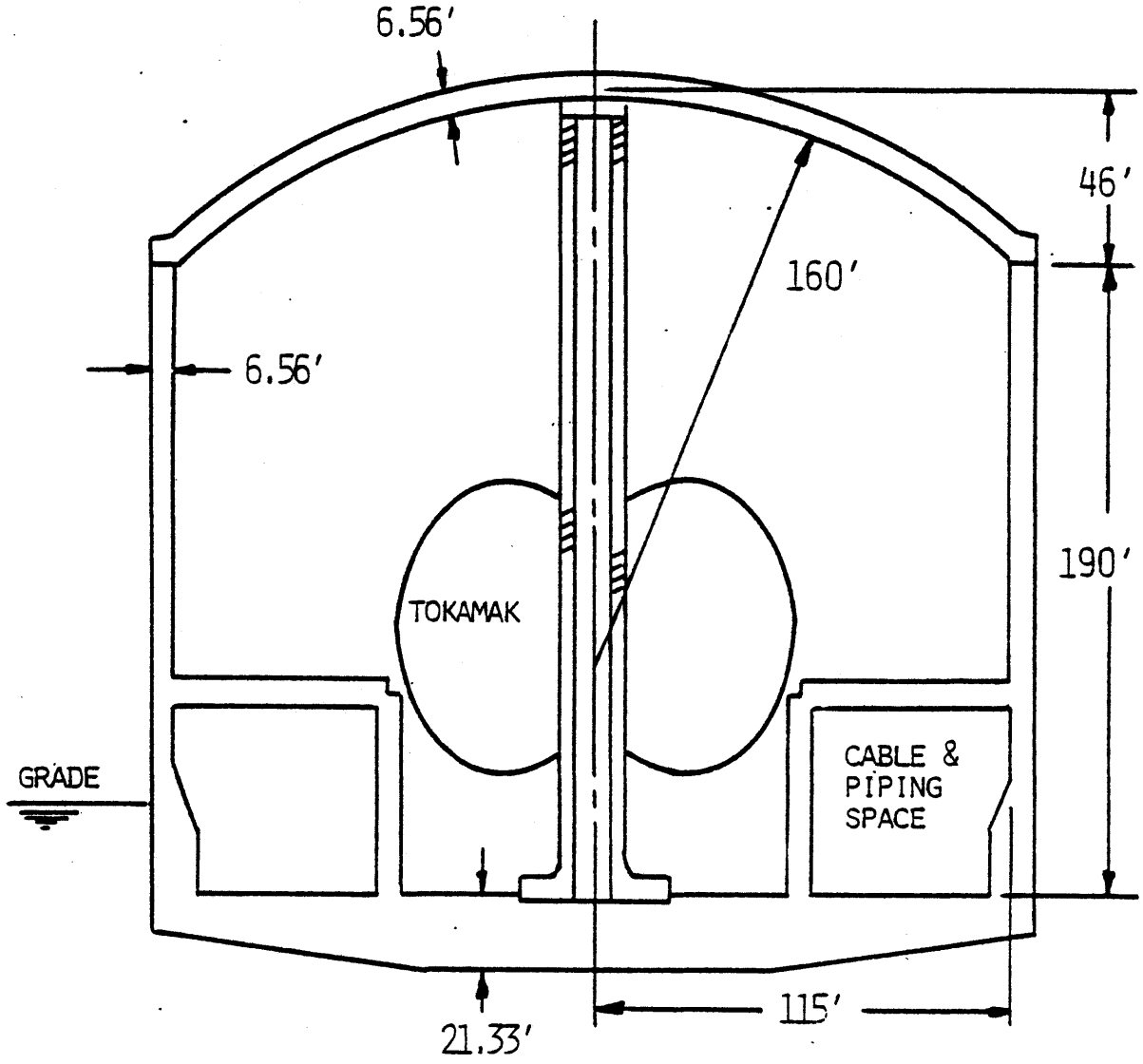

TOTAL FLOOR AREA	41548	SQ. FT.
TOTAL VOLUME	8855700	CUBIC FT.
WALL AREA	183532	SQ. FT.
TOTAL LITHIUM MASS	870975	LBM.
1/18 TOTAL LITHIUM	48388	LBM.
AMBIENT TEMPERATURE	538	°R
INITIAL PRESSURE	14.7	PSIA

LINED WITH 0.25 INCH STEEL PLATE WITH A 0.025 IN. GAS GAP BETWEEN THE PLATE AND THE CONCRETE SURFACE.

of the resultant fire. The selection of values for the important parameters is discussed below. A summary is presented in Table 4.1.

The initial containment gas composition was assumed to be a normal atmosphere of 23.1% oxygen and 76.9% nitrogen by weight. This was done in order to get some idea of the maximum consequences of a lithium fire. With an inert operating atmosphere, only lithium-concrete reactions need to be seriously considered. If the containment were breached, the containment over-pressure would no longer be important since the containment would already be vented to the outside.

UWMAK-III uses roughly 1/4 the amount of lithium that UWMAK-I uses. This results from different blanket designs. In UWMAK-I the entire blanket uses liquid lithium. In UWMAK-III lithium is used only in the outer half of the torus blanket. The inner half (guarding the donut hole) is helium cooled. Helium is also used to cool the inner wall and the magnet shield. Both designs use a small amount of lithium to cool the plasma divertors. UWMAK-III uses 18 toroidal field coils. The blanket therefore consists of 18 modular sections. In this study, it was assumed that a header pipe broke in such a manner as to drain one blanket section i.e. 1/18 (5.56%) of the total lithium inventory is spilled. Because of lithium hold-up in piping and the heat exchangers, one blanket section would contain less than 1/18 of the total lithium inventory so that 1/18 is probably a conservative number. The lithium blanket sections are supplied and drained by two ring-shaped headers, one

TABLE 4.1

Input Values for the Base Case

Spill size	SPILL = 48,388 lbm. Li
Fraction of spill mass consumed as spray	SPRAY = 1%
Lithium pool surface area	ASLI = 10,387 ft^2
Oxygen content of cell gas	WO2 = 23.1% by weight
Initial lithium spill temperature	TLII = 2256 °R
Water vapor content of cell gas	WWA = 0.0%
Thermal emissivity of combustion zone	EMCZ = 0.5
Thermal emissivity of steel liner	EMSTL = 0.85
Thermal emissivity of concrete	EMCONC = 0.9
Initial temperature of combustion zone	TCZI = 2300 °R
Fraction of reaction products released as aerosols	FRA = 0.75
Mean radius of aerosol particles	RA = 300 microns
Thickness of wall node	W.N.T. = 3.94 inches
Thickness of floor node	F.N.T. = 12.8 inches
Method of integration used	IMETH = 3 (Simpson's Rule)
Initial containment gas pressure	PAZERO = 14.7 psia
Containment volume	V = 8,855,700 ft^3
Containment and structural wall area	AW = 183,532 ft^2

above and one below the reactor. These are connected to two lithium-sodium heat exchangers in an adjacent building. It may be possible for a break to occur which would drain two or more blanket sections. A break might also occur in the heat exchanger building. The latter possibility was not investigated.

The lithium pool area was chosen to be 25% of the total floor area. Cable rooms surrounding the reactor form a hot well of that size. It seems likely that the lithium emerging from a break would pool there.

The thermal emissivity of the oxidized, carbon-steel liner (inside and out, wall and floor) is assumed to be 0.85. The emissivity of concrete is chosen as 0.9, while that of the lithium pool surface and combustion zone are 0.2 and 0.5 respectively. The range of possible values is given by Kreith[31] and Siegel and Howell.[40]

The blanket exit temperature of lithium in UWMAK-III is 2256 °R. This was taken to be the spill temperature.

Studies of sodium spray fires show that only a very small fraction of the spray is consumed. Shire[42] reports pressure rises caused by a sodium jet impacting a deflector. In 5 of the 6 cases reported, pressure readings indicate that no more than 3% of the sodium reacted. In the sixth case, 15% may have reacted. The experiment was done in low oxygen atmospheres, and the average drop size was 0.21 inches in diameter. Krolikowski[41] reports a calculation, for 0.026 inch sized drops under large driving pressures, which shows less than a 2%

decrease in diameter. This would constitute less than 6% decrease in mass. In a severe break only a small portion would be sprayed. We assume 20%. If 5% of the spray is consumed then only 1% of the total spill mass is consumed in the spray fire. This was used as the base case.

The remaining 99% of the spilled lithium is assumed to collect as a pool on the reactor containment floor instantaneously. However, Kastenberg et al.[26] indicated that it may take up to 1 hour for lithium to drain out of the blanket. A computer run using a modified version of SPOOL-FIRE was made assuming that the spill rate decays exponentially.[27] 1/18 of the total lithium inventory was assumed to spill over a period of 3600 seconds which constituted 3 time seconds. The result was a negligible difference in the containment thermal response between the base case and the slow ejection of lithium case. Hence, the assumption of instantaneous ejection of liquid lithium in LITFIRE appears reasonable.

The release of aerosols into the containment gas is important because this effect increases the heat capacity of the gas and prevents radiation heat transfer from the combustion zone or pool surface to the containment walls. In SOFIRE II and SPOOL-FIRE, the method used for accounting for such an effect as aerosol release is to change the radiation heat transfer coefficient in the cell gas at some arbitrary time. In SOFIRE II for example, the emissivity view-factor between the pool surface and cell walls is changed from 0.5 to 1.0 five

minutes after the initiation of combustion. This means that the heat radiated from the combustion zone is captured by the aerosol particles so that no heat can be absorbed by the walls.

However, for the case of lithium fires, no information can be found on the aerosol properties of lithium combustion properties (size, distribution, density, shape, chemical nature, etc.). For the base case of this study, a mean aerosol radius of between 30 and 30,000 μm was considered. The sensitivity study discussed in 4.2.3 shows that the effect of changing the mean aerosol radius from 30 to 300 μm is negligible. However, values above 1000 μm result in large effects, although it is doubtful that particles of such size would be experienced in light of experimental values obtained for sodium oxide aerosols.[28] A base case value of 300 μm was chosen for this study. In addition, 75% of the reaction products were assumed to be released into the atmosphere as aerosols, with 25% of the reaction products remaining in the pool.

4.2.3 Results of Sensitivity Study

The important results of the sensitivity study are compiled in Table 4.2. Information is given on the maximum temperatures calculated for the containment structures and gas, as well as the maximum overpressurization experienced by the containment. The input parameters to which the sensitivity of the results was investigated include:

1) EMCZ, the combustion zone thermal emissivity;
2) TCZI, the initial temperature of the combustion zone following lithium spill;

3) EMCONC, the thermal emissivity of the concrete floor and wall surfaces;

4) EMSTL, the thermal emissivity of the steel liner, wall and floor, inside and out;

5) EMLI, the thermal emissivity of the lithium pool surface;

6) WO2, the initial oxygen concentration inside the cell gas;

7) WWA, the initial water vapor concentration inside the cell gas;

8) ASLI, the lithium pool surface area;

9) SPRAY, the fraction of lithium spilled which burns as a spray;

10) TLII, the initial spill temperature of lithium;

11) SPILL, the mass of lithium spilled;

12) FRA, the fraction of lithium products evolved as aerosols;

13) RA, the mean radius of the aerosol particle;

14) W.N.T., the wall node thickness used in the LITFIRE computation;

15) F.N.T., the floor node thickness.

The sensitivity analysis showed that changes in the following parameters had little effect on the thermal response of UWMAK-III to lithium fire:

1) EMCZ (cases 55 and 52)

2) TCZI (case 91)

3) EMSTL (case 74)

4) EMLI (cases 62 and 64)

5) SPRAY (case 66)

6) SPILL (values above 97,000, cases 70, 75, and 82)

7) RA (values below 1000, cases 80, 84, and 85)

TABLE 4.2

Compilation of Sensitivity Study

Case No.	Max. Gas Overpressure (psig)	Max. Gas Temp. (°F)	Max. Steel Floor Temp. (°F)	Max. Steel Wall Temp. (°F)	Max. Concrete Floor Temp. (°F)	Max. Concrete Wall Temp. (°F)
56 BASE	23.5	1051	1793	560	1302	330
Effect of changing combustion zone properties						
55 EMCZ=0.7	23.4	1034	1695	567	1159	338
52 EMCZ=0.9	23.1	1013	1626	570	1109	339
91 TXZI=1800	23.5	1050	1792	560	1301	330
Effect of changing thermal emissivity values						
57 EMCONC=0.0	38.9	1664	2308	1118	469	180
59 EMCONC=0.5	26.9	1171	1928	654	1065	276
74 EMSTL=0.5	26.8	1167	1926	647	1084	346
62 EMLI=0.1	23.6	1055	1793	562	1305	295
64 EMLI=0.3	23.4	1048	1794	559	1300	292

TABLE 4.2 continued

Case No.	Max. Gas Overpressure (psig)	Max. Gas Temp. (°F)	Max. Steel Floor Temp. (°F)	Max. Steel Wall Temp. (°F)	Max. Concrete Floor Temp. (°F)	Max. Concrete Wall Temp. (°F)
Effect of changing initial oxygen and water vapor concentrations						
69 WO2=0.00	9.9	489	1565	255	415	130
79 WO2=0.05	11.0	532	1703	269	391	132
78 WO2=0.08	13.3	623	1706	316	470	147
77 WO2=0.10	15.2	699	1711	356	544	161
76 WO2=0.14	17.8	804	1685	409	695	189
63 WWA=0.05	20.8	1062	1802	558	1274	330
Effect of changing lithium spill conditions						
65 ASLI=4000 ft^2	18.4	848	1902	499	1837	358
66 SPRAY=0.05	23.8	1054	1790	563	1279	334
61 TLII=1460 °R	23.0	1032	1766	548	1261	325
70 SPILL=97,000 lb.	25.0	1094	1623	677	1556	576

TABLE 4.2 continued

Case No.	Max. Gas Overpressure (psig)	Max. Gas Temp. (°F)	Max. Steel Floor Temp. (°F)	Max. Steel Wall Temp. (°F)	Max. Concrete Floor Temp. (°F)	Max. Concrete Wall Temp. (°F)
71 SPILL=24,000 lb.	19.6	847	1842	430	770	193
75 SPILL=97,000 lb. ASLI=20,772 ft^2	29.0	1345	1758	738	1177	449
82 SPILL=193,000 lb.	27.2	1310	1755	812	1707	680
Effect of changing aerosol properties						
83 FRA=0.0	17.7	826	1918	568	1465	310
80 RA=30μm	23.6	1052	1768	560	1295	331
84 RA=100μm	23.6	1052	1770	560	1296	331
85 RA=1000μm	23.0	1036	1854	557	1327	327
73 RA=3000μm	21.4	972	1903	553	1380	320
72 RA=30,000μm	15.6	741	1934	556	1472	306
Effect of changing wall and floor node thicknesses						
93 W.N.T.=0.50 in. F.N.T.=1.25 in.	31.9	1389	2111	786	2019	608

TABLE 4.2 continued

Case No.	Max. Gas Overpressure (psig)	Max. Gas Temp. (°F)	Max. Steel Floor Temp. (°F)	Max. Steel Wall Temp. (°F)	Max. Concrete Floor Temp. (°F)	Max. Concrete Wall Temp. (°F)
94 W.N.T.=0.25 in. F.N.T.=1.25 in.	32.1	1396	2111	798	2019	627
95 W.N.T.=0.25 in. F.N.T.=0.50 in.	32.3	1402	2126	804	2030	637
96 W.N.T.=0.50 in. F.N.T.=0.50 in.	32.2	1396	2126	792	2030	616
92 W.N.T.=0.50 in. F.N.T.=1.25 in. WO2=0.08	13.62	636	1808	308	1629	209

Case 57 shows the importance of thermal radiation between the steel wall liner and the concrete in providing a heat sink for heat generation. However, the thermal emissivity of 0.0 for concrete is grossly unrealistic. A value of EMCONC = 0.5 as given in case 59 results in a similar thermal response as the base case.

As shown in Table 4.2, a decrease in oxygen concentration within the containment greatly reduces the consequences of lithium fire. Case 63 indicates that although the presence of water vapor increases the combustion rate of liquid lithium, the containment overpressurization decreases. Even though the reaction of lithium with water releases hydrogen, the stoichiometric combustion ratio of lithium to water is so much higher than that of lithium to oxygen or lithium to nitrogen that a small fraction of the containment gas consumes large amounts of lithium. In all of the cases studied thus far, the mass of liquid lithium has been the limiting effect on total energy release.

Cases 65, 70, and 75 show how LITFIRE is relatively sensitive to the surface area of the lithium pool - the greater the surface area, the greater the rate of total energy release to the containment. Cases 70, 71, and 82 indicate that the consequences of lithium fires is relatively insensitive for spills of over 97,000 pounds of lithium since oxygen in the containment becomes the limiting constraint.

Case 83 indicates the removal of aerosols from the containment gas will allow for better heat radiation transfer between

the lithium pool combustion zone and the containment walls and structures, resulting in smaller consequences. However, the mean aerosol particle radius chosen is unimportant except at unreasonably large values above 3000 microns.

In cases 93, 94, 95, 96, and 92, the wall and floor node thicknesses were changed to study the effect of node size on the output of LITFIRE. It was clearly shown that LITFIRE is quite sensitive to these node thicknesses at least for conditions of high oxygen concentration. However, below node thicknesses of about 0.50 inches, the sensitivity is greatly diminished.

For this reason, the input values for case 93 are assumed to represent the best estimates available for predicting the consequences of lithium fire within the UWMAK-III containment. Figures 4.2 and 4.3 give the temperature-pressure history of the UWMAK-III containment for case 93.

4.3 Inherent Safety Features of Fusion Reactor Containment and Cooling Systems

4.3.1 Multiplicity of Parallel Cooling Systems

The use of a large number of parallel, lithium cooling systems offers a number of advantages from the viewpoint of lithium fire protection. Assuming the total mass flow rate of lithium through the fusion reactor to be fixed for a given thermal output, then a large number of cooling systems would mean smaller lithium inventories per system. Rupture of a single lithium system will lead to the release of a small fraction of the total lithium inventory. The UWMAK-III design employs 18

FIGURE 4.2

BEST ESTIMATE OF THE CONTAINMENT THERMAL RESPONSE TO LITHIUM FIRE IN UWMAK-III

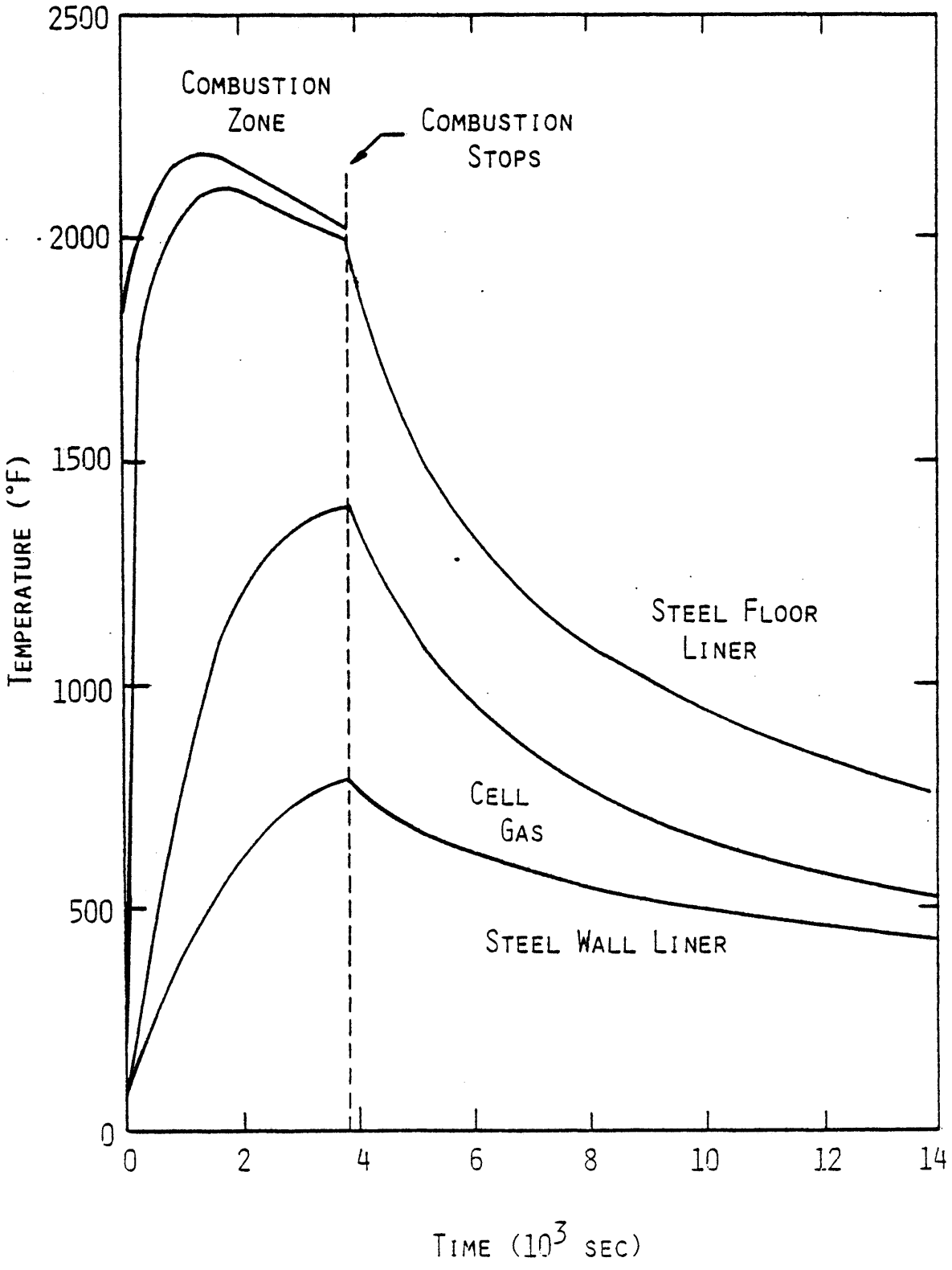

FIGURE 4.3

BEST ESTIMATE OF THE CONTAINMENT GAS PRESSURE RESPONSE TO LITHIUM FIRE IN UWMAK-III

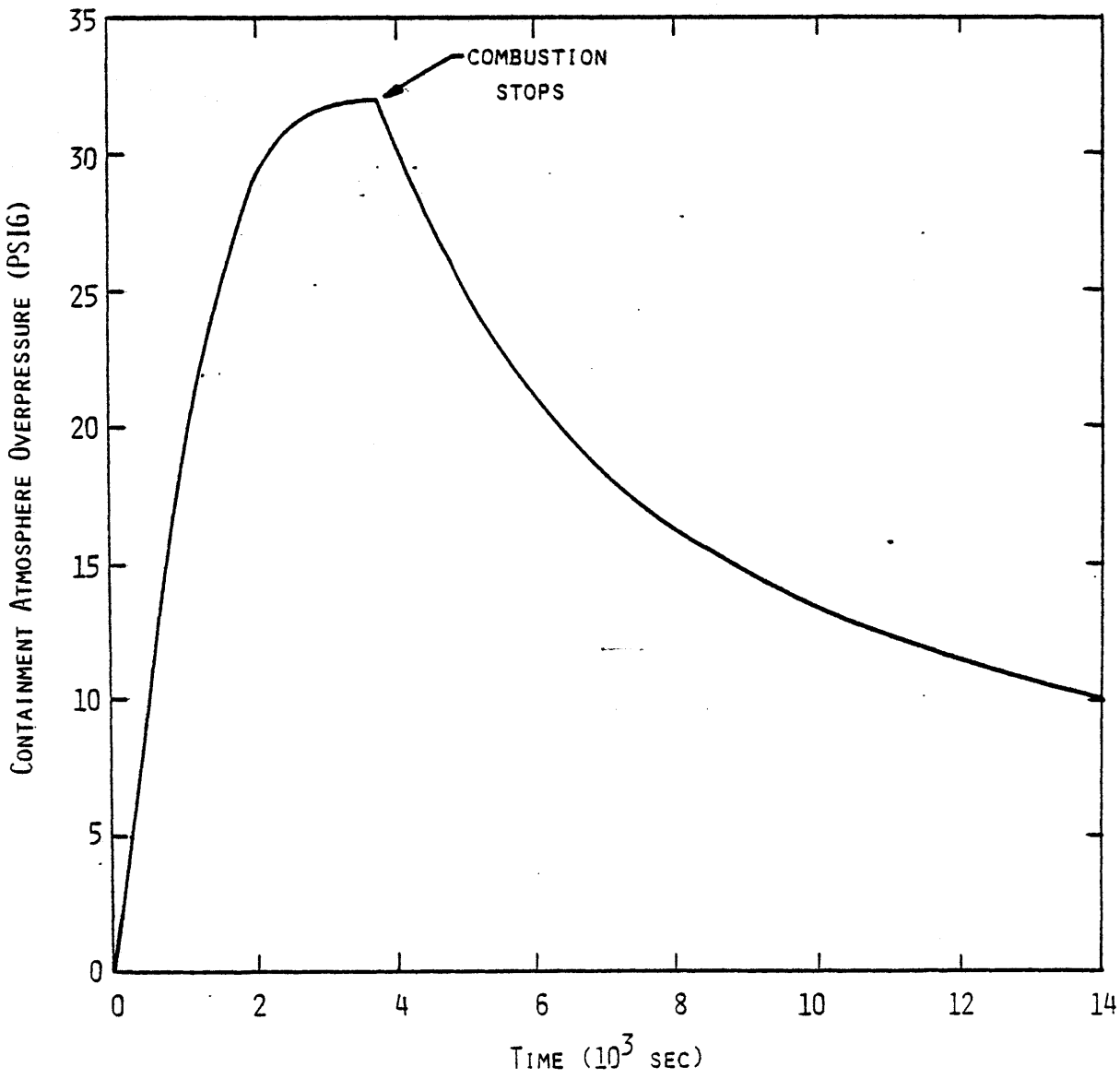

parallel systems whereas EBTR would use up to 48 loops. The lithium inventory for a sinlge lithium loop in UWMAK-III is 48,400 lbs. Doubling the number of cooling loops to 36 would presumably reduce this inventory to 24,200 lbs.

In the event of the rupture of a loop and release of the lithium inventory into the containment, less serious consequences would be experienced in the 36-loop design. For example, LITFIRE predicts maximum containment gas overpressures of 31.9 psig for 18-loop design versus 24.9 psig for 36-loop design. The maximum steel wall temperature in the 18-loop design is 786 °F versus 520 °F for the 36-loop case. Similar reductions in the temperatures of other structures occur with the employment of 36 loops while reductions in the consequences of lithium fire result from using still greater numbers of cooling systems although economic consideration would probably limit the maximum number of systems that are feasible.

4.3.2 Modularization of Fusion Reactor into Individual Compartments

The ELMO Bumpy Torus Reactor (EBTR) design has a much larger aspect ratio than the Tokamak-type fusion reactor designs, and therefore employs a primary containment similar to those used for large underground particle accelerators. Furthermore, the reactor is modularized into as many as 48 individual compartments, each isolated from the next by concrete structures. Presumably, these concrete moats would be lined with steel plates to prevent lithium-concrete reactions. Figure 4.4 is a simple illustration of the modular design and

FIGURE 4.4

MODULARIZATION OF FUSION REACTOR AS ILLUSTRATED IN THE ELMO BUMPY TORUS REACTOR

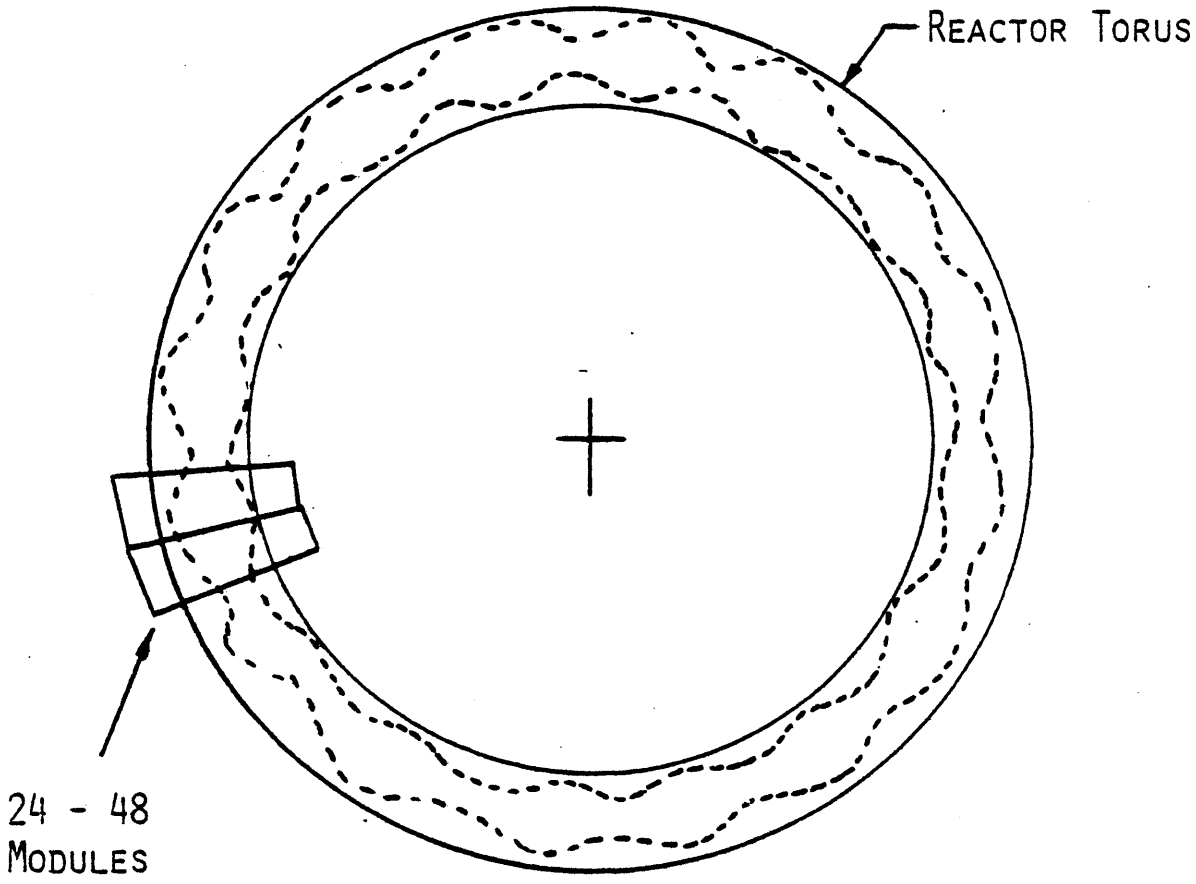

TOP VIEW

primary containment of EBTR.

Because of the relatively small free volume of the EBTR compartments (approximately 3.5×10^4 ft^3), the mass of oxygen and nitrogen is the limiting factor when considering the total energy release from lithium fires. Figure 4.5 shows the temperature history of the containment structures during a lithium fire. Note that the temperatures are significantly below corresponding temperatures for UWMAK-III structures as indicated in Figure 4.1. This is because the initial release temperature is much lower for EBTR (896 °F versus 1796 °F for UWMAK-III) and also because of the limiting amount of reactive gases in the EBTR module.

Figure 4.6 shows the containment gas pressure history for EBTR. If the inert gas flooding rate is automatically controlled, the pressure within the containment levels off just above normal atmospheric pressure to prevent in-leakage of oxygen and nitrogen. Without inert gas flooding, the cell pressure decreases until depletion of oxygen and nitrogen is sufficient to stop combustion. This latter case assumes no significant in-leakage of reactive gases. More detailed information of the proposed design of EBTR is required before the importance of in-leakage can be determined. In either case, the EBTR design offers important advantages over the UWMAK-III design from the viewpoint of lithium fire protection.

4.3.3 Reduction of Oxygen Concentration in the UWMAK-III Containment

FIGURE 4.5

TEMPERATURE HISTORY OF THE STRUCTURES AND GAS WITHIN AN EBTR MODULE DURING LI FIRE (60,000 LBS. LI SPILLED)

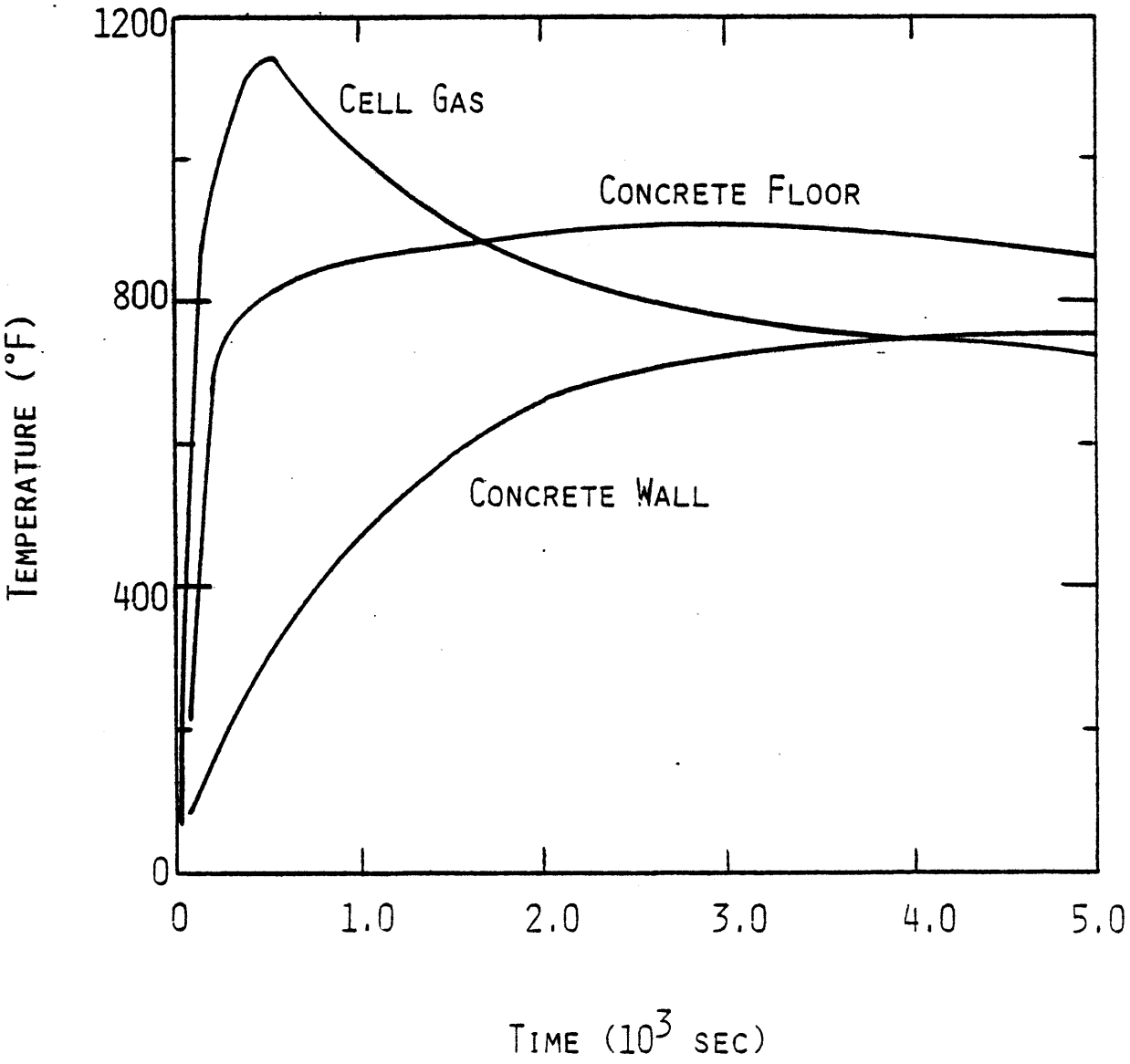

FIGURE 4.6

PRESSURE HISTORY OF THE AIR WITHIN AN EBTR MODULE DURING LI FIRE (60,000 LB. LI SPILLED)

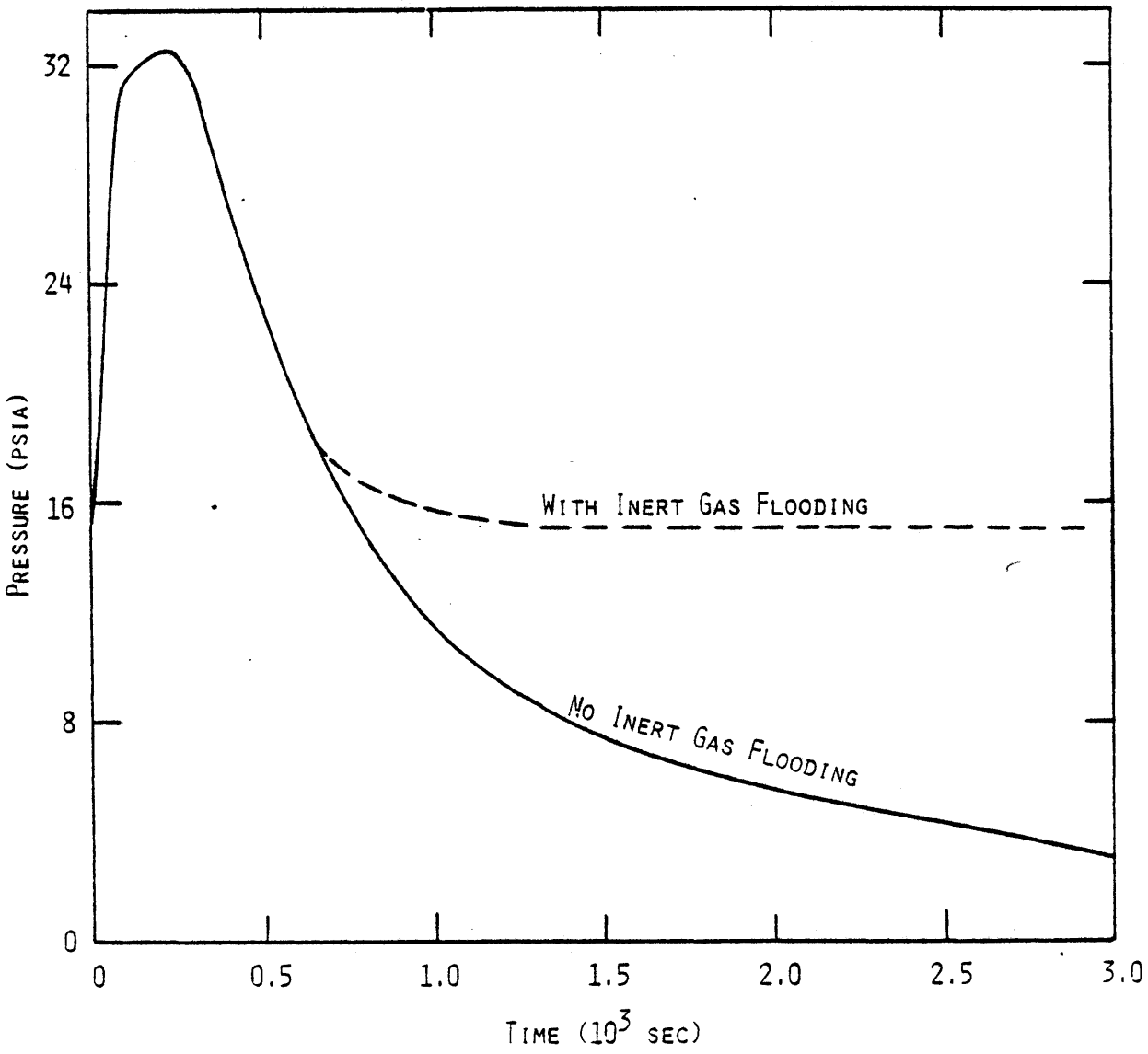

Important advantages can be gained by using less-than-normal concentrations of oxygen within the UWMAK-III containment. Lithium-nitrogen reactions release four and one-half times less energy per pound of lithium than do lithium-oxygen reactions. Figure 4.7 gives the maximum containment gas overpressure during a lithium fire as a function of the initial oxygen concentration, all other factors equal. In addition, the maximum temperatures experienced during a fire would be less for low oxygen concentrations. The maximum steel wall liner and cell gas temperatures calculated are 200 and 387 °F respectively for purely nitrogen atmospheres as opposed to 786 and 1389 °F for normal atmosphere.

4.3.4 Reduction of Initial Containment Gas Pressure

Depending on the particular CTR containment design, it may be advantageous to maintain the cell gas at a subatmospheric pressure. This option serves two purposes: First, it will reduce the leakage of tritium or other radioactive products out of the containment during normal operation. Second, it will mitigate the consequences of lithium fire should an accidental spill of lithium occur. Figure 4.8 shows the relationship between the maximum containment gas overpressure calculated by LITFIRE versus the initial gas pressure for the UWMAK-III containment. The substantial reduction in maximum overpressure with decreasing initial pressure arises because of the reduction of the lithium-air combustion rate. Also, a reduction in the cell gas density results in a proportional decrease in the

FIGURE 4.7

MAXIMUM UWMAK-III CONTAINMENT GAS OVERPRESSURE DURING Li FIRE AS FUNCTION OF INITIAL O_2 CONCENTRATION

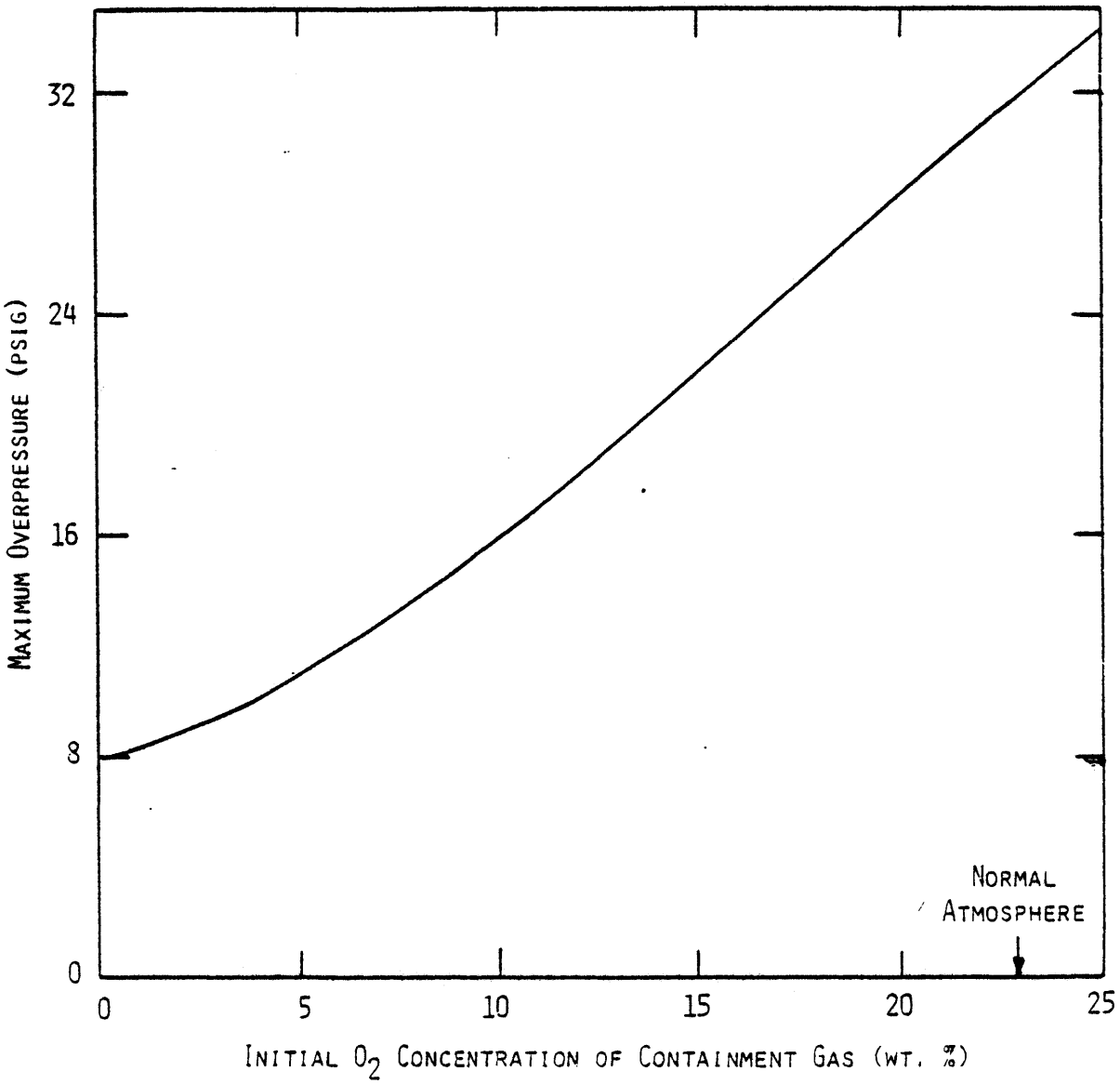

FIGURE 4.8
MAXIMUM UWMAK-III CONTAINMENT GAS OVERPRESSURE
DURING LI FIRE AS FUNCTION OF INITIAL PRESSURE

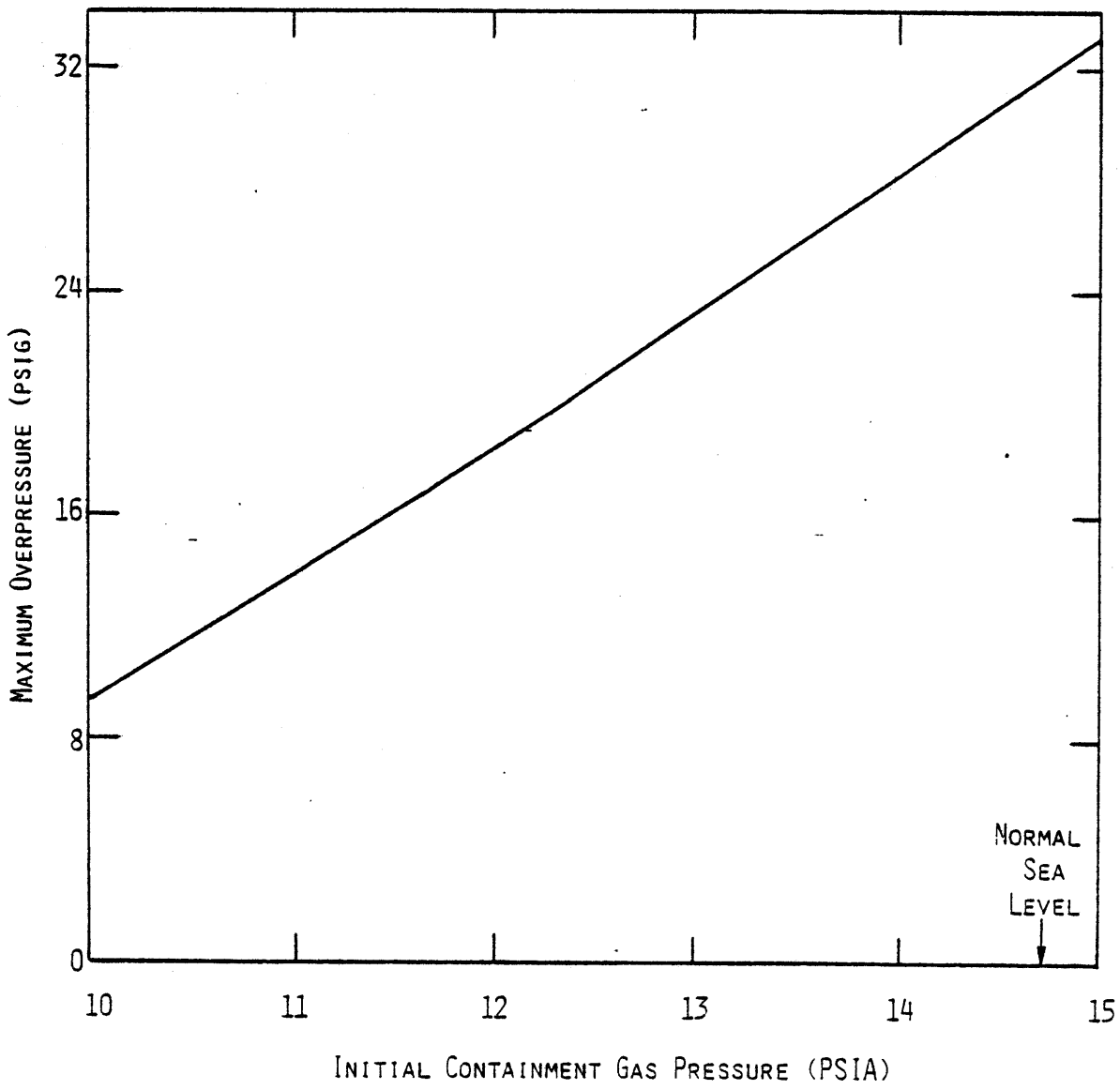

gas pressure as calculated by the ideal gas law.

For a readily achievable initial gas pressure of 12.4 psia, the maximum gas temperature is reduced from 1389 °F in the best estimate case to 1175 °F, whereas the maximum steel wall temperature is reduced by nearly 100 °F and the maximum overpressure is lowered by 12 psi.

4.3.5 Introduction of Structures with High Heat Capacities and Thermal Conductivities

The large thermal conductivity and heat capacity of steel has prompted Huber et al.[29] to suggest inserting high heat capacity material into similar pools of sodium for quick cooling, and eventually extinguishment of the fire.

During the course of a hypothetical lithium fire, the relatively large heat capacities of the steel and concrete structures provide the primary mechanism for heat removal from the hot lithium and cell gas. The rate at which heat is transferred from the cell gas to the structures depends on the heat transfer coefficient as well as the temperature differences.

A figure of merit for determining the ability of structures to conduct heat away from the air-structure interface is the value $A\sqrt{\rho\ C_p\ k}$. For instance, in a one-dimensional semi-infinite solid suddenly exposed to a temperature T_s at the surface, the transient temperature distribution is

$$T_s - T(x,t) = (T_s - T_i)\ \text{erf}\left(\frac{x}{2\sqrt{at}}\right) \qquad (4.1)$$

where t = time

x = distance from surface

T_s = surface temperature

T_i = initial temperature of the solid

a = thermal diffusivity

The heat flow is then given by

$$q(x,t) = -k\, A_w \frac{\delta T(x,t)}{\delta x} \tag{4.2}$$

Taking $x = 0$, the thermal energy which enters the wall through the surface in the whole time t, beginning with the instant of sudden change of the surface will be

$$Q = \int_o^t q(x,t)\, dt \tag{4.3}$$

By substitution and assuming constant physical properties with regard to temperature, integration of 4.3 gives[53]

$$Q = -k\, A_w (T_i - T_s)\, 2\sqrt{t/\pi a} \tag{4.4}$$

Substitution of $k/\rho C_p$ for a in 4.4 results in

$$Q \propto A_w \sqrt{\rho\, C_p\, k} \tag{4.5}$$

Therefore, to a first approximation, the amount of heat removed by the containment structures is proportional to $A_w\sqrt{\rho\, C_p\, k}$. Using values for ρ, C_p, and k given in Table 3.2 the ratio of heat removal by steel to that of concrete is approximately 11.

Hence, there is a substantial advantage to using thick steel liners and structures wherever possible.

Using LITFIRE, it was found that a 50 percent increase in the surface area A_w of steel-lined structures reduced the maximum overpressures from 31.9 psig in the best estimate case to 25.7 psig. A corresponding temperature decrease of 150 °F was calculated for the outer structural materials. Presumably, further decrease in temperatures and cell gas pressure could be achieved with proper selection of structural materials.

4.4 Engineered Safety Features of Fusion Reactor Containments

4.4.1 Emergency Cooling of Containment Atmosphere

Many light-water reactor containments employ cooling systems for normal operation and in the event of a loss of coolant accident and steam release into the primary containment.[54] Each cooling unit embodies a cooling coil and axial flow fan. For normal operation, three fans operate and each of the companion coils is supplied with 800 gpm of cooling water, while two cooling assemblies are on standby. For emergency operation, five fans operate and each of the companion coils is fed by 1200 gpm of cooling water. Total emergency cooling capacity is 67×10^3 BTU/sec. Each fan is capable of handling 32,500 cubic feet per minute during emergency operation.

The employment of such a system within fusion reactor containments is feasible provided adequate assurances are made that leakage of water would not occur. As seen earlier in

Chapter 2, lithium-water reactions release large amounts of heat and hydrogen.

Using LITFIRE, the thermal response of the UWMAK-III containment to lithium fires with this design feature was investigated. The maximum containment overpressure as a function of cooling rate is shown in Figure 4.9. For the emergency space cooling rate of 67 X 10^3 BTU/sec, the maximum overpressure is reduced to 18.8 psig from the best estimate value of 31.9 psig. Corresponding reductions of the steel wall liner and cell gas temperatures occur.

4.4.2 Ventilation of Containment Atmosphere

During a hypothetical lithium spill and fire, it may be possible to relieve some of the containment atmosphere pressure using a purge exhaust (or pressure relief) system provided that the release of radioactive products into the cell gas is minimal. Light-water reactor containments employ such systems for normal operation.[55]

The purge exhaust system consists of two identical subsystems, each having a capacity of 25,000 cfm air flow. Each subsystem in the purge exhaust system is equipped with a belt-driven fan, prefilter, absolute filter, carbon filter, second absolute filter, ducts, Reactor Building isolation valves, and air sampling lines and radioactivity monitors. The exhausted air is filtered by prefilters and final filters having an efficiency of 95 per cent when tested according to National Bureau of Standards discoloration test method using atmospheric dust.

FIGURE 4.9

MAXIMUM UWMAK-III CONTAINMENT GAS OVERPRESSURE
DURING LI FIRE AS FUNCTION OF EMERGENCY SPACE COOLING RATE

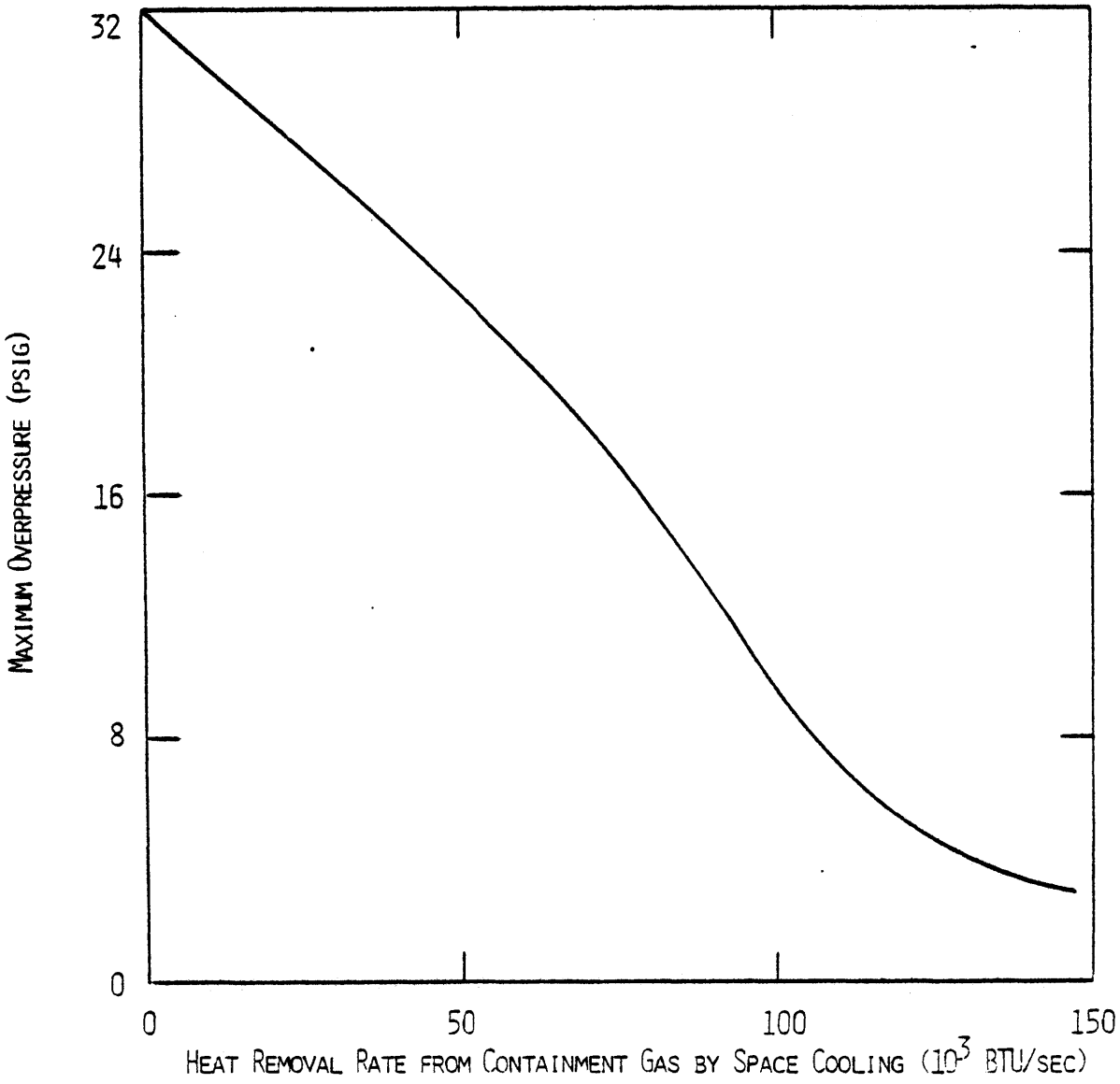

Using LITFIRE, the effectiveness of this design feature was studied under conditions of large lithium fires within the UWMAK-III containment. Figure 4.10 shows the maximum containment gas overpressure as a function of the ventilation rate. A ventilation rate of 50,000 standard cubic feet per minute (SCFM) reduced the maximum overpressure to 9.1 psig from the best estimate value of 31.9 psig. The maximum cell gas and steel wall liner temperatures were also reduced by 500 and 380 °F respectively from the best estimate values. However, further research is required to determine the feasibility of such a system in light of the large amounts of tritium likely to be released from an accident and the difficulty of removing tritrium gas from the exhaust stream.

4.4.3 Emergency Cooling of Steel Floor Liner

Another possible means of mitigating the consequences of lithium fire is the employment of a steel floor liner cooling system. This system would reduce the excessively large temperatures in the containment floor which otherwise would result from a lithium spill and fire.

The Fort St. Vrain High Temperature Gas Cooled Reactor[56] utilizes such a system for cooling the pre-stressed concrete reactor vessel liner. Two 100 percent capacity pumps provide 1650 gpm of water flow. The wall liner cooling tube spacing is 3.75 inches. The maximum heat flux through the walls is calculated to be 7.2×10^3 BTU/hr-ft^2 for accident conditions. This results in a heat flux through the cooling tubes of

FIGURE 4.10

MAXIMUM UWMAK-III CONTAINMENT GAS OVERPRESSURE DURING LI FIRE AS FUNCTION OF EMERGENCY VENTILATION RATE

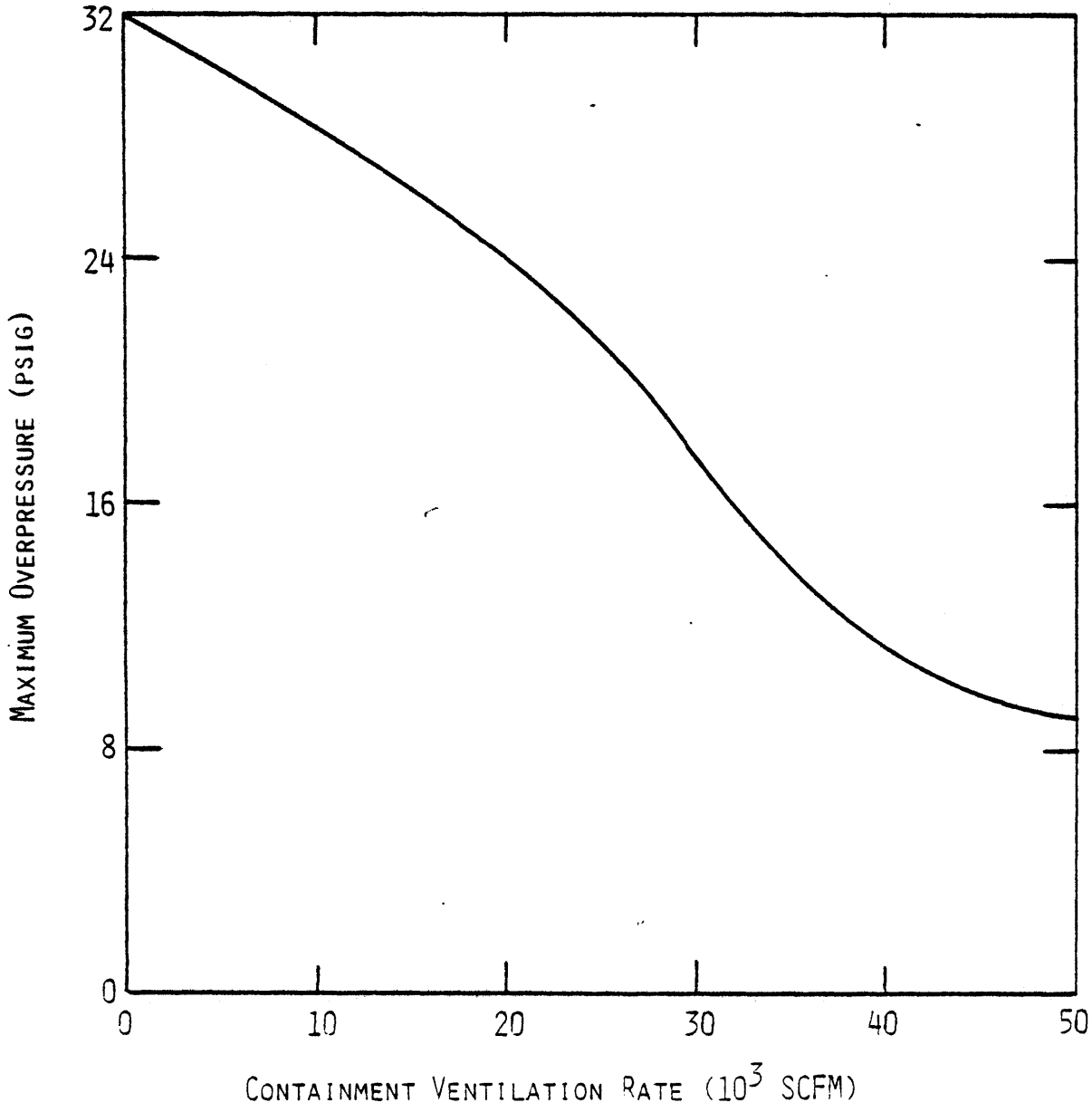

54,000 BTU/hr-ft^2 which is 27% of subcooled boiling and 9% of CHF (critical heat flux). Together, the 2 loops are capable of removing 13,000 BTU/sec under accident conditions.

With the employment of several cooling systems in the UWMAK-III containment, it may be possible to provide 50,000 BTU/sec of cooling, corresponding to a heat flux of 1.8 X 10^4 BTU/hr-ft^2 through the steel floor liner for a lithium pool area of 10,000 square feet. However, because of the potential for lithium-water reaction should the steel liner and coolant piping fail, it would be more practical to use a gas coolant such as helium. Heat could then be rejected to a secondary cooling system.

Using LITFIRE, the effectiveness of deploying a steel floor liner cooling system was examined. Figure 4.11 shows the maximum overpressure calculated during lithium fire as a function of the floor liner cooling rate. For a reasonable cooling rate of 50,000 BTU/sec, the maximum containment gas overpressure is reduced to 24.7 psig from the best estimate value of 31.9 psig. The maximum steel floor liner and concrete floor temperatures are also reduced by 300 °F from the best estimate values of 2111 and 2019 °F respectively. However, further research is needed to determine the ability of concrete structures to withstand such high temperatures. Undoubtedly, the concrete would lose most of its physical characteristics because of the evolution of water.

FIGURE 4.11

MAXIMUM UWMAK-III CONTAINMENT GAS OVERPRESSURE DURING LI FIRE AS FUNCTION OF EMERGENCY STEEL FLOOR LINER COOLING RATE

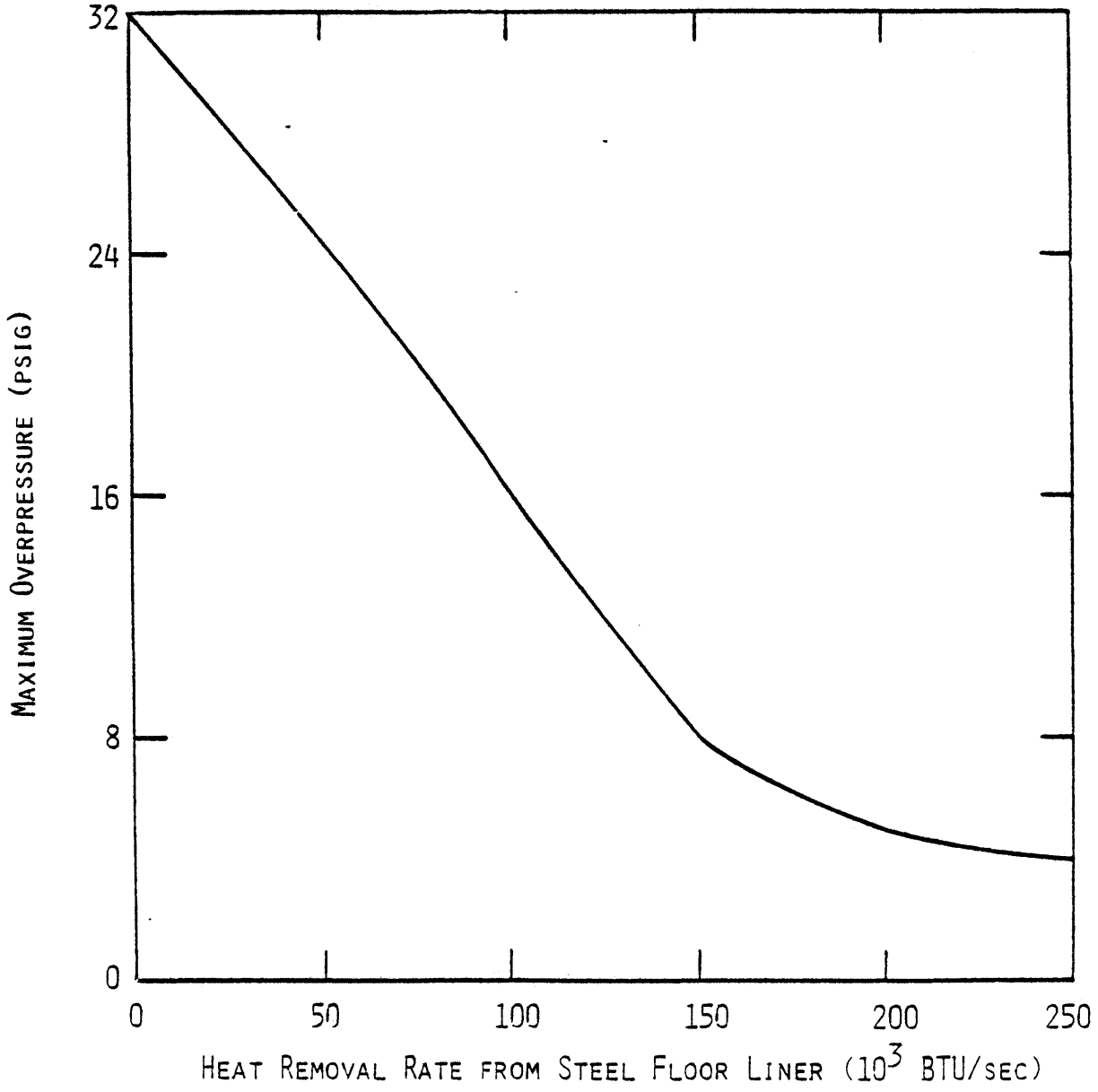

4.4.4 Other Possible Design Features

A number of possible design features have been considered for mitigating the consequences of sodium fires or small lithium fires. These include the use of catch pans and dump tanks on the floor of the reactor containment, inert gas flooding of the containment, and the addition of chemicals to the lithium pool for suppressing the fire.

4.4.4.1 Use of Catch Pans

Huber et al.[29] constructed such a catch pan system together with perforated covers. The covers consisted of a folded plate like a roof, thereby generating parallel collecting drains. The system was designed for 50 m^3 of sodium and a base area of 100 m^2. It was subdivided in pan sections of 1 X 2 m base area. Five sections form a pan row with the outlet to the drain tank in the center. The pan system works automatically without any action from outside.

Catching pans provided with a grooved cover yielded the following significant results vis-a-vis open pools:

1) The percentage of reacted sodium entrained as aerosols was reduced from 36% for open pool fires to 1% using catch pans.

2) Compared to open area conflagration, the environmental pollution by aerosols was lower by a factor of 300.

3) The specific combustion rate of sodium (lb/hr-ft^2) was reduced by a factor of 8 with the deployment of catch pans.

The effect of using catch pans is primarily to reduce the combustion rate of liquid metal with air. A reduction of the pool surface area likewise reduces the consequences of lithium fire. Using LITFIRE for example, a reduction in the pool surface area by a factor of 5 reduced the maximum containment gas overpressure from the best estimate value of 31.9 psig to 15.7 psig. Significant decreases in peak temperatures of the containment structures was also calculated. For example, the maximum steel wall temperature dropped from 786 to 490 °F by reducing the lithium pool surface area.

4.4.4.2 Lithium Fire Extinguishment with Chemicals

Ballif et al.,[14] Rodgers and Everson,[17] and Bulmer[16] summarize research performed on lithium fire extinguishment using chemicals. The number of materials suitable for controlling lithium fires is small and include graphite, lithium chloride, and a mixture of sodium chloride and graphite. However, these chemicals were applied to small fires on the order of 0.75 to 14 pounds in size. The effectiveness of using chemicals in large lithium spills (48,000 pounds) is yet to be determined. The quantity of chemicals required for extinguishing large lithium fires might well be in excess of the total inventory of liquid metal. Although the use of chemicals should be given further consideration, it is questionable whether this should be the primary mechanism for mitigating the consequences of large lithium pool fires.

4.4.4.3 Inert Gas Flooding of Containment

As discussed earlier, inert gas flooding of the EBTR cell is an effective means of preventing the in-leakage of oxygen and nitrogen into the primary containment atmosphere during lithium fires. However, inert gas flooding in itself would not smother the lithium fire, especially in large containments such as the UWMAK-III design. The volume of inert gas, presumably helium or argon, needed to displace oxygen or nitrogen would be prohibitively expensive. There is also evidence that the application of an inert gas like argon to a well established lithium fire, with a pool surface area on the order of 10 square feet or greater, is completely ineffective.[57] Direct application to the burning surface did retard the fire somewhat but removal of the argon gas source caused combustion to immediately resume for lithium remaining in the liquid state.

4.4.5 Combined Effect of Safety Features

Using LITFIRE, the combined effect of various safety systems in mitigating the consequences of lithium fire within the UWMAK-III containment were considered. The results are summarized in Table 4.3. A readily achievable and cost effective design strategy employs a containment air cooling system of 67,000 BTU/sec capacity combined with an atmosphere of 5 percent oxygen or less. Case 108 in Table 4.3 summarizes the consequences of lithium fire under these conditions. Although the lithium-nitrogen reaction is not retarded, because

TABLE 4.3

Summary of Effectiveness of Designed Safety Features

Case No.	Max. Gas Overpressure (psig)	Max. Gas Temp. (°F)	Max. Steel Floor Temp. (°F)	Max. Steel Wall Temp. (°F)	Max. Concrete Floor Temp. (°F)	Max. Concrete Wall Temp. (°F)
93 Best Estimate	31.9	1389	2111	786	2019	608
111 ESCR=67,000 ESFLCR=50,000	9.5	483	1769	413	1647	310
119 ESCR=67,000 ESFLCR=50,000 EXHSTV=25,000	2.42	208	1634	273	1453	190
108 WO2=5% ESCR=67,000	3.65	247	1764	226	1524	141
109 WO2=5% ESFLCR=50,000	10.38	509	1674	247	1386	152

ESCR = emergency space cooling rate (BTU/sec)
ESFLCR = emergency steel floor liner cooling rate (BTU/sec)
EXHSTV = exhaust rate of containment gas (ft^3/min)

of the 95% nitrogen concentration within the containment, the consequences are found to be greatly diminished. The temperature-pressure histories of the containment structures and gas are shown in Figures 4.12 and 4.13. Note however that the concrete floor is not protected because of the high temperature of the liner. The concrete floor will substantially erode, although the reduction in the concrete wall temperature will assure the integrity of the wall.

FIGURE 4.12

TEMPERATURE HISTORY OF THE UWMAK-III STRUCTURES DURING LI FIRE AND EMPLOYING READILY AVAILABLE DESIGN STRATEGIES

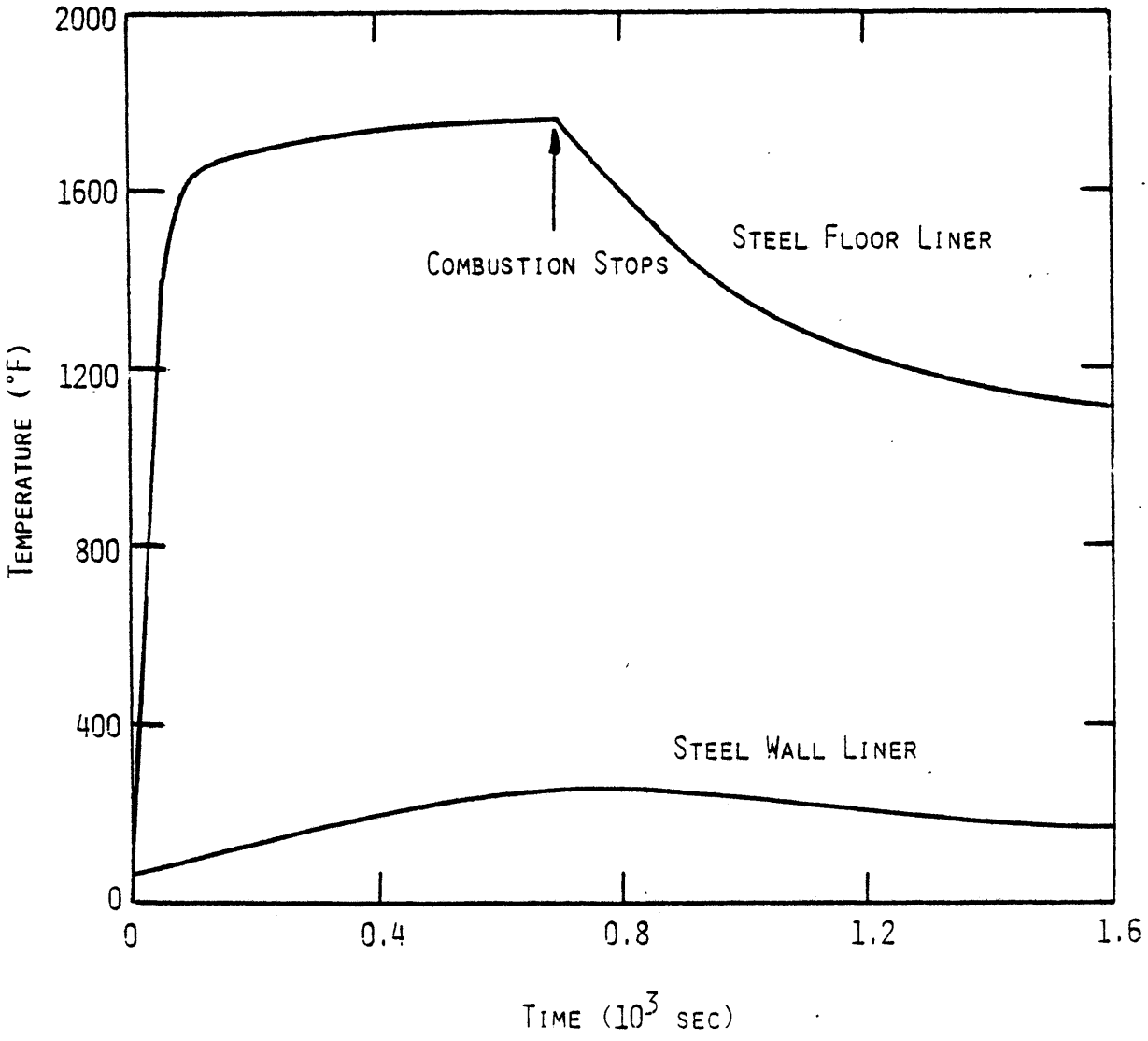

FIGURE 4.13

PRESSURE HISTORY OF THE UWMAK-III CONTAINMENT GAS DURING LI FIRE AND EMPLOYING READILY AVAILABLE DESIGN STRATEGIES

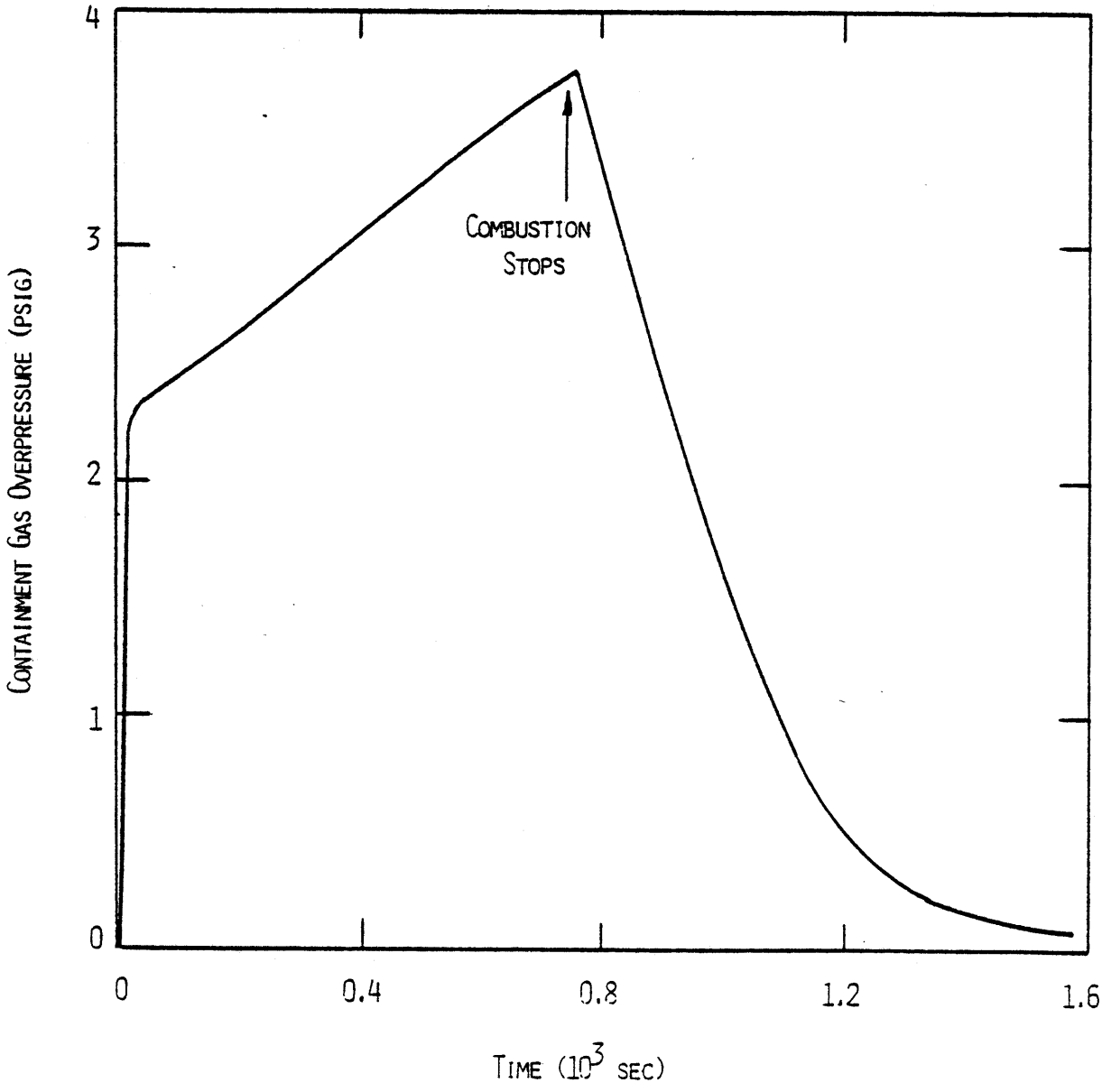

V. CONCLUSIONS AND RECOMMENDATIONS

5.1 Conclusions

There exist several large sources of energy and heat release within conceptual fusion reactor designs. One of these is lithium fire resulting from a hypothetical rupture of the coolant piping and lithium spill within the containment.

Analysis of lithium-air reactions has shown that in the event of a fire, the maximum temperatures produced would lie below the boiling point of all, and the melting point of most, structural materials. However, sufficiently high temperatures would be reached to damage instrumentation as well as the outer layers of concrete structures.

Without adequate protective measures, containment gas overpressures as high as 31.9 psig could be experienced from the spill and combustion of one coolant loop of the UWMAK-III design. In addition, large temperatures on the order of 1500 °F or greater would be attained by structures. With the incorporation of inherent and engineered safety designs, the consequences can be greatly reduced. In particular, consideration should be given to the following design strategies:

1) Reducing the lithium inventory per cooling loop by increasing the number of cooling systems;

2) Reducing the oxygen concentration within the containment, or completely replacing the cell atmosphere with an inert gas if possible;

3) Decreasing the initial containment pressure if normal atmospheres are employed;

4) Using structural materials with high heat removal potential (by maximizing $A\sqrt{\rho\ k\ C_p}$);

5) Installing a containment atmosphere cooling system (fan-coil type) as used in many light water reactor designs;

6) Employing a catch pan-dump tank system below likely areas of lithium spill;

7) Enclosing likely spill areas into air-tight compartments to prevent in-leakage of reactive gases in the event of fire;

8) Installing a containment building pressure relief system capable of handling large air flow rates through an efficient aerosol filtering system;

9) Storing large quantities of fire fighting chemicals for the eventual extinguishment of possible fires.

The ELMO Bumpy Torus Reactor reference design offers an advantage over the Tokamak-type designs from the viewpoint of lithium fire safety. The containment thermal responses of other conceptual fusion reactor designs to lithium fire have not been considered in this study because of the lack of detailed information on the cooling systems and containment designs. However, the LITFIRE program could be used for investigating lithium fire under different circumstances given adequate design specifica-

tions.

5.2 Recommendations for Future Study

The following items are recommended for further study:

1) Experimental verification of the lithium combustion zone model developed in this study is needed, particularly for large-scale fires. Specifically, more information is required on the properties of lithium aerosol products, i.e. percentage of reaction products released as aerosol particles, particle size, distribution, chemical nature, and so forth.

   Presently, experimental work on lithium fire is underway at the Hanford Engineering Development Laboratory. It is expected that the series of tests being conducted will provide adequate information for verifying the applicability of LITFIRE under a variety of circumstances.

2) A more detailed model is needed to account for large gradients in temperature and concentration of various gases and aerosols within the containment. In addition, the effect of multi-component diffusion (i.e. water vapor, nitrogen, oxygen) on the combustion rate should be considered. These effects were not accounted for in this study.

3) LITFIRE presently calculates mass transport to the combustion zone on the basis of Reynold's analogy

between heat an mass transport. It is assumed that steady-state convection is established immediately following a lithium spill. In reality, a finite amount of time is required for steady state conditions to be reached within a containment. A transient natural convection model for large containments, internally heated from below, would be useful.

4) Calculations made with LITFIRE have shown that the concrete floor layer just below the steel liner would reach temperatures in excess of 1300 °F under all postulated accident scenarios involving a lithium spill within the UWMAK-III containment. At such high temperatures, there would be significant erosion of the concrete and evolution of water. Further analysis is required to determine the integrity of concrete and the enitre floor structure under such conditions.

5) Although this study considers the spectrum of possible consequences from lithium fire, no mention is made of the probabilities of initiating a particular event. A more detailed analysis of coolant piping failure mechanisms pertaining to fusion reactors is needed.

REFERENCES

1. J. O. Cowles and A. D. Pasternak, "Lithium Properties Related to Use as a Nuclear Reactor Coolant," Lawrence Radiation Laboratory, Rept. UCRL-50647 (1968).

2. The University of Wisconsin Fusion Feasibility Study Group, "UWMAK-III, A Non-Circular Tokamak Power Reactor Design," UWFDM-150, July, 1976.

3. The University of Wisconsin Fusion Feasibility Study Group, "UWMAK-I, A Wisonsin Toroidal Fusion Reactor Design," UWFDM-68, March 15, 1974.

4. D. G. McAlees et al., The ELMO Bumpy Torus Reactor (EBTR) Reference Design, ORNL-TM5669, November 1976.

5. JANAF Thermochemical Tables, (Midland, Mich.: Dow Chemical Co., 1970)

6. I. M. Klotz, Chemical Thermodynamics, rev. ed., (New York: Benjamin, Inc., 1964).

7. F. U. Zeggeren and S. H. Storrey, The Computation of Chemical Equilibrium, (London: Cambridge University Press, 1970).

8. S. Gordon and B. J. McBride, "Computer Program for Calculations of Complex Chemical Equilibrium Compositions, Rocket Performance, Incident and Reflected Shocks, and Chapman-Jouguet Detonation," NASA SP-273 (1971).

9. D. Okrent, et al., "On the Safety of Tokamak-Type, Central Station Fusion Power Reactors," Nucl. Eng. Design, (1976).

10. I. Charak and L. W. Person, "SPOOL-FIRE: Analysis of Spray and Pool Na Fire," ANL, presented at the ANS International Meeting on Fast Reactor Safety and Related Physics, Oct., 1976, Chicago.

11. P. R. Shire, "Reactor Sodium Coolant Hypothetical Spray Release for Containment Accident Analysis: Comparison of Theory with Experiment," HEDL, April, 1974.

12. P. Beireger, et al., "SOFIRE II User Report," AI-AEC-13055, April, 1973.

13. R. D. Peak and D. D. Stepnewski, "Computational Features of the CACECO Containment Analysis Code," HEDL SA-922, May 29, 1975.

14. J. L. Ballif et al., "Lithium Literature Review: Lithium's Properties and Interactions," HEDL, TC-1000 January, 1978.

15. Yu I. Ostroushko, et al., Lithium, Its Chemistry and Technology, USAEC Division of Technical Information, AEC-tr-4940, July, 1962.

16. G. H. Bulmer, "The Thermonuclear Fusion Reactor: Some Aspects of Lithium Fire Safety," FTSG(M&C) (71) p. 26, FRESG (71) p.3.

17. S. J. Rodgers and W. A. Everson, "Extinguishment of Alkali Metal Fires," Technical Documentary No. APL TDR 64-114, October 1964.

18. H. C. Hottel, Review of "Certain Laws Governing the Diffusion Burning of Liquids," by V. I. Blinov and Khudiakov of USSR, Fire Research Abstracts and Reviews, Volume 1, pp. 41-44, (1958).

19. D. B. Spalding, "The Burning Rate of Liquid Fuels from Open Trays by Natural Convection," Fire Research Abstracts and Reviews, v. 4, P. 234, (1962).

20. K. Akita and T. Yumoto, "Heat Transfer in Small Pools and Rates of Burning of Liquid Methanol," Tenth Symposium (International) on Combustion, pp. 943-948, The Combustion Institute, (1965).

21. M. Michaud, et al., "Oxygen and Combustion - Theoretical and Experimental Fundaments," Revue Générale de Thermique, Volume 4, pp. 527-551, (1965).

22. C. S. Kelly, "The Transfer of Radiation from a Flame to its Fuel," Journal of Fire and Flammability, Volume 4, p. 56, (1973).

23. N. H. Afgan and J. M. Beer, Editors, Heat Transfer in Flames, John Wiley and Sons, N.Y., (1974), pp. 413-439.

24. P. L. Blackshear, Editor, Heat Transfer in Fires: Thermophysics, Social Aspects, Economic Impact, John Wiley and Sons, N.Y., (1974), pp. 73-195.

25. A. M. Kanury, "Modeling of Pool Fires with a Variety of Polymers," Fifteenth Symposium (International) on Combustion, The Combustion Institute, (1974), p. 193.

26. W. E. Kastenberg et al., "Loss-of-Coolant Accidents in Lithium Cooled Fusion Blankets," Trans. Am. Nucl. Soc., (26) pp. 32-33, (1977).

27. M. S. Kazimi et al., "Aspects of Environmental and Safety Analysis of Fusion Reactors," Massachusetts Institute of Technology, MITNE-212, October 1977.

28. R. L. Koontz et al., "Aerosol Modeling of Hypothetical LMFBR Accidents," Atomics International, AI-AEC-12977, August, 1970.

29. F. Huber, et al., "Behavior of Na Area Conflagrations and Suitable Protecting Systems," presented at the ANS International Meeting on Fast Reactor Safety and Related Physics, October 1976, Chicago.

30. M. Fishender and O. A. Saunders, An Introduction to Heat Transfer, Oxford University Press, first edition, (1950), p. 97.

31. Frank Kreith, Principles of Heat Transfer, 3rd Ed., (New York: Intext Educational Publishers, (1973).

32. B. U. Sarma, et al., "Review of Current Sodium Fire Analytical Methods," GEAP-14148, September 1976.

33. M. Jakob, Heat Transfer, John Wiley & Sons, Inc., New York, N.Y., Volume 1, p. 534, 1949.

34. W. V. R. Malkus, "Discrete Transitions in Turbulent Convection," Proceedings of the Royal Society (London), series A, Volume 225, 1954, p. 185.

35. S. Globe, D. Dropkin, "Natural Convection Heat Transfer in Liquids Confined by Two Horizontal Plates and Heated from Below," Trans. of the ASME, J. of Heat Transfer, February 1959.

36. P. Beiriger et al., "SOFIRE II User Report," AI-AEC-13055, Atomics International, (1973).

37. E. R. G. Eckert and R. M. Drake Jr., Heat and Mass Transfer, McGraw-Hill, N.Y., (1959).

38. N. H. Chen and D. F. Othmer, J. Chem. Engr. Data, v. 7, p. 37, (1962).

39. Liquid Metals Handbook, 2nd ed., NAVEXOS-P-733, rev. (June 1952).

40. R. Siegel and J. R. Howell, Thermal Radiation Heat Transfer, McGraw-Hill, N.Y., (1972).

41. Theresa S. Krolikowski, "Violently Sprayed Sodium-Air Reaction in an Enclosed Volume" ANL-7472 (September 1968).

42. P. R. Shire, "Reactor Sodium Coolant Hypothetical Spray Release for Containment Accident Analysis: Comparison of Theory with Experiment," Proc. of the Fast Reactor Safety Meeting, Beverly Hills, Calif., April 2-4, 1974, CONF-740401-P1.

43. P. R. Shire, "A Combustion Model for Hypothetical Sodium Spray Fire Within Containment of an LMFBR,: M.S. Thesis, Univ. of Wash., 1972.

44. Letter, D. E. Simpson to K. Hikido, "Transmittal of SPRAY Computer Code," w/FFTFC-750140, Jan. 6, 1975.

45. P. R. Shire, et al., "A Sodium Droplet Combusion Model for Reactor Accident Analysis," Trans. Am. Nucl. Soc. (15), P. 812, (1972).

46. R. D. Peak, "CACECO Code," private transmittal, April 1974.

47. L. W. Person, "The Application of SPOOL-FIRE in Theoretical Analysis and Experimental Comparison," Nuclear Technology, Volume 32, March 1977.

48. B. U. Sarma, et al., "Review of Sodium Fire Analytical Models," GEAP-14053, June 1975.

49. S. S. Tsai et al., "Containment Design Basis Accident for LMFBR's: Review of Methods," BNL-NUREG-23221, September, 1977.

50. International Business Machines Corporation, "Continuous System Modeling Program II (CSMP II) - Program Reference Manual, Publication No. GH20-0367-4, 3rd, ed. (September 1972).

51. J. R. Humphreys, Jr., "Sodium-Air Reactions as They Pertain to Reactor Safety and Containment," Proceedings of the Second International Conference on the Peaceful Uses of Atomic Energy, Geneva, Paper 1893 (1958).

52. R. K. Hilliard et al., "Sodium Fire Protection by Space Isolation with Inert Gas Flooding," presented at the ANS International Meeting on Fast Reactor Safety and Related Physics, October, 1976, Chicago.

53. M. Jakob and G. A. Hawkins, Elements of Heat Transfer and Insulation, John Wiley and Sons, Inc., N.Y., (1950), pp. 66-68.

54. Metropolitan Edison Company, Jersey Central Power and Light Company, Three Mile Island Nuclear Station - Unit 2, PSAR, revised March 10, 1969, Docket No. 50-320, section 6, p. 14.

55. Ibid, section 5, p. 19.

56. Public Service Company of Colorado, Fort St. Vrain Nuclear Generating Station, PSAR, Amendment No. 10, February 12, 1968, Docket No. 50-267-1.

57. "Final Report on Development of Fire Extinguishing Agents for Lithium," Arthur D. Little, Inc., Contract No. AT-(30-1)-2527, C-62839, Dec. 30, 1960.

58. K. E. Torrance et al., "Experiments on Natural Convection in Enclosures with Localized Heating from Below," J. Fluid Mech. (1969), vol. 36, pp. 21-31.

59. K. E. Torrance and J. A. Rockett, "Numerical Study of Natural Convection in an Enclosure with Localized Heating from Below - Creeping Flow to the Onset of Laminar Instability, J. Fluid Mech. (1969), vol. 36, pp. 33-54.

APPENDIX A

Complete Listing of LITFIRE

```
C      LITFIRE COMPUTER CODE IS A MODIFICATION OF THE CODE SPOOL-FIRE DEVELOPED
C      AT ARGONNE NATIONAL LABORATORY.  LITFIRE DESCRIBES THE TEMPERATURE-
C      PRESSURE HISTORY OF A FUSION REACTOR CONTAINMENT TO LITHIUM FIRE
C      AND WAS DEVELOPED IN THE NUCLEAR ENGINEERING DEPARTMENT AT MIT IN 1978.
C
C     DEFINITION OF VARIABLES AND UNITS
C
C      AKLI     THERMAL CONDUCTIVITY OF LITHIUM   BTU/FT.-HR.-DEG.F
C      AK1,AK2   PROD. OF THERMAL COND. AND PRANDTL NO.   BTU/HR-FT-DEG. F
C      ASLI SURFACE AREA OF LITHIUM      FT2
C      AW      EXPOSED WALL AREA    FT2
C      B   USED IN CALC. THERMAL RESIST. OF LINER-GAP-CONC.    IN.
C      B1 & B2   COEFFICIENT OF GAS EXPANSION      1/DEG. F
C      BLIN   TIME AFTER SPILL AT WHICH INERT GAS FLOODING AND
C             EXHAUST BEGINS   SEC
C      BLOUT   TIME AFTER SPILL AT WHICH FLOODING AND EXHAUST STOPS  SEC
C      BLOWR  INERT GAS INPUT RATE  LB/SEC
C      BLOWV   INERT GAS INPUR RATE   FT3/MIN
C      CH    CONTAINMENT HEIGHT      FT
C      CLIG,CGLI,CLIST,CSBLI    SPECIFIC THERMAL DIFFUSIVITIES
C                              OF VARIOUS NODES      1/SEC
C      CMBR      TOTAL COMBUSTION RATE     LB. LI/SEC.-FT2
C      CMBRH     TOTAL COMBUSTION RATE     LB. LI/HR.-FT2
C      CMBRHI    INITIAL COMBUSTION RATE   LB. LI/HR-FT2
C      CMBRN  COMB. RATE FOR NITROGEN REACTION  LB. LI/SEC.-FT2
C      CMBRO  COMB. RATE FOR OXYGEN REACTION   LB. LI/SEC.-FT2
C      CMBRW  COMB. RATE FOR WATER VAPOR REACTION   LB. LI/SEC.-FT2
C      CPA  INERT GAS SPECIFIC HEAT  BTU/LB.-DEG. F
C      CPAB   SPEC. HEAT OF FLOODING GAS  BTU/LB-DEG.F
C      CPCZ,CGCZ,CCZG,CCZP,CLIG,CGLI  SPECIFIC THERMAL DIFFUSIVITIES OF
C                          VARIOUS NODES     1/SEC
C      CPLI SPECIFIC HEAT OF LI      BTU/LB. -DEG. F
C      CPLIN  SPEC. HEAT OF LITHIUM NITRIDE        BTU/LB.-DEG. F
C      CPLIO      SPECIFIC HEAT OF LITHIUM OXIDE   BTU/LB.-DEG. F
C      CPLIOH    SPECIFIC HEAT OF LITHIUM HYDROXIDE   BTU/LB.-DEG. F
C      CPMCZ     EFFECTIVE HEAT CAPACITY OF COMB. ZONE   BTU/DEG F
```

```
C       CPMH2     HEAT CAPACITY OF HYDROGEN IN CONTAINMENT    BTU/DEG. F
C       CPMLIH    HEAT CAP. OF LITH. HYDROXIDE IN CONT.       BTU/DEG. F
C       CPMLIN    HEAT CAP. OF LITH. NITRIDE IN CONT.       BTU/DEG. F
C       CPMLIO    HEAT CAP. OF LITHIUM OXIDE IN CONTAINMENT    BTU/DEG. F
C       CPMNI    HEAT CAPACITY OF NITROGEN IN CONTAINMENT    BTU/DEG. F
C       CPMOX    HEAT CAPACITY OF OXYGEN IN CONTAINMENT    BTU/DEG. F
C       CPMWA     HEAT CAP. OF WATER VAP. IN CONTAINMENT     BTU/DEG. F
C       CPWA      SPEC. HEAT OF WATER VAPOR     BTU/LB.-DEG. F
C       C1,C2,...C10  SPECIFIC THERMAL DIFFUSIVITY OF NODES    1/SEC.
C       DELOUT    OUT TIME STEP    SEC.
C       DELT      INTEGRATION TIME STEP     SEC.
C       DFILM        LITHIUM VAPOR FILM THICKNESS       FT
C       DIFF       DIFFUSION  OEFF. TO COMB. ZONE     FT2/HR.
C       DIFFLI       LITHIUM VAPOR DIFFUSION COEFFICIENT     FT2/SEC
C       DTBDT(I)    CONC. FLOOR TEMP. RATE OF CHANGE, NODE I    DEG. F/SEC.
C       DTCDT(I)    CONC. WALL TEMP. RATE OF CHANGE, NODE I    DEG. F/SEC.
C       DTMIN    MINIMUM TIME STEP TO BE USED    SEC.
C       DT1,...DT4    USED IN CALCULATING TIME STEP    SEC.
C       DYNAMI    SUBROUTINE USED IN CONTROLLING INTEGRATION LOOPS
C       D1,D2    KINEMATIC VISCOSITY OF CELL GAS (SQUARED)    FT4/SEC2
C       EMCONC      THERMAL EMISSIVITY OF CONCRETE
C       EMCZ       THERMAL EMISSIVITY OF COMBUSTION ZONE
C       EMG    THERMAL EMISSIVITY OF CELL GAS
C       EMLI      THERMAL EMISSIVITY OF LITHIUM POOL
C       EMSTL       THERMAL EMISSIVITY OF STEEL LINER
C       ESCR    HEAT REMOVAL RATE BY EMERGENCY SPACE COOLING    BTU/SEC
C       ESCTIN    TIME AFTER SPILL WHEN ESCR BEGINS    SEC
C       EXHSTR   RATE OF CONTAINMENT GAS EXHAUST   LB/SEC
C       EXHSTV    RATE OF CONTAINMENT GAS EXHAUST    FT3/SEC
C       EXX    USED IN CALC. MASS & HEAT TRANSF. COEFF.    1/FT3
C       EX1,EX2    USED IN CALCULATING MASS & HEAT TRANSF. COEFF.   1/FT
C       FF1,FF2    USED IN HEAT BALANCE EQS. FOR SPRAY FIRE    BTU
C       FMLEAK    FRACT. OF MASS LEAKED OUT OF CONTAINMENT
C       FMLEFT       FRACTION OF MASS STILL WITHIN CONTAINMENT
C       FNI    WT. FRACTION OF NITROGEN IN CELL GAS
C       FOX    WT. FRACTION OF OXYGEN IN CELL GAS
```

```
C       FRA     FRACTION OF COMBUSTION PRODUCTS EVOLVED INTO CELL GAS
C       FWA     WT. FRACTION OF WATER VAPOR IN CELL GAS
C       G    AIR GAP BETWEEN STEEL LINER AND CONCRETE FLOOR    IN.
C       GIN    GRAVITATIONAL CONSTANT      32.2 FT/SEC2
C       H    INTERIOR FILM COEF.     BTU/HR-FT**2-DEG. F
C       HA       EXTERIOR FILM COEF.  BTU/HR-FT**2-F
C       HB     HEAT TRANSF. COEFF. FROM POOL    BTU/HR.-FT2-DEG. F
C       HF     GAS TRANSPORT COEFF. TO POOL     FT/HR
C       HTCAPG  HEAT CAPACITY OF CONTAINMENT ATMOSPHERE  BTU/DEG.F
C       INIT    INITIALIZING SUBROUTINE FOR INTEGRATION CALCULATIONS
C       INTGRL    ARITHMETIC STATEMENT FUNCTION FOR FINDING INTEGRALS
C       K     LEAK RATE CONSTANT FROM CONTAINMENT    2.588E-09
C       KFILM     THERM. COND. OF LI POOL/COMB. ZONE FILM    BTU/HR-FT-F
C       L    CONCRETE WALL ELEMENT THICKNESS    IN.
C       LEAK    CELL GAS LEAKAGE RATE FROM CONTAINMENT    1/SEC.
C       LEAKO    INITIAL CELL GAS LEAKAGE RATE FROM CONTAINMENT  1/SEC.
C       LIBP     LITHIUM BURNED IN POOL FIRE        LB.
C       LIC        MASS OF LITHIUM IN CONTAINMENT        LB.
C       LIS      LITHIUM USED IN SPRAY FIRE         LB.
C       LIT         MASS OF LITHIUM IN POOL INITIALLY       LB.
C       L1    CONCRETE FLOOR ELEMENT THICKNESS    IN.
C       MA    WT. OF INERT GAS IN CELL     LB.
C       MAIR    WT. OF CELL GAS    LB.
C       MH2     WT. OF HYDROGEN IN CONT. CELL GAS     LB.
C       MLIH      WT. OF LITHIUM HRYDROXIDE IN CONT. CELL GAS    LB.
C       MLIN      WT. OF LITHIUM NITRIDE IN CONT. GAS CELL      LB.
C       MLINI    MASS OF LITHIUM NITRIDE IN CONT. INITIALLY    LB
C       MLIO    WEIGHT OF LITHIUM OXIDE IN CELL GAS. PRESENTLY ALL OT THE
C               SPRAY FIRE PRODUCT REMAINS IN THE CELL GAS.  A FRACTION
C               OF THE PRODUCTS FROM THE POOL FIRE IS ADDED      LB.
C       MLIOI    MASS OF LITHIUM OXIDE IN CONT. INITIALLY    LB
C       MNI      WEIGHT OF NITROGEN IN CONTAINMENT CELL GAS      LB.
C       MNII    INITIAL WEIGHT OF NITROGEN IN CONTAINMENT    LB
C       MOX     WEIGHT OF OXYGEN IN CELL GAS     LB.
C       MOXI    INITIAL WEIGHT OF OXYGEN IN CONTAINMENT    LB.
C       MWA     WEIGHT OF WAT. VAP. IN CONTAINMENT CELL GAS     LB.
```

```
C       MWAI     MASS OF WATER VAPOR IN CONT. CELL GAS INITIALLY   LB
C       NAME(I)    INPUT CONTAINING PROGRAM TITLE AND HEADING
C       OUTINT       LEAK FRACTION
C       OVERP    CONTAINMENT OVER PRESSURE    PSIG
C       OXLB OXYGEN BURNED    LB.
C       OXLBI    OXYGEN BURNED INITIALLY    LB.
C       OXLFS    OXYGEN LEFT AFTER SPRAY FIRE    LB.
C       PA     GAS PRESSURE IN CELL     PSIA
C       PAZERO    INITIAL CELL PRESSURE    PSIA
C       PLIV      PARTIAL PRESSURE OF LITHIUM VAPOR       PSIA
C       QCN   HEAT OF COMB. FOR NITROGEN REACTION    BTU/LB. LI
C       QCO       HEAT OF COMBUSTION FOR OXYGEN REACTION     BTU/LB. LI
C       QCW     HEAT OF COMB. FOR REACTION WITH WATER VAPOR     BTU/LB. LI
C       QIN    HEAT ADDITION TO CELL GAS FROM SPRAY FIRE    BTU
C       QOUT1,2,3,4     USED IN HEAT BALANCE EQS. FOR SPRAY FIRE     BTU
C       QRADC,QRADG,QRADB,QRADW,QRADP    VARIOUS RADIANT HEAT
C                                        TRANSFER RATES     BTU/HR.
C       QVAP     HEAT OF VAPORIZATION OF LITHIUM      BTU/LB
C       RA         MEAN RADIUS OF COMBUSTION PRODUCT PARTICLES     MICRONS
C       RCMBH2    STOICH. COMB. RATIO FOR H2O VAPOR REACT.    LB. LI/LB. H2
C       RCMBN    STOICH. COMB. RATIO OF NITROGEN REACT.    LB. LI / LB. N
C       RCMBO    STOICH. COMB. RATIO FOR OXYGEN REACTION   LB. LI/LB. O
C       RCMBW    STOICH. COMB. RATIO FOR WAT. VAP. REACT.   LB. LI/LB. H2O
C       RELERR    MAXIMUM ALLOWABLE FRACTIONAL TEMP. CHANGE ACROSS A SINGLE
C                  INTEGRATION STEP.  USED TO VARY TIME STEP.
C       RHLI     DENSITY OF LITHIUM    LB. / FT3
C       RHOA    DENSITY CELL GAS LB/FT3
C       RHOAI    INITIAL DENSITY OF CELL GAS    LB/FT3
C       RHOLIH     DENSITY OF LITHIUM HYDROXIDE    LB/FT3
C       RHOLIN     DENSITY OF LITHIUM NITRIDE     LB/FT3
C       RHOLIO      DENSITY OF LITHIUM OXIDE    LB/FT3
C       RHOLIV     LITHIUM VAPOR DENSITY ABOVE POOL       LB/FT3
C       RIFCZG    RADIATIVE INTERCHANGE FACTOR BETWEEN COMB. ZONE AND THE
C              CELL GAS
C       RIFCZP    RADIATIVE INTERCHANGE FACTOR BETWEEN COMB. ZONE AND
C                  THE POOL SURFACE
```

```
C       RIFCZW   RADIATIVE INTERCHANGE FACTOR BETWEEN COMB. ZONE AND
C              CONTAINMENT WALLS
C       RIFPG    RAD. INT. FAC. BETWEEN POOL AND CELL GAS
C       RIFPW    RAD. INT. FACT. BETWEEN POOL AND WALL
C       RIFSLC    RADIATIVE INTERCHANGE FACTOR BETWEEN STEEL LINER
C                 AND CONCRETE SURFACE
C       RIN UNIVERSAL GAS CONSTANT   1545 FT. LBF./LB.MOLE-DEG. F
C       RNILB  RATE OF NITROGEN CONSUMPTION        LB./ SEC
C       RN2   DEGREE TO WHICH NITROGEN-LI REACTION OCCURS.  VALUE IS
C             BETWEEN ZERO AND ONE (=1 FOR NO REACTION,=0 FOR COMPLETE )
C       ROXLB    RATE OF OXYGEN CONSUMPTION BY POOL FIRE   LB./SEC.
C       RTLI,RTG,RADB,RADW,RADCB,RADCW          VARIOUS RATES OF TEMP.
C              CHANGE OF NODES   DEG. F/SEC.
C       RWALB    RATE OF WATER VAPOR CONSUMPTION       LB./SEC
C       RWCZ,RCZW,RCZG,RADB,RADW,RADCB,RADCW,RLIW,RWLI,RGLI,RLIG ----
C           VARIOUS RATES OF TEMP. CHANGE OF NODES   DEG. F/SEC
C       SFLCR    HEAT REMOVAL RATE BY EMERGENCY COOLING OF STEEL
C              FLOOR LINER   BTU/SEC
C       SFLTIN    TIME AFTER SPILL WHEN SFLCR BEGINS   SEC
C       SPILL     TOTAL WEIGHT OF LITHIUM SPILLED   LB.
C       SPRAY      WEIGHT FRACTION OF LITHIUM CONSUMED IN THE SPRAY FIRE
C       TA     AMBIENT TEMPERATURE   DEG. F
C       TB(I)    TEMP. OF ITH NODE OF CONCRETE FLOOR   DEG. R
C       TBIC(I)    INITIAL TEMP. OF ITH NODE OF CONCRETE FLOOR   DEG. R
C       TBF, TCF,TGF, ETC.   CORRESPONDING TEMP. IN DEGREES FAHRENHEIT
C       TBLOW  INERT GAS INLET TEMP.  DEG. R
C       TC(I)    TEMP. OF ITH NODE OF CONCRETE WALL   DEG. R
C       TCIC(I)    INITIAL TEMP. OF ITH NODE OF CONCRETE WALL   DEG. R
C       TE   EQUILIBRIUM TEMP. RESULTING FROM SPRAY FIRE   DEG. R
C       TFEFF  NORMALIZED TEMP. OF LI POOL/COMB. ZONE FILM
C       TG   GAS TEMP. AFTER SPRAY FIRE    DEG. R
C       TGZERO     INITIAL CELL GAS TEMP.     DEG. R
C       THF   CONCRETE FLOOR THICKNESS    IN.
C       THW   CONCRETE WALL THICKNESS    IN.
C       TIME   TIME AFTER SPILL HAS OCCURRED   SEC.
C       TIMEF   STOP INTEGRATION TIME   SEC.
```

```
C       TIMEO     OUTPUT TIME INDICATOR    SEC.
C       TLI      LITHIUM TEMP. IN POOL    DEG. R
C       TLIO    INITIAL LITHIUM POOL TEMP.     DEG. R
C       TMELT     MELTING TEMP. OF LITHIUM   DEG. R
C       TO    TEMP. OF CELL GAS AFTER SPRAY FIRE   DEG. R
C       TS    STEEL WALL LINER TEMP.  DEG. R
C       TSB     STEEL FLOOR LINER TEMP.  DEG. R
C       TSBI    INITIAL STEEL FLOOR LINER TEMP.   DEG.R
C       TSZERO    INITIAL STEEL WALL LINER TEMP.  DEG. R
C       TVAP     BOILING POINT OF LITHIUM    DEG. R
C       T1    FILM TEMP. BETWEEN CELL GAS AND POOL   DEG. R
C       T2    FILM TEMP. BETWEEN CELL GAS AND STEEL WALL LINER   DEG. R
C       USUBA    HEAT TRANSF. COEFF., CONTAINMENT-AMBIENT  BTU/SEC-FT2-DEG. F
C       V     CELL FREE VOLUME     FT3
C       W     THICKNESS OF STEEL POOL LINER     IN.
C       WA     WT. FRACTION OF INERT GAS IN ATMOSPHERE
C       WN2   WEIGHT FRACTION OF NITROGEN IN ATMOSPHERE
C       WN2B     WEIGHT FRACTION OF NITROGEN IN FLOODING GAS
C       WO2    WEIGHT FRACTION OF OXYGEN IN ATMOSPHERE
C       WO2B   WEIGHT FRCTION OF OXYGEN IN FLOODING GAS
C       WWAB    WT. FRACTION OF WATER VAPOR IN FLOODING GAS
C       XBLOW     USED IN CONJUNCTION WITH IBLOW
C       XESC    USED IN CONJUNCTION WITH IESC
C       XMAIR    AMOUNT OF GAS IN CONTAIMENT AFTER SPRAY   LB.-MOLES
C       XMOL    MOL. WEIGHT OF CONTAINMENT GAS   LB./LB.-MOLE
C       XMOLA      MOLECULAR WT. OF INERT GAS   LB./LB.-MOLE
C       XMOLAB    MOL. WT. OF INERT FLOODING GAS
C       XSFLC   USED IN CONJUNCTION WITH ISFLC
C       YALICZ    EFFECTIVE THERMAL ADMITTANCE,  FILM-COMB. ZONE BTU/SEC-DEG. F
C       YALIG      EFFECTIVE THERMAL ADMITTANCE, POOL-CELL GAS BTU/SEC-DEG. F
C       YAPCZ      EFFECTIVE THERMAL ADMITTANCE POOL-COMB. ZONE  BTU/SEC-DEG F
C       ZLI     THICKNESS OF LITHIUM NODE      IN.
C       ZZ1    POOL TEMP. RATE OF CHANGE   DEG. F/SEC.
C       ZZ4    CELL GAS TEMP. RATE OF CHANGE   DEG. F/SEC.
C       ZZ5    STEEL WALL LINER TEMP. RATE OF CHANGE   DEG. F/SEC.
C       ZZ6     COMB. ZONE TEMP. RATE OF CHANGE    DEG. F/SEC
```

```
C       ZZ7   FLOOR STRUCTURE TEMP. RATE OF CHANGE   DEG. F/SEC.
C       ZZ99   USED TO ENSURE POSITIVE COMBUSTION RATE
C
C     PROGRAM DECISION FLAGS
C
C       IBLOW = 1  FLOOD CONTAINMENT WITH INERT GAS.
C             = 0  NO CONTAINMENT FLOODING.
C       ICMB = 0  NO OXYGEN LEFT AFTER SPRAY FIRE.
C            = 1  THERE IS STILL OXYGEN LEFT AFTER SPRAY FIRE.
C                 SET INITIALLY TO 1 AND THEN RESET TO 0 WHEN THE
C                 PROGRAM CALCULATES THAT THE OXYGEN HAS RUN OUT.
C       ICNI = 1  NITROGEN REACTIONS POSSIBLE.
C            = 0  NITROGEN REACTIONS NOT POSSIBLE.
C       ICZ = 1  COMBUSTION ZONE MODEL USED
C           = 0  COMBUSTION ZONE MODEL NOT USED
C       IESC = 1  EMERGENCY SPACE COOLING OPTION
C            = 0  NO EMERGENCY SPACE COOLING
C       ILIT = 0  NO LITHIUM LEFT TO BURN.
C            = 1   LITHIUM LEFT TO BURN (INITIAL CONDITION).
C       IMETH = 1  RUNGE-KUTTA METHOD OF INTEGRATION USED.
C             = 3   SIMPSON'S RULE METHOD OF INTEGRATION USED.
C       IPAGE   NO. OUTPUT LINES PER PAGE
C       ISFLC = 1  EMERGENCY COOLING OF STEEL FLOOR LINER OPTION
C             = 0  NO EMERGENCY COOLING OF STEEL FLOOR LINER
C
      DIMENSION TCF(20),TBF(20),TB(20),TC(20),DTCDT(20),DTBDT(20),
     .          TCIC(20), TBIC(20), NAME(100)
      REAL INTGRL,K,L,LEAK,LEAKO,LIT,LIS,LIC,LIBP,L1,MA,MAIR,MH2,KFILM,
     .     MLIH,MLIN,MLIO,MNI,MOX,MWA,MOXI,LILP,MAI,MLIOI,MNII,MWAI,
     .     MLINI
      COMMON IMETH,ICOUNT,ISTORE,INOIN,IPASS,DELT,XIC(101),ZZZ(501)
C
C     READ IN TITLE AND HEADINGS
C
  998 CONTINUE
      READ(5,707,END=999)  (NAME(I),I=1,100)
```

```
  707 FORMAT(20A4)
C
C     READ IN CONTAINMENT SPECIFICATIONS
C
      READ(5,702)AW,V,CH,G,THW,W,K,HA,WO2,THF,WWA,WA
C
C     READ IN SPILL PARAMETERS
C
      READ(5,702) ASLI,SPILL,SPRAY,FRA,RA,XMOLA
  702 FORMAT(6F12.4)
C
C     READ IN REACTION CONSTANTS
C
      READ(5,702) QCO,QCN,QCW,RCMBO,RCMBN,RCMBW,RCMBH2,TMELT,TVAP,QVAP,
     .     EMCZ,TCZI
C
C     READ IN PHYSICAL CONSTANTS
C
      READ(5,702) RHOLIO,RHOLIN,RHOLIH,CPA
      READ(5,702) CPLI,RHLI,AKLI,EMSTL,EMLI,EMCONC
C
C     READ IN INITIAL CONDITIONS
C
      READ(5,702) PAZERO,TGZERO,TSZERO,TSBI,TA,TLII
C
C     READ IN INTEGRATION CONTROL PARAMETERS
C
      READ(5,706) IMETH, DTMIN, TIMEF, RELERR, DELOUT
  706 FORMAT(I4,5F12.4)
C
C     CONTAINMENT FLOODING WITH INERT GAS OPTION
C
      READ(5,708) IBLOW
  708 FORMAT(I4)
      IF(IBLOW.EQ.1) READ(5,702) WO2B,WWAB,WN2B,XMOLAB,CPAB,TBLOW,BLOWV,
     .                           EXHSTV,BLIN,BLOUT
```

```
      XBLOW=0.
      WAB=1.-WO2B-WN2B-WWAB
      IF(IBLOW.EQ.1) GO TO 437
      BLIN=0.
      BLOUT=0.
      WO2B=0.
      WAB=0.
      WN2B=0.
      WWAB=0.
      XMOLAB=1.
      CPAB=1.
      TBLOW=1.
      BLOWV=0.
      EXHSTV=0.
  437 CONTINUE
      BLOWR = 1.35E-03 * BLOWV
      EXHSTR = 1.35E-03 * EXHSTV
C
C     EMERGENCY SPACE COOLING OF CONTAINMENT OPTION
C
      READ(5,708) IESC
      IF(IESC.EQ.1) READ(5,702) ESCR,ESCTIN
      XESC=0.
      IF(IESC.EQ.1) GO TO 439
      ESCR= 0.
      ESCTIN=0.
  439 CONTINUE
C
C     EMERGENCY STEEL FLOOR LINER COOLING OPTION
C
      READ(5,708) ISFLC
      IF(ISFLC.EQ.1) READ(5,702) SFLCR,SFLTIN
      XSFL=0.
      IF(ISFLC.EQ.1) GO TO 440
      SFLCR=0.
      SFLTIN=0.
```

```
  440 CONTINUE
C
C     INITIALIZE PROGRAM VARIABLES
C
      RIFSLC=(EMSTL*EMCONC)/(EMSTL+EMCONC-EMSTL*EMCONC)
      RIFCZP=(EMLI*EMCZ)/(EMCZ+EMLI-EMCZ*EMLI)
      DELT=DTMIN
      LIS=SPILL*SPRAY
      LIT=SPILL-LIS
      WN2=1.-WO2-WWA-WA
      XMOL=1./(WO2/32.+WN2/28.+WWA/18.+WA/XMOLA)
      RIN=1545./XMOL
      TIME=0.0
      TIMEO=-.001
      TLI=TLII
      LILP=LIT
      ZLI=LILP*12./RHLI/ASLI
      LIBP=0.
      TCZ=TCZI
      LEAKO=0.
      FMLEFT=1.0
      OUTINT=0.
      GIN=32.2
      MLINI=0.
      MLIN=0.
      MLIH=0.
      MH2=0.
      CMBRHI=0.
      OXLB=0.
      OXLBI=0.
      TS=TSZERO
      TSB=TSBI
      DO 801 I=1,20
      TCIC(I)=TSZERO
      TBIC(I)=TSBI
      TC(I)=TSZERO
```

```
      TB(I)=TSBI
  801 CONTINUE
      ICZ=1
      ICMB=1
      ILIT=1
      RHOA=PAZERO*144./RIN/TGZERO
      RHOAI=RHOA
      WRITE(6,802) (NAME(I),I=1,60)
  802 FORMAT(3(20X,20A4,/),/)
      IPAGE=50
      MNII=WN2*RHOAI*V
      MNI=MNII
      MOXI=WO2*RHOAI*V
      MLIOI= LIS*(1.+RCMBO)/RCMBO
      MWAI=WWA*RHOAI*V
      MWA=MWAI
      MAI=WA*RHOAI*V
      MA=MAI
      LIC=LIS
C
C     PRINT OUT THE INPUT
C
      WRITE(6,142)
  142 FORMAT(5X,' INPUT ',/)
      WRITE(6,143)AW,V,G,THW,W,K,HA,WO2,THF,ASLI,SPILL,SPRAY,FRA,QCO,
     .      RCMBO,TMELT,TVAP,CPLI,RHLI,AKLI,EMSTL,EMLI,EMCONC,EMCZ,
     .      PAZERO,TGZERO,TSZERO,TSBI,TA,TLII,IMETH,DTMIN,TIMEF,RELERR,
     .      DELOUT,IBLOW,WO2B,WN2B,XMOLA,CPA,TBLOW,BLOWV,EXHSTV,QCW,
     .      QVAP,QCN,RCMBN,RCMBW,BLIN,BLOUT,IESC,ESCR,ESCTIN,ISFLC,
     .      SFLCR,SFLTIN,CH,WWA,RA,RCMBH2,TCZ
      WRITE(6,144)RHOLIO,RHOLIN,RHOLIH,WWAB,WA,XMOLAB,CPAB
  143 FORMAT(' AW= ',F12.4,/,' V = ',F12.4,/,' G = ',F12.4,/,' THW = ',
     .      F12.4,/,' W = ',F12.4,/,' K = ',E12.5,/,' HA = ',F12.4,/,
     .      ' WO2 = ',F12.4,/,' THF = ',F12.4,/,' ASLI = ',F12.4,/,
     .      ' SPILL = ',F12.4,/,' SPRAY = ',F12.4,/,' FRA  = ',F12.4,/,
     .      ' QCO= ',F12.4,/,' RCMBO= ',F12.4,/,' TMELT = ',F12.4,/,
```

```
     .     ' TVAP  = ',F12.4,/,' CPLI = ',F12.4,/,' RHLI = ',F12.4,/,
     .     ' AKLI = ',F12.4,/,' EMSTL = ',F12.4,/,' EMLI  = ',F12.4,/,
     .     ' EMCONC= ',F12.4,/,' EMCZ  = ',F12.4,/,' PAZERO = ',F12.4,/,
     .     ' TGZERO = ',F12.4,/,' TSZERO = ',F12.4,/,' TSBI = ',F12.4,/,
     .     ' TA = ',F12.4,/,' TLII = ',F12.4,/,' IMETH = ',I4,/,
     .     ' DTMIN = ',F12.4,/,' TIMEF = ',F12.4,/,' RELERR = ',F12.4,/,
     .     ' DELOUT = ',F12.4,/,' IBLOW = ',I4,/,' WO2B = ',F12.4,/,
     .     ' WN2B = ',F12.4,/,' XMOLA = ',F12.4,/,' CPA = ',F12.4,/,
     .     ' TBLOW = ',F12.4,/,' BLOWV = ',F12.4,/,' EXHSTV = ',F12.4,/,
     .     ' QCW = ',F12.4,/,' QVAP = ',F12.4,/,' QCN = ',F12.4,/,
     .     ' RCMBN = ',F12.4,/,' RCMBW = ',F12.4,/,' BLIN = ',F12.4,/,
     .     ' BLOUT = ',F12.4,/,' IESC = ',I4,/,' ESCR = ',F12.4,/,
     .     ' ESCTIN = ',F12.4,/,' ISFLC = ',I4,/,' SFLCR = ',F12.4,/,
     .     ' SFLTIN = ',F12.4,/,' CH = ',F12.4,/,' WWA = ',F12.4,/,
     .     ' RA = ',F12.4,/,' RCMBH2 = ',F12.4,/,' TCZI = ',F12.4)
 144 FORMAT(' RHOLIO =',F12.4,/,' RHOLIN =',F12.4,/,' RHOLIH =',F12.4,/
     .     ,' WWAB = ',F12.4,/,' WA = ',F12.4,/,' XMOLAB= ',F12.4,/,
     .     ' CPAB = ',F12.4,/)
C
C      CHECK THAT ENOUGH OXYGEN IS LEFT FOR POOL FIRE AFTER THE SPRAY FIRE
C
      OXLFS=WO2*RHOA*V- LIS/RCMBO
      IF(OXLFS.LT.0.0)  LIS=RCMBO*WO2*RHOAI*V
      IF(OXLFS.LT.0.0) OXLFS=0.0
C
C      SPRAY FIRE COMPUTATION STARTED
C
      IF(LIS.LE.0.0) GO TO 627
      TO=TGZERO
      QIN= LIS*(QCO+CPLI*(TLI-TO))
      FF2=QIN
      TE=TGZERO+1.
 140  CONTINUE
C
C     SPECIFIC HEAT FOR DILITHIUM OXIDE
C     CP = .0602*T**.326  T = DEG. R
```

```
C     IF A DIFFERENT REACTION PRODUCT IS DESIRED, THE INTEGRAL OF THE
C     DESIRED PRODUCT MUST BE SUBSTITUTED IN QOUT1.
C
      QOUT1=(1.+RCMBO)/RCMBO*LIS*(0.0602/1.326)*(TE**1.326-TO**1.326)
      QOUT2=WN2*RHOA*V*(.172*(TE-TO)+8.57E-6/2.*(TE**2.-TO**2.)+1.02E-9
     .      /3.*(TE**3.-TO**3.))
      QOUT3=OXLFS*(.184*(TE-TO)+3.2E-6/2.*(TE**2.-TO**2.)+1.36E04*
     .           (1./TE-1./TO))
      QOUT4=WWA*RHOA*V*(0.44*(TE-TO))+WA*RHOA*V*CPA*(TE-TO)
      FF1=QIN-QOUT1-QOUT2-QOUT3-QOUT4
      IF(FF1*FF2.LT.0.) GO TO 150
      TE=TE+1.
      IF(TE.GT.1.0E06) GO TO 910
      FF2=FF1
      GO TO 140
C
C      PORTION OF PROGRAM FOR GETTING INITIAL GAS TEMP. AND PRESS.
C
  627 CONTINUE
      TE=TGZERO
  150 CONTINUE
      TG=TE
      MOX=MOXI-LIS/RCMBO
      MOXI=MOX
      MLIO=MLIOI
      XMAIR=MNI/28.+MOX/32.+MA/XMOLA+MWA/18.
      PZERO=1545.*XMAIR*TG/144./V
      PA=PZERO
      TGZERO=TG
      WRITE(6,726) TG,PZERO
  726 FORMAT(5X,'TGZERO =    ',F6.1,'   PZERO =    ',F6.3,/)
C
C      SPRAY FIRE COMPUTATION CONCLUDED
C
      L=THW/20.
      L1=THF/20.
```

```
      CALL INIT
C
C     START OF DYNAMIC CYCLE
C     START OF INTEGRATION CYCLE
C
  200 CONTINUE
C
C     CALCULATE AIR COMPOSITION AND SPECIFIC HEAT AT CONST. VOLUME
C
      MAIR=MOX+MNI+MWA+MH2+MA
      RHOA=MAIR/V
      FOX=MOX/MAIR
      FWA=MWA/MAIR
      FNI=MNI/MAIR
      CPMOX= (0.184 + 3.2E-06*TG - 1.36E04 /(TG**2))*MOX
      CPMNI = (0.172 + 8.57E-06*TG + 1.02E-09*TG**2)*MNI
C     DESIRED FORMULAE FOR SPECIFIC HEAT OF REACTION PRODUCTS MUST BE
C     SUBSTITUTED HERE
      CPWA=0.44
      CPH2=3.76
      CPLIH=0.67
      CPN2=(0.172+8.57E-06*TG+1.02E-09*TG**2)
      CPLIO=.0602*TG**.326
      CPLIN=.3368+3.67E-4*TG
      CPMLIO=CPLIO*MLIO
      HTCAPG=CPMOX+CPMNI+CPMLIO+CPA*MA+CPLIN*MLIN+CPLIH*MLIH+CPH2*MH2
     .       +CPWA*MWA
C
C      CALCULATING GAS HEAT TRANSFER COEFF.
C
      EMG=1.-EXP(-(MLIO/RHOLIO+MLIN/RHOLIN+MLIH/RHOLIH)*2.27E05*CH/V/RA)
      IF(EMG.LE.0.05) EMG=0.05
      RIFPW=1./((1.-EMLI)/EMLI+(1.-EMSTL)*ASLI/EMSTL/AW+1./((1.-EMG)
     .       +EMG/(1.+ASLI/AW)))
      RIFCZW=1./((1.-EMCZ)/EMCZ+(1.-EMSTL)*ASLI/EMSTL/AW+1./((1.-EMG)
     .       +EMG/(1.+ASLI/AW)))
```

```
      RIFPG=(EMLI*EMG)/((1.-EMLI)*EMG+EMLI)
      RIFCZG=(EMCZ*EMG)/((1.-EMCZ)*EMG+EMCZ)
      IF(ICZ.EQ.1) T1=0.5*(TG+TCZ)
      IF(ICZ.EQ.0) T1=0.5*(TG+TLI)
      T2 = 0.5*(TG +TS )
      B1 = 1.0/T1
      B2 = 1.0/T2
      D1 = ((4.94E-05*T1 +0.0188)/(RHOA*3600.0))**2
      D2 = ((4.94E-05*T2 +0.0188)/(RHOA*3600.0))**2
      AK1 = 0.014+1.92E-05*(T1-460.)
      AK2 = 0.014+1.92E-05*(T2-460.)
      EX2 = (GIN*B2*ABS(TG -TS)/D2)**0.3333
      H=0.14*AK2*EX2
      B=30.*L+W+4000.*G
      USUBA=6.67E-3*HA/(24.+L*HA)
      C1=-(.2*AW*H/(720.+W*H))/HTCAPG
      C3=.1068/(B*L)
      C4=1.781E-3/L**2
      C5=.534*USUBA/L
      C6=.0408*H/(W*(720.+W*H))
      C7=0.0408/(B*W)
      C8=.0408/(W*(30.*L1+W+4000.*G))
      C9=.1068/(L1*(30.*L1+W+4000.*G))
      C10=1.781E-3/L1**2.
      IF(ICZ.EQ.1) EXX=(GIN*B1*ABS(TCZ-TG)/D1)
      IF(ICZ.EQ.0) EXX=(GIN*B1*ABS(TLI-TG)/D1)
      IF   (EXX .LE. 0.0) GO TO 300
      EX1 = (EXX)**0.3333
C
C       CALCULATING GAS CONVECTION COEFF.
C
      DIFF = 241.57/(132.0 + T1/1.8)*(T1/493.2)**2.5
      HF = 0.140*DIFF*EX1
      HB = 0.14*AK1*EX1
      IF(TIME.GT.ESCTIN) XESC=1.
      IF(TIME.GT.SFLTIN) XSFL=1.
```

```
C
C       COMPUTING RATE OF LITHIUM COMBUSTION
C
        ICNI=0
        IF(TCZ.LE.2340..AND.TCZ.GE.900..AND.FOX.LE.0.14) ICNI=1
        IF(ILIT.EQ.0 .OR.(ICMB.EQ.0 .AND. ICNI.EQ.0) .OR. TLI.LT.TMELT)
     .                    ICZ=0
        IF(ICZ.EQ.0) GO TO 522
C
C
C
C       COMPUTATIONS USING COMBUSTION ZONE MODEL
C
        RN2=1.
        IF(TCZ.LE.2340..AND.TCZ.GE.900..AND.FOX.LE.0.14) RN2=((TCZ-1620.)
     .       /720.)**2*FOX/0.14
        CMBRO = ((HF*FOX*RHOA)/3600.)*RCMBO
        CMBRN = ((HF*FNI*RHOA)/3600.)*RCMBN*(1.-RN2)
        CMBRW = ((HF*FWA*RHOA)/3600.)*RCMBW
        CMBR = CMBRO + CMBRN + CMBRW
        RNILB=CMBRN*ASLI/RCMBN
        ROXLB=CMBRO*ASLI/RCMBO
        RWALB=CMBRW*ASLI/RCMBW
C
C         COMPUTATION OF LITHIUM VAPOR DIFFUSION
C
        TFEFF=0.002*(TG+TLI)/2.-3.92
        KFILM=PA*(0.04032+0.0078*TFEFF-8.2E-04*TFEFF*TFEFF-2.08E-04*TFEFF
     .       *TFEFF*TFEFF)/14.7
        PLIV=(10.**(4.8831-14180.2/TLI))*14.7
        RHOLIV=PLIV*144./RIN/TLI
        DIFFLI=3.56E-03*((TLI/460.)**1.81)/PA
        DFILM=DIFFLI*RHOLIV/CMBR
C
C       COMPUTATION OF HEAT TRANSFER COEFFICIENTS
C
```

```
      YAPCZ=6.666E-03*AKLI*KFILM*ASLI/(DFILM*AKLI+ZLI*KFILM)
      CPMCZ=ASLI*((1.+RCMBO)/RCMBO*CMBRO*CPLIO+(1.+RCMBN)/RCMBN*CMBRN*
     .   CPLIN+((1.+RCMBW)/RCMBW-(1./RCMBH2))*CMBRW*CPWA+(1.+RCMBH2)/
     .   RCMBH2*CMBRW*CPH2+RN2*HF*FNI*RHOA*CPN2/3600.)*300.
      CCCZ=HB*ASLI/3600./CPMCZ
      CCZG=HB*ASLI/3600./HTCAPG
      CPCZ=YAPCZ/CPMCZ
      IF(LILP.GT. 0.1*LIT) CCZP=YAPCZ/(CPLI*LILP)
      IF(LILP.LE.0.1*LIT) CCZP=YAPCZ/(CPLI*0.1*LIT)
      QRADP=0.1714E-08*ASLI*(TCZ**4-TLI**4)*RIFCZP
      QRADW=0.1714E-08*ASLI*(TCZ**4-TS**4)*RIFCZW
      QRADG=0.1714E-08*ASLI*(TCZ**4-TG**4)*RIFCZG
      RCZW=12.*QRADW/(W*AW*490.*0.12*3600.)
      RCZP=12.*QRADP/(RHLI*CPLI*ASLI*ZLI*3600.)
      RCZG=QRADG/(HTCAPG*3600.)
      QRADB=0.1714E-08*ASLI*(TSB**4-TB(1)**4)*RIFSLC
      QRADC=0.1714E-08*AW*(TS**4-TC(1)**4)*RIFSLC
      RADB=12.*QRADB/(W*ASLI*490.*0.12*3600.)
      RADC=12.*QRADC/(W*AW*490.*0.12*3600.)
      RADCB=12.*QRADB/(L1*ASLI*144.*0.156*3600.)
      RADCC=12.*QRADC/(L*AW*144.*0.156*3600.)
      CCZ=(CMBRO*QCO+CMBRN*QCN+CMBRW*QCW)*ASLI
      IF(LILP.GT. 0.1*LIT) CLIST=(0.2*AKLI)/(LILP*CPLI
     .     *(30.*ZLI+W*AKLI))*ASLI
      IF(LILP.LE.0.1*LIT) CLIST=(0.2*AKLI)/(0.1*LIT*CPLI*
     .  (30.*ZLI+W*AKLI))*ASLI
      CSBLI=(2.4*AKLI)/(58.8*ASLI*W*(30.*ZLI+W*AKLI))*ASLI
C
C     CALCULATE COMB. ZONE TEMP. RATE OF CHANGE   DEG. R/SEC
C
      ZZ6=(CCZ-(QRADP+QRADW+QRADG)/3600.)/CPMCZ+QVAP*CMBR*ASLI/CPMCZ
     .          -CPCZ*(TCZ-TLI)-CGCZ*(TCZ-TG)
C
C    CALC. LITHIUM TEMP. RATE OF CHANGE     DEG. R/SEC
C
      ZZ1=CCZP*(TCZ-TLI)+RCZP-CLIST*(TLI-TSB)-QVAP*CMBR*ASLI*CCZP/YAPCZ
```

```
C
C     CALC. CELL GAS TEMP. RATE OF CHANGE   DEG. R/SEC.
C
      ZZ4=C1*(TG-TS)+CCZG*(TCZ-TG)+RCZG+XBLOW*BLOWR*CPAB*(TBLOW-TG)
     .    /HTCAPG-ESCR*XESC/HTCAPG
C
C     CALC. WALL STRUCTURE TEMP. RATE OF CHANGE
C
      ZZ5=C6*(TG-TS)-C7*(TS-TC(1))+RCZW-RADC
      GO TO 523
C
C
C
C       COMPUTATIONS WITHOUT COMBUSTION ZONE MODEL
C
  522 CONTINUE
      CMBR=0.0
      YALIG=6.666E-03*(HB*ASLI*AKLI)/(ZLI*HB+24.0*AKLI)
      CLIG=YALIG/HTCAPG
      QRADW=0.1714E-08*ASLI*(TLI**4-TS**4)*RIFPW
      QRADG=0.1714E-08*ASLI*(TLI**4-TG**4)*RIFPG
      RLIW=12.*QRADW/(W*AW*490.*0.12*3600.)
      RWLI=12.*QRADW/(RHLI*CPLI*ASLI*ZLI*3600.)
      RGLI=12.*QRADG/(RHLI*CPLI*ASLI*ZLI*3600.)
      RLIG=QRADG/(HTCAPG*3600.)
      QRADB=0.1714E-08*ASLI*(TSB**4-TB(1)**4)*RIFSLC
      QRADC=0.1714E-08*AW*(TS**4-TC(1)**4)*RIFSLC
      RADB=12.*QRADB/(W*ASLI*490.*0.12*3600.)
      RADC=12.*QRADC/(W*AW*490.*0.12*3600.)
      RADCB=12.*QRADB/(L1*ASLI*144.*0.156*3600.)
      RADCC=12.*QRADC/(L*AW*144.*0.156*3600.)
      IF(LILP.GT. 0.1*LIT) CGLI=YALIG/(LILP*CPLI)
      IF(LILP.LE.0.1*LIT) CGLI=YALIG/(0.1*LIT*CPLI)
      IF(LILP.GT. 0.1*LIT) CLIST=(0.2*AKLI)/(LILP*CPLI*(30.*ZLI+W*AKLI))
     .       *ASLI
      IF(LILP.LE.0.1*LIT) CLIST=(0.2*AKLI)/(0.1*LIT*CPLI*
```

```
     .  (30.*ZLI+W*AKLI))*ASLI
      CSBLI=(2.4*AKLI)/(58.8*ASLI*W*(30.*ZLI+W*AKLI))*ASLI
C
C       CALCULATE LITHIUM TEMP. RATE OF CHANGE  DEG. F/SEC
C
      ZZ1=CGLI*(TG-TLI)-CLIST*(TLI-TSB)-RWLI-RGLI
C
C       CALCULATE CELL GAS TEMP. RATE OF CHANGE   DEG. F/SEC
C
      ZZ4=C1*(TG-TS)+CLIG*(TLI-TG)+RLIG+XBLOW*BLOWR*CPAB*(TBLOW-TG)
     .    /HTCAPG-ESCR*XESC/HTCAPG
C
C       CALC. WALL STRUCTURE TEMP. RATE OF CHANGE   DEG. F/SEC
C
      ZZ5=C6*(TG-TS)-C7*(TS-TC(1))+RLIW-RADC
C
C
  523 CONTINUE
      DTCDT(1)=C3*TS+C4*TC(2)-(C3+C4)*TC(1)+RADCC
      DTCDT(20)=C4*(TC(19)-TC(20))-C5*(TC(20)-TA)
      DO 5 I=2,19
    5 DTCDT(I)=C4*(TC(I-1)+TC(I+1)-2.*TC(I))
C
C     CALC. FLOOR STRUCTURE TEMP. RATE OF CHANGE
C
      ZZ7=CSBLI*(TLI-TSB)-C8*(TSB-TB(1))-RADB-XSFL*SFLCR*12./(W*ASLI
     .     *490.*0.12)
      DTBDT(1)=C9*TSB+C10*TB(2)-(C9+C10)*TB(1)+RADCB
      DTBDT(20)=C10*(TB(19)-TB(20))
      DO 50 IB=2,19
   50 DTBDT(IB)=C10*(TB(IB-1)+TB(IB+1)-2.*TB(IB))
C
C       CALCULATING OVERPRESSURE
C
      XMAIR=MOX/32.+MNI/28.+MA/XMOLA+MWA/18.
      PA=1545.*XMAIR*TG/144./V
```

```
      OVERP=PA-PAZERO
      IF (TIME.GT.BLIN) XBLOW=1.
      IF (TIME.GT.BLOUT) XBLOW=0.
C
C       CALCU. TOTAL LEAKAGE
C
      IF (OVERP)10,10,11
   10 LEAK=0.
      GO TO 12
   11 LEAK = K*OVERP**0.5
   12 CONTINUE
      FOUT=EXHSTR/MAIR*XBLOW+LEAK
      FMLEFT= EXP(-OUTINT)
      FMLEAK = 1. -FMLEFT
C
C     DO INTEGRATIONS
C
      LIBP=INTGRL(0.,CMBR*ASLI)
      OXLB=INTGRL(OXLBI,ROXLB)
      IF(ILIT.EQ.0) OXLB=LIT/RCMBO
      IF(ICMB.EQ.0) OXLB=OXLFS
      MOX=INTGRL(MOXI,WO2B*BLOWR*XBLOW-MOX*FOUT-ROXLB)
      MNI=INTGRL(MNII,WN2B*BLOWR*XBLOW-MNI*FOUT-RNILB)
      MA=INTGRL(MAI,WAB*BLOWR*XBLOW-MA*FOUT)
      MWA=INTGRL(MWAI,WWAB*BLOWR*XBLOW-MNI*FOUT-RWALB)
      MLIO=INTGRL(MLIOI,-MLIO*FOUT+(1.+RCMBO)/RCMBO*CMBRO*ASLI*FRA)
      MLIN=INTGRL(MLINI,-MLIN*FOUT+(1.+RCMBN)/RCMBN*CMBRN*ASLI*FRA)
      MLIH=INTGRL(0.,-MLIH*FOUT+((1.+RCMBW)/RCMBW-1./RCMBH2)*CMBRW
     .     *ASLI*FRA)
      MH2=INTGRL(0.,-MH2*FOUT+(1.+RCMBH2)/RCMBH2*CMBRW*ASLI)
      TCZ=INTGRL(TCZI,ZZ6)
      TLI=INTGRL(TLII,ZZ1)
      IF(TLI.GE.TVAP) GO TO 820
      TG=INTGRL(TGZERO,ZZ4)
      TS=INTGRL(TSZERO,ZZ5)
      DO 750 I=1, 20
```

```
      TB(I)=INTGRL(TBIC(I),DTBDT(I))
      TC(I)=INTGRL(TCIC(I),DTCDT(I))
  750 CONTINUE
       TSB=INTGRL(TSBI,ZZ7)
      OUTINT=INTGRL(LEAKO,LEAK)
C
      CALL DYNAMI(TIME,&200)
C
C     POST-INTEGRATION SECTION
C     CHECK OVERP AND TLI FOR STOP CONDITION
C     CHECK AND CORRECT FOR LITHIUM AND OXYGEN SUPPLY
C
  180 CONTINUE
      LILP=LIT-LIBP
      IF(LILP.LE.0.) LILP=0.0
      IF(ICZ.EQ.0) TCZ=460.
      IF(TG.LT.500. .AND. OVERP.LT.1.) GO TO 745
      IF(TLI.LT.TMELT) GO TO 743
      IF(ICMB.EQ.0 .OR. ILIT.EQ.0) GO TO 500
      IF((OXLFS - OXLB) .GE. 0.0) GO TO 201
      OXLB=OXLFS
      ICMB=0
      CMBRO=0.0
      ROXLB=0.0
  201 CONTINUE
      IF(LILP.GE. 0.1) GO TO 500
      OXLB=LIT/RCMBO
      LILP=0.0
      ILIT=0
      LIT=LIBP
      CMBR=0.0
      CMBRO=0.0
      CMBRN=0.0
      CMBRW=0.0
      ROXLB=0.0
      RNILB=0.0
```

```
      RWALB=0.0
  500 CONTINUE
      IF(MNI.GE.0.0) GO TO 202
      MNI=0.0
      ICNI=0
      CMBRN=0.
      RNILB=0.0
  202 CONTINUE
      IF(MWA.GE.0.0) GO TO 502
      MWA=0.0
      CMBRW=0.0
      RWALB=0.0
  502 CONTINUE
      IF(CMBRH.GE.0.2 .OR. TIME.LE.10.) GO TO 503
      ICZ=0
      CMBRO=0.0
      CMBRN=0.0
      CMBRW=0.0
      ROXLB=0.0
      RNILB=0.0
      RWALB=0.0
  503 CONTINUE
C
C     CONVERT TEMP. TO DEG. F
C
      DO 6  I=1,20
      TBF(I) =TB(I)-460.
    6 TCF(I)=TC(I)-460.
      TGF=TG-460.
      TSBF=TSB -460.
      TSF=TS-460.
      TCZF=TCZ-460.
      TLIF=TLI-460.
      CMBRH=3600.*(CMBRO+CMBRN+CMBRW)
C
C     TIME STEP CONTROL
```

```
C
      DT1=ABS(RELERR*TLI/ZZ1)
      DT2=ABS(RELERR*TG/ZZ4)
      DT3=ABS(RELERR*TS/ZZ5)
      IF(ILIT.EQ.0 .OR. ICZ.EQ.0) GO TO 735
      DT5=ABS(RELERR*TCZ/ZZ6)
      ZZ99=(CMBRH-CMBRHI)/DELT
      IF(ZZ99.EQ.0.) GO TO 735
      DT4=ABS(RELERR*CMBRH/(CMBRH-CMBRHI)*DELT)
      CMBRHI=CMBRH
      IF(IPASS.EQ.1) DT4=1.E06
      GO TO 736
  735 CONTINUE
      DT4=1.0E06
      DT5=1.0E06
  736 CONTINUE
      DELT=AMIN1(DT1,DT2,DT3,DT4,DT5)
      IF(TIME.LT.8000.) DELOUT=100.
      IF(TIME.GT.8000.)  DELOUT=1000.
      IF(DELT.LT.DTMIN) DELT=DTMIN
      IF(DELT.GT.DELOUT) DELT=DELOUT
      IF(TIME.LT.1.0) DELT=.10
C
C     OUTPUT SECTION
C
      IF(TIME.LT.TIMEO) GO TO 810
      TIMEO=TIMEO+DELOUT
      IF(IPAGE.EQ.50) WRITE(6,803) (NAME(I),I=1,92)
  803 FORMAT('1',3(20X,20A4,/),//,32A4)
      IF(IPAGE.EQ.50) IPAGE=0
      IPAGE=IPAGE+1
      WRITE(6,804) TIME,TSF,TGF,OVERP,EMG,TCZF,TLIF,
     .     CMBRH,MOX,LILP,TCF(1),DELT,TSBF,MNI,TBF(1)
  804 FORMAT(F8.1,2F7.1,F7.2,E10.3,2F7.1, E11.3,2F9.1,F10.3,F8.2,
     .       F6.0,F9.0,F7.0)
  810 CONTINUE
```

```
      IF(TIME.GT.TIMEF) GO TO 900
C     RETURN TO TOP OF DYNAMIC CYCLE
      GO TO 200
C
C       ERROR POINTERS
C
  743 CONTINUE
      WRITE(6,744)
  744 FORMAT(' POOL TEMP. HAS DROPPED TO LITHIUMS MELTING TEMP.')
      GO TO 900
  745 CONTINUE
      WRITE(6,746)
  746 FORMAT(' CELL GAS TEMP. AND PRESS. HAVE RETURNED TO NORMAL')
      GO TO 900
  820 CONTINUE
      WRITE(6,821)
  821 FORMAT(' LITHIUM TEMP. ABOVE BOILING POINT')
      GO TO 900
  910 CONTINUE
      WRITE(6,725)
  725 FORMAT(1X,'NO ROOT FOUND FOR SPRAY FIRE FOR TEMP.S LESS THAN ',
     .       '1 MILLION DEG. R')
      GO TO 900
  300 CONTINUE
      WRITE(6,710)
  710 FORMAT(' EXX IS NEGATIVE--CANNOT TAKE ROOT')
      WRITE(6,711) TCZ,CMBRH,ZZ6,ZZ5,RN2
  711 FORMAT(' MESSED UP VARIABLES',5E10.3)
  900 CONTINUE
      WRITE(6,713)
  713 FORMAT(' PROGRAM EXECUTION STOPPED BY PROGRAM')
      WRITE(6,101) DT1,DT2,DT3,DT4,DT5
  101 FORMAT(' VALUES', 5E10.3)
C     RETURN TO BEGINNING OF PROGRAM AND READ IN NEW DATA.  IF NO NEW DATA IS
C     AVAILABLE, PROGRAM EXECUTION WILL AUTOMATICALLY BE STOPPED BY END
C     PARAMETER IN THE FIRST STATEMENT.
```

```
      GO TO 998
  999 CONTINUE
      CALL EXIT
      END
C     THESE 3 SUBROUTINES ARE DESIGNED TO BE USED IN A MAIN PROGRAM WHICH
C     SIMULATES A DYNAMIC SYSTEM EXPRESSED AS A SET OF ODE'S. THESE ODE'S
C     MAY BE REEXPRESSED AS A SET OF INTEGRALS WHICH MUST BE INTEGRATED
C     SIMULTANEOUSLY THROUGH THE DOMAIN OF INTEREST STARTING WITH THE APPROPRIATE
C     INITIAL CONDITIONS.  FOR EXAMPLE, THE FUNCTION Y MAY BE FOUND FROM THE
C     SOLUTION OF  DY/DT = RATE = F(Y,T) AND Y=YO AT T=TO. THIS MAY BE
C     REWRITTEN Y = INTGRL(YO, RATE), THE OPEN INTEGRAL OF RATE OVER T STARTING
C     AT YO. A SET OF ODE'S MAY BE TREATED IN A SIMILIAR MANNER.
C         THE MAIN PROGRAM SHOULD CONSIST OF TWO MAIN PARTS, THE INITIALIZATION
C     SECTION AND THE DYNAMIC SECTION.  THE DYNAMIC SECTION IS FURTHER DIVIDED
C     INTO INTEGRATION AND POST-INTEGRATION SECTIONS.
C         THE INITIAL SECTION SHOULD BE USED FOR INPUT, CALCULATION OF NECESSARY
C     CONSTANTS, AND FOR CALCULATING AND SETTING OF INITIAL CONDITIONS. IT
C     SHOULD CONTAIN THE REAL INTGRL, COMMON, AND CALL INIT STATEMENTS.
C         THE INTEGRATION SECTION SHOULD START WITH A NUMBERED CONTINUE
C     STATEMENT AND END WITH THE CALL DYNAMI  STATEMENT.  IT SHOULD CONTAIN
C     ALL CALCULATIONS OF PROGRAM VARIABLES AND NON-CONSTANT RATES. ALL INTGRL
C     FUNCTION STATEMENTS SHOULD APPEAR IN A GROUP IMMEDIATELY PRECEDING THE
C     CALL DYNAMI STATEMENT.
C         THE INTEGRATION SECTION WILL BE LOOPED SEVERAL TIMES DURING EACH
C     INTEGRATION STEP (SIMPSON'S RULE USES 4 LOOPS PER STEP, RUNGE-KUTTA USES
C     5 LOOPS PER STEP).  DYNAMI CONTROLS THE INTEGRATION BY TELLING THE
C     INTGRL FUNCTION WHAT STEP IT SHOULD PERFORM NEXT. THE INTEGRATION
C     VARIABLE TIME IS ALSO CONTROLED BY DYNAMI.  IT MAY OR MAY NOT BE INCREMENT-
C     ED DURING EACH LOOP. TIME SHOULD BE INITIALIZED IN THE INTIAL SECTION.
C     DYNAMI UTILIZES MULTIPLE RETURNS TO CONTROL PROGRAM FLOW.  THE STATEMENT
C     NUMBER PASSED TO DYNAMI SHOULD BE THAT OF THE FIRST STATEMENT IN THE
C     INTEGRATION SECTION. THIS CAUSES THE PROPER INTEGRATION LOOPING. AT THE
C     END OF EACH INTEGRATION STEP A NORMAL RETURN IS EXECUTED AND CONTROL
C     RETURNS TO THE FIRST STATEMENT FOLLOWING CALL DYNAMI. THIS SHOULD BE
C     THE FIRST STATEMENT OF THE POST-INTEGRATION SECTION.
C         BECAUSE VARIABLE VALUES MAY DIFFER FROM THEIR TRUE VALUE DURING THE
```

```
C     INTEGRATION LOOPING, ALL PROGRAM LOGIC AND VARIABLE TIME STEP CALCULATIONS
C     SHOULD BE MADE IN THE POST-INTEGRATION SECTION. THIS SECTION WILL BE
C     EXECUTED ONCE AT THE END OF EACH INTEGRATION STEP. TIME AND ALL VARIABLES
C     CONTAINED WITHIN THE INTEGRATION SECTION WILL BE UPDATED TO THEIR 'TRUE'
C     VALUES BEFORE CONTROL IS TRANSFERED TO THE POST-INTEGRATION SECTION.
C     THIS SECTION SHOULD CONTAIN AT LEAST ONE IF STATEMENT WHICH STOPS PROGRAM
C     EXECUTION. AND THE LAST STATEMENT SHOULD BE A GO TO ST.NO. WHERE ST.NO.
C     IS THE STATEMENT NUMBER OF THE FIRST STATEMENT IN THE INTEGRATION SECTION.
C         APPROXIMATELY 100 INTEGRATIONS MAY BE PERFORMED SIMULTANEOUSLY.
C
C     VARIABLE LIST
C
C       A    MATRIX WHICH STORES THE INTERMIATE VALUES CALCULATED DURING EACH LOOP
C       DELT    INTEGRATION TIME STEP
C       DXDT    RATE BEING INTEGRATED. CALCULATED USING  INTEGRAL VALUE AS
C               RETURNED BY INTGRL DURING THE PREVIOUS LOOP AND TIME SET BY
C               DYNAMI.  USED BY INTGRL AS CALLED FOR BY ICOUNT.
C       ICOUNT    TELLS INTGRL WHICH INTEGRATION LOOP IS PRESENTLY BEING DONE
C       IMETH = 1 USE RUNGE-KUTTA METHOD
C             = 3 USE SIMPSON'S RULE
C       INOIN    TELL DYNAMI HOW MANY INTGRL STATEMENTS THERE ARE IN THE MAIN
C                PROGRAM.
C       IPASS    TELLS INTGRL TO DO TWO SPECIAL FUNCTIONS DURING THE FIRST TWO
C                EXECUTIONS OF THE INTEGRATION SECTION.
C       ISTORE    TELLS INTGRL WHERE TO STORE THE RESULT OF ITS INTERMEDIATE
C                 CALCULATION IN MATRIX A.
C       XIC    MATRIX WHICH STORE  INTIAL CONDITIONS AND THEN IS UPDATED TO THE
C              PRESENT INTEGRAL VALUE AT THE END OF EACH INTEGRATION STEP.
C       XXIC    INITIAL CONDITION
C
      SUBROUTINE DYNAMI(TIME,*)
      COMMON IMETH,ICOUNT,ISTORE,INOIN,IPASS,DELT,XIC(101),A(501)
      IF(IPASS.EQ.0) GO TO 40
      IF(IMETH.EQ.1) GO TO 10
C
C     SIMPSON'S RULE (DEFAULT) IMETH>2
```

```
C
      IF(ICOUNT.EQ.4) GO TO 4
      IF(ICOUNT.EQ.3) GO TO 3
      TIME=TIME+DELT/2.
      ICOUNT=ICOUNT+1
      RETURN 1
    4 CONTINUE
      ISTORE=0
      ICOUNT=1
      IPASS=IPASS+1
      INOIN=0
      RETURN
    3 CONTINUE
      ICOUNT =4
      RETURN 1
C
C     RUNGE-KUTTA METHOD -FIXED STEP-   IMETH=1
C
   10 CONTINUE
      IF(ICOUNT.EQ.5) GO TO 4
      IF(ICOUNT.EQ.4) GO TO 14
      IF(ICOUNT.EQ.2) GO TO 12
      TIME=TIME+DELT/2.
      ICOUNT=ICOUNT+1
      RETURN 1
   12 CONTINUE
      ICOUNT=3
      RETURN 1
   14 CONTINUE
      ICOUNT= 5
      RETURN 1
   40 CONTINUE
      IPASS=1
      RETURN
      END
C     THIS SUBROUTINE INITIALIZES VARIABLES USED BY THE INTEGRATION ROUTINES.
```

```
C     IT SHOULD BE PLACED IN THE INITIALIZATION SECTION OF THE MAIN PROGRAM
C     BEFORE THE FIRST STATEMENT OF THE DYNAMIC SECTION.  SEE DYNAMI FOR VARIABLE
C     LIST AND INTEGRATION DESCRIPTION.
C
      SUBROUTINE INIT
      COMMON IMETH,ICOUNT,ISTORE,INOIN,IPASS,DELT,XIC(101),A(501)
      IPASS=0
      ISTORE=0
      ICOUNT=1
      INOIN=0
      RETURN
      END
C       FUNCTION INTGRL PERFORMS THE ACTUAL INTEGRATIONS. IN THE MAIN
C     PROGRAM, ALL INTGRL STATEMENTS SHOULD BE PLACED IN A GROUP AT THE END
C     OF THE INTEGRATION SECTION.  ALL RATE CALCULATIONS SHOULD PRECEDE THIS
C     GROUP AND IT SHOULD BE IMMEDIATELY FOLLOWED BY THE CALL DYNAMI STATEMENT.
C     FOR VARIABLE LIST AND DESCRIPTIONS SEE DYNAMI.
C
      REAL FUNCTION INTGRL(XXIC,DXDT)
      COMMON IMETH,ICOUNT,ISTORE,INOIN,IPASS,DELT,XIC(101),A(501)
      IF(IPASS.EQ.0) GO TO 40
      ISTORE=ISTORE+1
      IF(IMETH.EQ.1) GO TO 10
C
C     SIMPSON'S RULE (DEFAULT) IMETH GREATER THAN 2
C
      IF(ICOUNT.EQ.4) GO TO 4
      IF(ICOUNT.EQ.3) GO TO 3
      IF(ICOUNT.EQ.2) GO TO 2
    1 CONTINUE
      INOIN=INOIN+1
      IF(IPASS.EQ.1) XIC(INOIN)=XXIC
      A(ISTORE)=DXDT
      INTGRL=XIC(INOIN)+DELT*DXDT/2.
      A(500-ISTORE)=INTGRL
      RETURN
```

```
     2 CONTINUE
       A(ISTORE)=DXDT
       INTGRL=A(500+INOIN-ISTORE)+DELT*DXDT/2.
       RETURN
     3 CONTINUE
       INTGRL=XIC(ISTORE-2*INOIN)+DELT/6.*(A(ISTORE-2*INOIN)+4.*
      .                A(ISTORE-INOIN)+DXDT)
       XIC(ISTORE-2*INOIN)=INTGRL
       RETURN
     4 CONTINUE
       INTGRL=XIC(ISTORE-3*INOIN)
       RETURN
C
C     RUNGE-KUTTA METHOD -FIXED STEP-   IMETH=1
C
    10 CONTINUE
       IF(ICOUNT.EQ.5) GO TO 15
       IF(ICOUNT.EQ.4) GO TO 14
       IF(ICOUNT.EQ.3) GO TO 13
       IF(ICOUNT.EQ.2) GO TO 12
    11 CONTINUE
       INOIN=INOIN+1
       IF(IPASS.EQ.1) XIC(INOIN)=XXIC
       A(ISTORE)=DELT*DXDT
       INTGRL=XIC(INOIN)+.5*A(ISTORE)
       RETURN
    12 CONTINUE
       A(ISTORE)=DELT*DXDT
       INTGRL=XIC(ISTORE-INOIN)+.5*A(ISTORE)
       RETURN
    13 CONTINUE
       A(ISTORE)=DELT*DXDT
       INTGRL=XIC(ISTORE-2*INOIN)+A(ISTORE)
       RETURN
    14 CONTINUE
       AA=DELT*DXDT
```

```
      INTGRL=XIC(ISTORE-3*INOIN)+1./6.*(A(ISTORE-3*INOIN)+2.*
     .  A(ISTORE-2*INOIN)+2.*A(ISTORE-INOIN)+AA)
      XIC(ISTORE-3*INOIN)=INTGRL
      RETURN
   15 CONTINUE
      INTGRL=XIC(ISTORE-4*INOIN)
      RETURN
   40 CONTINUE
      INTGRL=XXIC
      RETURN
      END
```

APPENDIX B

Sample Input to LITFIRE

INPUT

```
AW=  183532.0000          ISFLC =      0
V = 8855700.0000          SFLCR =        0.0
G =       0.02500         SFLTIN =       0.0
THW =       10.0000       CH =       150.0000
W =          0.2500       WWA =          0.0
K =  0.25880E-08          RA =       300.0000
HA =         0.3000       RCMBH2 =         6.9300
WO2 =        0.2310       TCZI =     2300.0000
THF =       25.0000       RHOLIO =     124.0000
ASLI =   10386.0000       RHOLIN =      86.9400
SPILL =  48387.5000       RHOLIH =     160.0000
SPRAY =       0.0100      WWAB =         0.0
FRA =         0.7500      WA =         0.0
QCO=   18510.0000         XMOLAB=        1.0000
RCMBO=        0.8674      CPAB =         1.0000
TMELT =     816.5999
TVAP =     2949.0000
CPLI =        1.0000
RHLI =       27.4000
AKLI =       36.3000
EMSTL =       0.8500
EMLI =        0.2000
EMCONC=       0.9000
EMCZ =        0.5000
PAZERO =     14.7000
TGZERO =    538.0000
TSZERO =    538.0000
TSBI =      538.0000
TA =        538.0000
TLII =     2256.0000
IMETH =       3
DTMIN =       1.0000
TIMEF =   15000.0000
RELERR =      0.0060
DELOUT =   2000.0000
IBLOW =       0
WO2B =        0.0
WN2B =        0.0
XMOLA =       1.0000
CPA =         1.0000
TBLOW =       1.0000
BLOWV =       0.0
EXHSTV =      0.0
QCW =   13783.5977
QVAP =     83.9000
QCN =    4079.7000
RCMBN =       1.4870
RCMBW =       0.3830
BLIN =        0.0
BLOUT =       0.0
IESC =        0
ESCR =        0.0
ESCTIN =      0.0
```

APPENDIX C

Sample Output of LITFIRE

LITFIRE TEST RUN FOR LITHIUM FIRE IN UNMAK III CONTAINMENT
ASSUMING THAT 5.5 PERCENT OF THE TOTAL LITHIUM INVENTORY IS SPILLED
RUN NO. 88 CONC. TEMP. PROFILE, THW=10 IN., THF=25 IN.

TIME	TSF	TGF	OVERP	EMG	TCZF	TLIF	CMBRH	MOX	LILP	TCF(1)	DELT	TSBF	MNI	TBF(1)
0.0	78.0	167.0	2.42	0.102E 00	1840.0	1796.0	0.538E 01	149647.8	47903.6	78.000	0.10	78.	500036.	78.
105.8	106.6	194.9	3.14	0.310E 00	1837.1	1657.2	0.530E 01	147827.3	46325.5	80.485	4.07	1567.	500035.	348.
200.6	134.4	237.1	4.24	0.461E 00	1946.9	1767.9	0.551E 01	146124.9	44849.2	85.624	7.93	1675.	500034.	642.
306.5	167.7	299.0	5.86	0.594E 00	2018.8	1846.3	0.562E 01	144166.9	43151.4	93.933	7.10	1757.	500033.	958.
405.9	199.4	365.0	7.59	0.689E 00	2054.4	1897.8	0.563E 01	142309.7	41540.8	103.727	7.18	1816.	500032.	1213.
501.0	229.6	431.5	9.33	0.760E 00	2082.9	1939.3	0.562E 01	140530.1	39997.6	114.556	7.52	1866.	500031.	1408.
601.7	261.5	503.2	11.20	0.817E 00	2111.0	1979.8	0.561E 01	138651.7	38368.7	127.341	8.03	1916.	500030.	1565.
701.3	293.1	574.2	13.03	0.860E 00	2137.9	2016.1	0.558E 01	136800.4	36763.4	141.213	8.58	1961.	500030.	1680.
801.3	324.6	644.3	14.84	0.893E 00	2157.0	2047.9	0.553E 01	134956.3	35164.2	156.248	8.95	1999.	500029.	1766.
902.7	356.1	713.1	16.59	0.918E 00	2171.6	2074.2	0.547E 01	133106.2	33559.8	172.521	9.01	2030.	500028.	1832.
1004.6	387.0	779.1	18.27	0.937E 00	2181.9	2095.0	0.539E 01	131271.1	31968.6	189.791	8.79	2056.	500027.	1882.
1106.1	416.7	841.0	19.83	0.952E 00	2188.3	2110.5	0.530E 01	129470.9	30407.5	207.765	8.53	2075.	500027.	1920.
1206.7	445.0	898.4	21.26	0.962E 00	2191.5	2121.5	0.520E 01	127718.5	28887.9	226.166	8.35	2089.	500026.	1949.
1305.9	471.6	950.8	22.55	0.971E 00	2192.2	2128.8	0.510E 01	126022.3	27417.1	244.740	8.20	2099.	500025.	1970.
1403.5	496.3	998.3	23.72	0.977E 00	2191.1	2133.1	0.500E 01	124387.0	25999.2	263.267	8.05	2105.	500024.	1986.
1507.1	521.1	1044.4	24.84	0.982E 00	2188.2	2135.2	0.489E 01	122686.9	24525.1	283.074	7.87	2109.	500024.	1999.
1600.6	542.1	1082.5	25.75	0.985E 00	2184.5	2135.3	0.479E 01	121184.1	23221.9	300.960	7.71	2111.	500023.	2007.
1707.2	564.5	1121.7	26.68	0.989E 00	2179.3	2133.7	0.468E 01	119509.8	21770.1	321.199	7.50	2111.	500022.	2013.
1803.6	583.4	1153.8	27.43	0.991E 00	2173.7	2131.1	0.458E 01	118028.8	20486.0	339.288	7.32	2110.	500021.	2017.
1904.8	602.0	1184.1	28.12	0.993E 00	2167.3	2127.2	0.448E 01	116509.5	19168.8	357.941	7.12	2107.	500020.	2019.
2003.2	618.8	1210.5	28.72	0.994E 00	2160.6	2122.6	0.438E 01	115064.9	17916.2	375.699	6.92	2104.	500019.	2019.
2105.6	635.1	1235.2	29.27	0.995E 00	2153.2	2117.1	0.428E 01	113595.0	16641.8	393.714	6.72	2100.	500018.	2018.
2205.0	649.9	1256.5	29.73	0.996E 00	2145.7	2111.3	0.418E 01	112201.1	15433.3	410.691	6.52	2095.	500017.	2016.
2301.3	663.2	1274.9	30.12	0.997E 00	2138.2	2105.1	0.409E 01	110878.8	14286.7	426.652	6.32	2089.	500017.	2014.
2400.8	676.1	1291.8	30.47	0.997E 00	2130.3	2098.5	0.401E 01	109542.3	13128.1	442.596	6.11	2084.	500016.	2010.
2502.8	688.5	1307.2	30.77	0.998E 00	2122.0	2091.3	0.392E 01	108201.4	11965.7	458.363	5.88	2077.	500014.	2006.
2601.1	699.6	1320.2	31.02	0.998E 00	2113.9	2084.1	0.384E 01	106938.0	10870.5	472.980	5.66	2071.	500013.	2002.
2701.0	710.2	1331.9	31.24	0.998E 00	2105.7	2076.6	0.376E 01	105680.4	9780.4	487.271	5.42	2064.	500012.	1997.
2801.7	720.2	1342.2	31.42	0.999E 00	2097.2	2068.9	0.368E 01	104439.0	8704.3	501.103	5.16	2057.	500011.	1992.
2902.3	729.5	1351.2	31.56	0.999E 00	2088.8	2060.9	0.360E 01	103224.6	7651.6	514.353	4.88	2050.	500010.	1986.
3001.7	738.2	1358.9	31.68	0.999E 00	2080.4	2052.9	0.353E 01	102049.1	6632.7	526.898	4.57	2043.	500009.	1981.
3102.9	746.4	1365.6	31.77	0.999E 00	2071.9	2044.5	0.346E 01	100877.2	5616.9	539.117	4.21	2036.	500007.	1975.
3203.1	754.1	1371.4	31.84	0.999E 00	2063.5	2035.9	0.339E 01	99738.8	4630.3	550.701	3.84	2028.	500006.	1969.
3302.4	761.3	1376.2	31.88	0.999E 00	2055.2	2028.4	0.333E 01	98632.8	3671.9	561.681	3.80	2021.	500004.	1963.
3400.6	768.0	1380.2	31.91	0.100E 01	2047.2	2021.0	0.326E 01	97559.5	2741.7	572.073	3.76	2014.	500002.	1957.
3501.5	774.5	1383.7	31.92	0.100E 01	2039.0	2013.5	0.320E 01	96477.4	1804.0	582.284	3.72	2007.	500001.	1950.
3601.3	780.5	1386.5	31.92	0.100E 01	2031.0	2006.2	0.314E 01	95426.9	893.7	591.942	3.68	2000.	499999.	1944.
3700.0	786.2	1388.7	31.90	0.100E 01	2023.2	1998.9	0.309E 01	94406.3	9.3	601.084	3.64	1992.	499997.	1938.
3804.8	771.3	1365.3	31.31	0.100E 01	0.0	1912.5	0.0	94368.3	0.0	606.489	8.01	1912.	499996.	1904.
3900.6	760.4	1342.1	30.73	0.100E 01	0.0	1863.7	0.0	94367.5	0.0	607.531	7.98	1863.	499996.	1860.
4004.3	750.5	1316.9	30.09	0.100E 01	0.0	1817.7	0.0	94366.7	0.0	607.118	7.98	1817.	499995.	1815.
4100.1	742.5	1294.0	29.51	0.100E 01	0.0	1778.8	0.0	94365.9	0.0	606.062	7.99	1777.	499994.	1777.
4203.9	734.6	1269.6	28.90	0.100E 01	0.0	1739.8	0.0	94365.1	0.0	604.498	7.99	1738.	499993.	1738.
4307.8	727.2	1245.7	28.30	0.100E 01	0.0	1703.6	0.0	94364.3	0.0	602.641	8.00	1702.	499992.	1702.
4403.8	720.7	1224.3	27.76	0.100E 01	0.0	1672.3	0.0	94363.6	0.0	600.731	8.00	1670.	499992.	1671.
4507.8	713.8	1201.9	27.19	0.100E 01	0.0	1640.4	0.0	94362.8	0.0	598.493	8.01	1638.	499991.	1640.
4603.9	707.7	1181.7	26.68	0.100E 01	0.0	1612.7	0.0	94362.0	0.0	596.297	8.01	1610.	499990.	1612.
4700.0	701.8	1162.3	26.19	0.100E 01	0.0	1586.3	0.0	94361.3	0.0	593.996	8.02	1584.	499989.	1586.
4804.2	695.5	1141.9	25.68	0.100E 01	0.0	1559.3	0.0	94360.4	0.0	591.404	8.02	1557.	499989.	1560.
4900.4	689.6	1123.7	25.22	0.100E 01	0.0	1535.5	0.0	94359.7	0.0	588.932	8.03	1533.	499988.	1536.

LITFIRE TEST RUN FOR LITHIUM FIRE IN UWMAK III CONTAINMENT
ASSUMING THAT 5.5 PERCENT OF THE TOTAL LITHIUM INVENTORY IS SPILLED
RUN NO. 88 CONC. TEMP. PROFILE, THW=10 IN., THF=25 IN.

TIME	TSF	TGF	OVERP	EMG	TCZF	TLIF	CMBRH	MOX	LILP	TCF(1)	DELT	TSBF	MNI	TBF(1)
5004.7	683.8	1104.7	24.74	0.100E 01	0.0	1511.0	0.0	94358.9	0.0	586.185	8.03	1508.	499987.	1512.
5101.0	678.4	1087.7	24.31	0.100E 01	0.0	1489.3	0.0	94358.1	0.0	583.594	8.03	1487.	499986.	1491.
5205.4	672.6	1070.0	23.87	0.100E 01	0.0	1466.9	0.0	94357.3	0.0	580.741	8.03	1464.	499985.	1469.
5301.8	667.4	1054.2	23.47	0.100E 01	0.0	1447.0	0.0	94356.6	0.0	578.072	8.04	1444.	499985.	1449.
5406.3	661.8	1037.6	23.05	0.100E 01	0.0	1426.3	0.0	94355.8	0.0	575.153	8.04	1424.	499984.	1429.
5502.7	656.8	1022.9	22.68	0.100E 01	0.0	1408.0	0.0	94355.0	0.0	572.438	8.04	1405.	499983.	1411.
5607.2	651.4	1007.5	22.29	0.100E 01	0.0	1388.8	0.0	94354.2	0.0	569.483	8.05	1386.	499982.	1392.
5703.7	646.6	993.7	21.94	0.100E 01	0.0	1371.8	0.0	94353.4	0.0	566.748	8.05	1369.	499982.	1375.
5800.3	641.8	980.4	21.61	0.100E 01	0.0	1355.4	0.0	94352.7	0.0	564.010	8.05	1353.	499981.	1359.
5904.9	636.8	966.4	21.26	0.100E 01	0.0	1338.1	0.0	94351.9	0.0	561.046	8.05	1335.	499980.	1342.
6001.5	632.2	954.0	20.94	0.100E 01	0.0	1322.8	0.0	94351.1	0.0	558.315	8.05	1320.	499979.	1327.
6106.1	627.3	940.9	20.61	0.100E 01	0.0	1306.6	0.0	94350.3	0.0	555.366	8.05	1304.	499978.	1311.
6202.7	622.9	929.3	20.32	0.100E 01	0.0	1292.2	0.0	94349.6	0.0	552.656	8.06	1289.	499978.	1297.
6307.5	618.2	917.0	20.01	0.100E 01	0.0	1277.1	0.0	94348.8	0.0	549.737	8.06	1274.	499977.	1282.
6404.1	614.0	906.1	19.73	0.100E 01	0.0	1263.6	0.0	94348.0	0.0	547.058	8.06	1261.	499976.	1269.
6500.8	609.8	895.5	19.47	0.100E 01	0.0	1250.4	0.0	94347.3	0.0	544.397	8.06	1248.	499975.	1256.
6605.5	605.4	884.3	19.19	0.100E 01	0.0	1236.6	0.0	94346.4	0.0	541.537	8.06	1234.	499975.	1242.
6702.3	601.3	874.4	18.93	0.100E 01	0.0	1224.1	0.0	94345.7	0.0	538.918	8.06	1221.	499974.	1230.
6807.1	597.1	863.9	18.67	0.100E 01	0.0	1211.0	0.0	94344.9	0.0	536.106	8.07	1208.	499973.	1217.
6903.8	593.2	854.5	18.43	0.100E 01	0.0	1199.3	0.0	94344.1	0.0	533.535	8.07	1196.	499972.	1206.
7000.6	589.4	845.4	18.20	0.100E 01	0.0	1187.8	0.0	94343.4	0.0	530.988	8.07	1185.	499971.	1194.
7105.4	585.4	835.7	17.96	0.100E 01	0.0	1175.7	0.0	94342.6	0.0	528.256	8.07	1173.	499971.	1183.
7202.2	581.7	827.1	17.74	0.100E 01	0.0	1164.9	0.0	94341.8	0.0	525.761	8.07	1162.	499970.	1172.
7307.1	577.8	818.1	17.51	0.100E 01	0.0	1153.4	0.0	94341.0	0.0	523.087	8.07	1151.	499969.	1161.
7403.9	574.3	809.9	17.31	0.100E 01	0.0	1143.1	0.0	94340.3	0.0	520.646	8.07	1140.	499968.	1151.
7500.8	570.8	802.0	17.11	0.100E 01	0.0	1133.0	0.0	94339.5	0.0	518.232	8.07	1130.	499968.	1141.
7605.7	567.2	793.6	16.90	0.100E 01	0.0	1122.3	0.0	94338.7	0.0	515.646	8.08	1119.	499967.	1130.
7702.5	563.8	786.1	16.71	0.100E 01	0.0	1112.7	0.0	94337.9	0.0	513.287	8.08	1110.	499966.	1121.
7807.5	560.3	778.2	16.51	0.100E 01	0.0	1102.5	0.0	94337.1	0.0	510.762	8.08	1100.	499965.	1111.
7904.3	557.0	771.1	16.33	0.100E 01	0.0	1093.3	0.0	94336.4	0.0	508.460	8.08	1090.	499964.	1102.
8001.2	553.9	764.1	16.15	0.100E 01	0.0	1084.4	0.0	94335.6	0.0	506.184	8.08	1081.	499964.	1093.
9002.9	524.1	701.2	14.57	0.100E 01	0.0	1001.7	0.0	94327.9	0.0	484.214	8.09	999.	499956.	1012.
10005.5	498.8	651.1	13.30	0.100E 01	0.0	933.9	0.0	94320.1	0.0	464.892	8.09	931.	499948.	945.
11000.4	477.3	610.5	12.28	0.100E 01	0.0	877.5	0.0	94312.4	0.0	448.043	8.09	875.	499941.	890.
12004.0	458.6	576.5	11.42	0.100E 01	0.0	829.0	0.0	94304.7	0.0	433.094	8.10	826.	499933.	842.
13007.8	442.4	547.9	10.70	0.100E 01	0.0	787.1	0.0	94296.9	0.0	419.927	8.10	784.	499925.	800.
14004.2	428.4	523.5	10.09	0.100E 01	0.0	750.8	0.0	94289.3	0.0	408.399	8.11	748.	499917.	764.
15000.7	416.0	502.5	9.56	0.100E 01	0.0	718.9	0.0	94281.6	0.0	398.204	8.10	716.	499910.	733.

PROGRAM EXECUTION STOPPED BY PROGRAM